Master's thesis

NTNU
Norwegian University of Science and Technology
Faculty of Information Technology and Electrical Engineering
Department of Engineering Cybernetics

Kristian Kjerstad

Collision Avoidance System for Ships Utilizing Other Vessels' Intentions

Master's thesis in Cybernetics and Robotics
Supervisor: Edmund Førland Brekke
June 2020

NTNU
Norwegian University of Science and Technology

DNV·GL

Kristian Kjerstad

Collision Avoidance System for Ships Utilizing Other Vessels' Intentions

Master's thesis in Cybernetics and Robotics
Supervisor: Edmund Førland Brekke
June 2020

Norwegian University of Science and Technology
Faculty of Information Technology and Electrical Engineering
Department of Engineering Cybernetics

NTNU

Kunnskap for en bedre verden

Problem Description

A collision avoidance system is of vital importance for the navigational safety of an autonomous ship. Such algorithms should be able to avoid both collisions and groundings while following the navigational rules defined by the International Regulations for Preventing Collisions at Sea (COLREGs). In this thesis, the research question to be answered is: *can data about other vessels' intentions be used to improve an existing short-term collision avoidance algorithm*? The main task of this thesis is to design and implement two collision avoidance algorithms, one that utilizes a priori information about other vessels' intentions and one algorithm that does not use intention data. Also, a simulator needs to be developed to perform simulations and compare the performance of the two algorithms. The performance will be quantified with a set of metrics. The following set of tasks are proposed:

- Perform a literature survey on navigational rules (COLREGs) and collision avoidance systems for autonomous ships.
- Study how ships are manually operated to avoid collisions. Identify the main reasons for collisions and how navigators solve collision situations.
- Develop a simulator for a vessel and the surroundings.
- Design and implement a collision avoidance system that utilizes other vessels' intentions to improve the collision avoiding abilities compared to an already existing collision avoidance method.
- Find a suitable vessel-to-vessel communication method for exchanging intention data.
- By using the developed simulator, compare the performance of the developed collision avoidance system utilizing intentions to a collision avoidance system that is not utilizing other vessels' intentions.
- Assess how a priori information about other vessels' intentions affects collision avoidance performance.

Preface

This master's thesis is the final part of my master's degree in Cybernetics and Robotics at the Norwegian University of Science and Technology (NTNU). The thesis has been written in collaboration with DNV GL as part of the Autosea project, a collaborative research project between NTNU, DNV GL, Maritime Robotics and Kongsberg Maritime.

The work done on this thesis is a continuation of my 5th-year specialization project from the fall of 2019, whose main contribution was the development of a vessel simulator. This simulator has been improved and extended to include two collision avoidance systems in this master's thesis. MATLAB R2017a and Simulink have been used for implementation and simulations. Data about ship models have been provided by DNV GL.

During the past year, I have learned a lot about the challenges regarding collision avoidance for autonomous vessels. I want to express my gratitude towards the people who have helped me with this thesis. First, I would like to thank my supervisor Edmund Førland Brekke (NTNU) and my co-supervisors Steinar Låg (DNV GL) and Tom Arne Pedersen (DNV GL). They have helped me with proofreading, answering my questions and discussing a wide range of topics. I would also like to thank Benjamin Bjørge, Olaf Gundersrud, Øystein Engelhardtsen, Frederik Tore Elter, Erlend Norstein and Tommi Juhani Rifaat from DNV GL for being available for interviews and useful discussions. I want to thank PhD candidate Inger Berge Hagen (NTNU) for her help regarding the implementation of the collision avoidance systems.

Finally, I want to give a special thanks to my family and my girlfriend for helping me stay motivated through all the hard work.

Kristian Kjerstad
Trondheim, June 2020

Abstract

Before autonomous vessels are commercially accepted, they need to be sufficiently safe. Having a collision avoidance system that complies with the navigational rules (COLREGs) is an essential step towards making autonomous vessels safer. There exists a wide range of research on different collision avoidance methods, but few researchers have investigated if data about other vessel's intentions can improve collision avoidance performance. This thesis aims to investigate if utilization of other vessels' intentions can improve the performance of an existing short-term collision avoidance method; the Simulation-Based Model Predictive Control (SBMPC) algorithm by Johansen et al. (2016). This algorithm is classified as short-term because it is concerned with avoiding immediate collisions.

In this thesis, two different collision avoidance algorithms have been implemented: the original SBMPC algorithm by Johansen et al. (2016) and a modified version of this algorithm called the modified SBMPC algorithm. The only difference between the original SBMPC and the modified SBMPC is that the modified SBMPC algorithm uses intention data about future trajectories and what COLREGs rules other vessels intend to follow. The two collision avoidance algorithms were implemented as part of a vessel simulator. This simulator performs simulations to compare the performance of the two algorithms. A set of metrics were developed to quantify the collision avoidance performance.

A wide range of simulation scenarios with varying difficulty were used to compare the two algorithms. Although the two implemented algorithms did have some problems with the choice of tuning parameters, they were able to avoid collision and grounding in all simulation scenarios. In the majority of the scenarios, the modified SBMPC algorithm utilizing intention data had better collision avoidance performance compared to the original SBMPC algorithm. The use of intention data made maneuvers safer, and it also increased compliance with the navigational rules.

Sammendrag

Før autonome skip kan bli kommersielt akseptert, må de være trygge nok. Å ha et automatisk antikollisjonssystem som følger navigasjonsreglene (COLREGs), er et viktig steg mot å gjøre autonome skip tryggere. Det finnes allerede mye forskning på ulike antikollisjonsmetoder, men få forskere har undersøkt om intensjonsdata kan brukes til å forbedre ytelsen til et eksisterende antikollisjonssystem. Denne masteroppgaven skal undersøke hvorvidt bruk av data om intensjoner kan forbedre den eksisterende SBMPC-antikollisjonsalgoritmen til Johansen et al. (2016). Dette er en kortsiktig antikollisjonsalgoritme fordi den prøver å unngå umiddelbar kollisjon.

I denne masteroppgaven har det blitt utviklet to forskjellige antikollisjonsalgoritmer: den originale SBMPC-algoritmen til Johansen et al. (2016) og en modifisert versjon av denne algoritmen, som vil bli kalt modifisert SBMPC. Den eneste forskjellen mellom den originale SBMPC-algoritmen og den modifiserte SBMPC-algoritmen er at den modifiserte SBMPC-algoritmen utnytter data om andre skip sine intensjoner. Denne dataen inneholder fremtidig rute i tillegg til hvilke navigasjonsregler andre skip har planlagt å følge. De to antikollisjonsalgoritmene har blitt implementert som en del av en skipssimulator. Denne simulatoren simulerer ulike situasjoner for å sammenligne ytelsen til de to algoritmene. Ulike metrikker har blitt utviklet for å kvantifisere ytelsen.

Et bredt utvalg av ulike situasjoner med ulik vanskelighetsgrad har blitt brukt for å sammenligne de to algoritmene. Selv om de to algoritmene hadde ytelsesproblemer på grunn av valg av parametere, så klarte begge algoritmene å unngå kollisjon og grunnstøting i alle situasjoner som ble testet. I flertallet av situasjoner som ble testet så hadde den modifiserte SBMPC-algoritmen, som bruker intensjonsdata, bedre ytelse enn den originale SBMPC-algoritmen. Bruk av intensjonsdata gjorde manøvere mer trygge, og bruk av intensjonsdata førte også til at skipet klarte å følge navigasjonsreglene bedre.

Table of Contents

List of Figures

List of Tables

Abbreviations

AIS	=	Automatic Identification System
ASM	=	Application Specific Messages
COLREGs	=	International Regulations for Preventing Collisions at Sea
CPA	=	Closest Point of Approach
DLSA	=	Distributed Local Search Algorithm
DOF	=	Degree Of Freedom
DSSA	=	Distributed Stochastic Search Algorithm
ECDIS	=	Electronic Chart and Display Information System
GNC	=	Guidance, Navigation and Control
GPS	=	Global Positioning System
LOS	=	Line Of Sight
MPC	=	Model Predictive Control
MTCAS	=	Maritime Traffic Alert and Collision Avoidance System
MVFF	=	Modified Virtual Force Field
NED	=	North-East-Down
PID	=	Proportional Integral Derivative
PSV	=	Platform Supply Vessel
RRT	=	Rapidly-exploring Random Tree
SBMPC	=	Simulation-Based Model Predictive Control
SOLAS	=	International Convention for the Safety of Life at Sea
SSL	=	Secure Sockets Layer
STCC	=	Ship Traffic Coordination Centre
TCP	=	Transmission Control Protocol
TCPA	=	Time to Closest Point of Approach
VDE	=	VHF Data Exchange
VDES	=	VHF Data Exchange System
VHF	=	Very High Frequency
VO	=	Velocity Obstacles
VSAT	=	Very-Small-Aperture-Terminal
VTS	=	Vessel Traffic Service
WP	=	Waypoint
XML	=	Extensible Markup Language

Nomenclature

$\boldsymbol{\eta}$	Position and orientation vector
$\boldsymbol{\nu}$	Velocity vector
$\boldsymbol{\tau}$	Force vector
x, y	Position along x- and y-axis
z	Position along z-axis
u, v	Speed in x- and y-direction
U	Total speed
r	Yaw rate
ψ	Heading angle
χ	Course angle
P	Waypoint position
Pr	Propulsion command
ψ_{ca}	Heading angle offset
$\mathcal{H}$	Total hazard
$\mathcal{R}$	Risk of collision
$\mathcal{C}$	Cost of collision
g	Risk of grounding
$\hat{x}, \hat{y}, \hat{U}, \hat{\psi}$	Estimated values for position, speed and heading angle
k	Scenario index
i	Obstacle ship index
α	Relative contact angle
β	Relative bearing angle
$\mathcal{P}$	Penalty metric
$\mathcal{S}$	Score metric
r_{cpa}	CPA distance
γ	Weight parameter for metric calculation
$(\cdot)_d$	Desired value for a variable
$(\cdot)_{\mathrm{ref}}$	Reference value for a variable

Chapter 1

Introduction

1.1 Background

In recent years, technological advances in the area of autonomous systems have made it possible to automate a wide range of tasks. Everything from industrial manufacturing to vacuum cleaning can now be performed by autonomous systems. In the marine industry, the development of autonomous ships has gained increasing interest among ship manufacturers. In 2018, Rolls-Royce and Finferries successfully demonstrated the world's first autonomous ferry in Finland (Hobbs, 2018). Another example is Yara Birkeland, a fully autonomous cargo ship developed by Yara and Kongsberg to reduce the number of diesel truck journeys between Yara's plant in Porsgrunn and the ports in Brevik and Larvik (Skredderberget, 2017).

There are several motivational factors for using unmanned autonomous ships instead of manually operated ships. When having no crew members, there are possibilities for reducing costs. According to the results from MUNIN (2016), the use of an autonomous bulk carrier instead of a manned bulk carrier can save over seven million dollars in crew costs and fuel consumption over a 25-year period. Having no crew members also has the potential to make the voyage safer. Allianz Global Corporate & Specialty (2017) estimates that human errors cause between 75% and 96% of all accidents in the shipping sector.

The collision avoidance system is an important aspect of autonomous ships. In addition to preventing collisions and grounding, a collision avoidance system must comply with the International Regulations for Preventing Collisions at Sea (COLREGs) published by the International Maritime Organization (1972). The COLREGs describe what maneuvers should be taken to prevent collisions. All navigators are required to follow these rules. Even though the COLREGs are written for human navigators, autonomous ships should

also be able to follow these rules when both manually operated ships and autonomous ships occupy the same areas of the sea.

Before autonomous ships can be commercially accepted and achieve regulatory approval, they need to demonstrate an equivalent level of safety as conventional ships (International Maritime Organization, 2013). Having a well-functioning collision avoidance system is necessary to ensure a safe voyage for an autonomous ship. Denker et al. (2016) expect the marine traffic density to increase in the near future. Therefore, the collision avoidance system will become more and more important in the years to come. It is of great interest to explore new ways of improving the performance of collision avoidance systems. This thesis will investigate how other vessels' intentions can be used to improve collision avoiding abilities.

1.2 Previous work

Over the last few decades, an extensive amount of research on collision avoidance methods for ships has been published. The review articles by Huang et al. (2020), Polvara et al. (2018) and Campbell et al. (2012) give an overview of recently published collision avoidance methods for unmanned vessels. According to Huang et al. (2020), the most common limitations of previous research include: not complying with COLREGs, no consideration of environmental disturbances and ignoring the own-ship's dynamics. In the literature, the term own-ship is used for the ship under control with a collision avoidance system.

Different collision avoidance algorithms are divided into two main classes: long-term and short-term methods (Eriksen et al., 2019). Figure 1.1 illustrates the difference between the two classes. Long-term methods are algorithms for path planning that can find a collision free path from start to destination. The path found avoids collision with static obstacles. On the other hand, short-term methods make the vessel deviate from the planned path to avoid immediate collision with dynamic obstacles.

Hybrid methods also exist. They use a combination of both short-term and long-term methods to avoid collisions. Such a hybrid architecture is suggested by Bitar et al. (2019) and Loe (2008).

Long-term collision avoidance methods are divided into two main groups: roadmap methods and complete path methods (Bitar et al., 2018). Roadmap methods generate a series of waypoints, and a path is created by connecting these waypoints. Rapidly-Exploring Random Tree (RRT), first introduced by LaValle (1998), is an example of a roadmap method. RRT generates a tree by using an iterative algorithm to find a set of vertices $\mathcal{T}$, i.e. waypoints, that connect an initial vertex x_{init} to the destination vertex x_{goal}. Complete path methods use a different approach where a continuous path is found by using optimization techniques. An example of this is the approach taken by Sundar and Shiller (1997), where the Hamilton-Jacobi-Bellman equation solves an optimization problem.

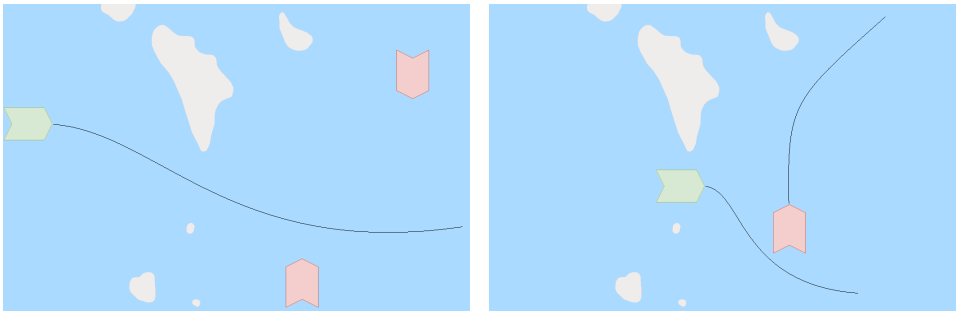

(a) Long-term collision avoidance. **(b)** Short-term collision avoidance.

Figure 1.1: The difference between long-term and short-term methods. Long-term path planning determines a path from start to destination that avoids static obstacles. Short-term collision avoidance makes the own-ship deviate from the desired path to avoid dynamic obstacles.

There are several short-term collision avoidance methods able to achieve COLREGs compliance. Lee et al. (2004) developed the Modified Virtual Force Field (MVFF) algorithm, an extension of the Virtual Force Field method by Borenstein and Koren (1989). The MVFF method finds a collision free path by using 210 different fuzzy rules to determine the heading angle necessary to avoid collision. Another example is the Velocity Obstacles (VO) algorithm by Kuwata et al. (2014). The main idea behind this algorithm is to calculate a velocity obstacle. If the own-ship's velocity vector lies outside the set of velocities defined by the velocity obstacle, there will not be any collision. A third example is the Simulation-Based Model Predictive Control (SBMPC) algorithm by Johansen et al. (2016). This was one of the first uses of model predictive control for ship collision avoidance with COLREGs compliance. The SBMPC algorithm simulates the behavior of the ship for different control behaviors and chooses the control behavior associated with the lowest risk. This algorithm will be discussed in more detail in chapter 5.

Several methods for short-term collision avoidance have been published. However, the amount of research regarding the use of intentions for short-term collision avoidance is very limited. Some research projects, such as STM BALT SAFE and its forerunner project MONALISA, have investigated a concept for exchanging intended routes to improve traffic control. Lindborg et al. (2019) explain how the route exchange method in the STM BALT SAFE project works. In short, a ship's planned route is sent to a shore-based Ship Traffic Coordination Centre (STCC), which examines the route for possible collisions with other ships. The STCC validates the suggested route if there is little chance of collision. If the route is not validated, the STCC returns an alternative route back to the ship.

During the research for this master's thesis, only four different collision avoidance methods that utilize intentions were found. Kim et al. (2017) developed the Distributed Stochastic Search Algorithm (DSSA). The work was inspired by the Distributed Local Search Algorithm (DLSA) by Kim et al. (2014). Both algorithms calculate the route for each vessel based on other vessels' intended course angles. Initially, each ship broadcasts her intended

course angle to all surrounding ships. Based on the received data, each ship chooses a new course angle. This process continues until all ships have chosen a course angle with the lowest possible risk of collision. Both DSSA and DLSA use many of the same principles, but DSSA requires fewer messages exchanged. Simulation results show that DSSA and DLSA have acceptable collision avoidance performance, but COLREGs compliance of the calculated maneuvers was not considered. Also, the simulations did not contain any static obstacles.

The method by Hornauer and Hahn (2013) uses information about other ships' intended routes to optimize the own-ship's route. Each ship creates an initial route and broadcasts this route to all other ships. After the routes from other ships are received, a negotiation procedure makes all ships agree on a common solution. This paper does not contain any simulation results and argues that simulation and evaluation of the algorithm will be given in future projects.

Another example of utilizing intentions for collision avoidance is the method by Hu et al. (2008), which extends the negotiation framework developed by Hu et al. (2006) to include data about planned routes. They concluded that the inclusion of intentions makes the behavior of the ships more efficient, but they do not consider whether safety or collision avoidance performance is improved. This method is designed for collision situations involving only two vessels, and would probably not scale very well to include more vessels. In addition, COLREGs compliance and the effect of including static obstacles is not considered.

To summarize, little research exists regarding the use of intentions for collision avoidance purposes. Only four examples of collision avoidance methods that utilize other vessels' intentions have been found. All of them can be categorized as negotiation procedures where several ships cooperate on calculating a route for each ship involved. None of the authors of these algorithms have addressed the degree of COLREGs compliance achieved or how the inclusion of static obstacles affects the performance.

1.3 Motivation and objective

The motivation behind this thesis is the desire to improve existing collision avoidance methods. The main objective of this thesis is to determine if the inclusion of intentions will improve the collision avoidance performance.

In this thesis, the previously developed SBMPC method by Johansen et al. (2016) will be modified to include data about other vessels' intentions. The collision avoidance performance of the original SBMPC method and the modified SBMPC will be compared in a wide range of scenarios to assess how the inclusion of intentions will affect collision avoidance performance. Several metrics, partly based on the work by Woerner (2016), will be used to quantify the performance.

Previous collision avoidance methods that use intentions are negotiation procedures that calculate the route for all ships involved. Such an approach would probably not work very well in environments with passive obstacle ships without a collision avoidance system. Therefore, the modified SBMPC developed in this thesis will not use a negotiation procedure. Unlike previous research about collision avoidance methods that use intentions, this thesis will investigate the degree of COLREGs compliance and the effect of including static obstacles.

1.4 Contributions

The main contributions of this thesis are:

- A study on how collision avoidance is performed for manually operated ships and a summary of common reasons for collisions.
- Implementation of a vessel simulator able to simulate scenarios with several obstacle ships and static obstacles.
- Modifying the SBMPC collision avoidance algorithm by Johansen et al. (2016) to utilize data about other vessels' intentions.
- Recommendation for a communication method for exchanging intention data.
- Implementation of an evaluation tool, consisting of several types of metrics, that quantifies the performance of collision avoidance algorithms.
- A comparison of the performance of the SBMPC and modified SBMPC algorithms in a wide range of scenarios. The scenarios will include both static obstacles and obstacle ships with and without a collision avoidance system.

1.5 Outline

This thesis is divided into ten chapters. Chapter 2 provides relevant background theory to familiarize the reader with important concepts related to the control of marine surface vessels and navigational rules. Chapter 3 contains information about how ships are manually operated to avoid collisions and common reasons for collisions at sea. In chapter 4, details about the simulator development and the implementation of the guidance and control systems for a vessel model will be presented. Chapter 5 introduces the SBMPC collision avoidance algorithm in detail and explains how intention data has been utilized in the modified SBMPC algorithm. A recommendation for a way of communicating intentions is also given. Chapter 6 provides details about the metrics used for quantifying collision avoidance performance. Chapter 7 contains the simulation results. The performance of the SBMPC and the modified SBMPC algorithms are compared in a wide range of scenarios. A discussion of these simulation results is given in chapter 8. Chapter 9 concludes the thesis, and suggestions for further work are given in chapter 10.

Chapter 2

Background Theory

This chapter will provide the relevant background theory for this thesis. The chapter starts with an introduction to guidance, navigation and control and continues with a description of a mathematical model for a marine craft. Details about optimization and model predictive control will also be given. Towards the end of the chapter, the International Regulations for Preventing Collisions at Sea (COLREGs) will be presented.

Some of the content in this chapter is similar to chapter 2 from the specialization project by the author (Kjerstad, 2019). Compared to the specialization project, this master's thesis contains a more thorough review of the motion control system for marine vessels, and a more in-depth discussion about the navigational rules.

2.1 Guidance, navigation and control

The motion control system for a marine vessel is divided into three separate components: Guidance, Navigation and Control (GNC) (Fossen, 2011). Figure 2.1 illustrates the three components and the connections between them. In the following, each component will be discussed in more detail.

2.1.1 Navigation

The navigation system's task is to determine the states of the vessel, including position, heading angle, speed and acceleration (Fossen, 2011). Typically, several sensors are being used in conjunction to provide proper situational awareness. Some of the sensor data is

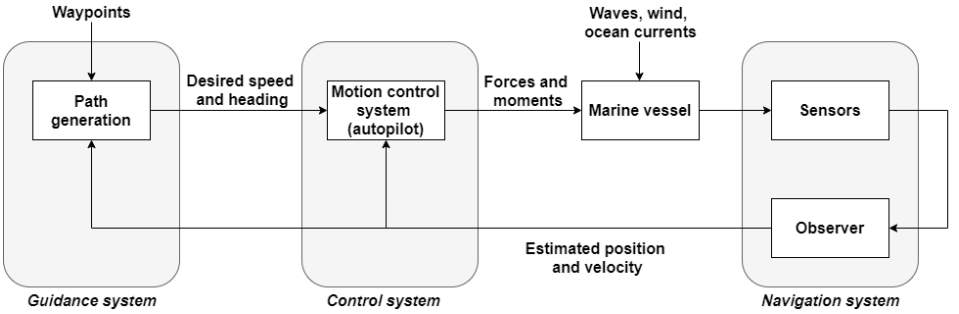

Figure 2.1: Connection between guidance, navigation and control. The figure is inspired by Figure 9.1 in Fossen (2011).

processed by an observer, typically a Kalman filter. This observer can estimate variables that cannot be directly measured, and can also combine data from several sensors to estimate states when the measurements are subject to noise (Fossen, 2011). Both the guidance and the control system use the estimated states.

There are several different types of sensors being used onboard a vessel. Global Positioning System (GPS) is commonly used to determine the position of a vessel and relies on a network of satellites that orbits around the Earth (Beard and McLain, 2012). A gyrocompass is often used to measure the heading angle of a vessel, which is the direction of the vessel's bow. This sensor can find the north direction by utilizing a spinning wheel and the rotation of the Earth (Bai and Bai, 2019).

Different sensors are also used for the detection of static and dynamic obstacles. By using two or more cameras in a stereo-vision setup along with a processing algorithm to process the data, a map of obstacles can be created (Huntsberger et al., 2011). Radar is also used for detecting obstacles. The technology is based on transmitting radio-waves from a rotating antenna and detection of the radio-waves reflected back from the surrounding obstacles (Elkins et al., 2010). Today's vessels often use radar tracking, as defined in the IEC 62388 standard. When an obstacle vessel is selected for tracking, the information about the tracked vessel's speed and direction is typically displayed on a monitor.

Automatic Identification System (AIS) can also be used for tracking obstacles. AIS uses Very High Frequency (VHF) radio to broadcast real-time data about a vessel's measured states and other vessel-related information. Some of the information broadcasted includes:

- Position
- Heading angle
- Speed
- Destination and time of arrival
- Type of ship and ship size
- Maritime mobile service identity number, a unique nine digit number
- Rate of turn

- UTC timestamp
- Navigational status (e.g. ”underway using engine” or ”at anchor”)
- Route plan and waypoints, entered manually at the start of the voyage and can be updated manually later

For a complete list of the data transmitted via AIS, the reader is referred to the AIS guidelines report by IMO (2002). The data received from AIS can be merged with the radar data, and the information is typically displayed on an Electronic Chart Display and Information System (ECDIS). Figure 2.2 shows a screenshot of an ECDIS displaying AIS data. According to the International Convention for the Safety of Life at Sea (SOLAS) issued by the International Maritime Organization (IMO) (1974), the majority of larger ships are required to be equipped with AIS. Fishing and military vessels typically do not use AIS.

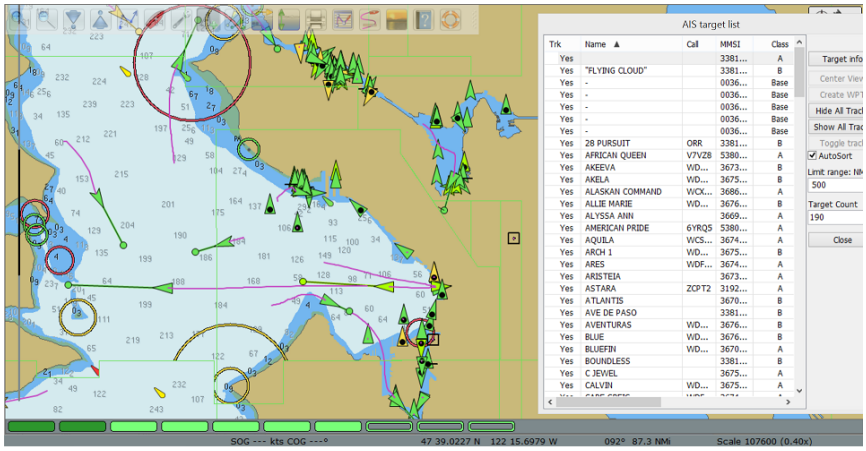

Figure 2.2: A screenshot of ECDIS that shows the location of other vessels and information about each vessel. The figure is taken from `http://www.tiarora.no/batdata/ais-receiver/`.

2.1.2 Guidance

The guidance system generates a desired path for the vessel to follow (Fossen, 2011). Vessels are required by regulations to have a path from start to destination before departure (Porathe et al., 2013). A common way to represent the path is to use waypoints, as illustrated in Figure 2.3. These waypoints can be generated based on weather data, geographical data as well as human operator inputs. Optimization methods can also be used for path generation to minimize time to destination or fuel consumption (Fossen, 2011).

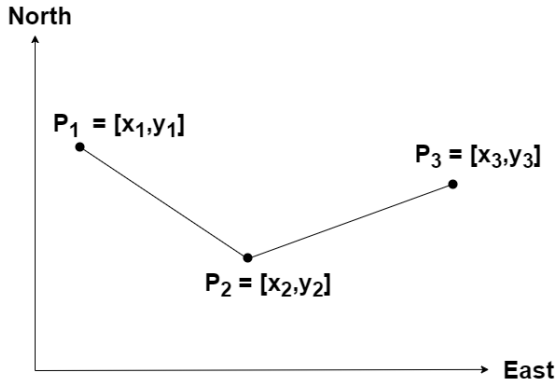

Figure 2.3: The desired path for the vessel can be represented as straight line segments between a set of waypoints $\{P_i\}$.

Guidance laws

Most of the literature on guidance laws are related to airborne systems, such as missiles (Naeem et al., 2003). However, guidance laws are also an essential aspect of the control of marine surface vessels. Guidance laws have two primary purposes: trajectory tracking and path following. Fossen (2011) defines trajectory tracking as the task of following a moving target and ultimately hit the target. Path following is defined as the task of following a path independent of time. In the context of collision avoidance, path following is of main interest. In this discussion, it will be assumed that the guidance laws do not consider collision avoidance.

For path following, the guidance law computes the desired course angle and speed necessary to make the ship follow the desired path generated by the guidance system. Course angle is the actual direction the ship is moving. Several approaches to achieve path following can be found in the literature, for instance deep reinforcement learning (Martinsen and Lekkas, 2018) or nonlinear adaptive controllers (Almeida et al., 2007). However, LOS guidance is one of the most popular guidance strategies (Naeem et al., 2003).

In the simulator for this thesis, the lookahead-based LOS steering law by Fossen (2011) is used to calculate the desired course angle χ_d necessary to make the vessel follow the desired path. The principle is explained below.

Lookahead-based LOS steering

Figure 2.4 illustrates the idea behind the lookahead-based LOS steering law from Fossen (2011). The goal is to make the vessel follow the straight path between the two waypoints $P_k = [x_k, y_k]$ and $P_{k+1} = [x_{k+1}, y_{k+1}]$. The vessel, currently located at position $[x(t), y(t)]$, is steered towards the point $[x_{\text{los}}, y_{\text{los}}]$ on the straight path between the two

waypoints. The lookahead distance Δ is the distance between the vessel and the point $[x_{\text{los}}, y_{\text{los}}]$, measured along the straight path. The closest distance between the vessel and the path is called the cross-track error e. The control objective is to let e converge to zero. To achieve this, the guidance law calculates the desired course angle χ_d necessary to make the ship converge to the path. This desired course angle is found by using equation (2.1).

$$\chi_d = \chi_p + \chi_r(e) \tag{2.1}$$

Here, $\chi_p = \text{atan2}(y_{k+1} - y_k, x_{k+1} - x_k)$ and $\chi_r(e) = \text{atan}(\frac{-e}{\Delta})$. The function $\text{atan2}(y, x)$ returns a value between $-\pi$ and π corresponding to the arctangent of y/x. Equation (2.2) can be used to find the cross-track error e.

$$e(t) = -(x(t) - x_k)\sin(\chi_p) + (y(t) - y_k)\cos(\chi_p) \tag{2.2}$$

A large value for Δ will make the vessel converge slowly towards the path, while a small value for Δ will give fast convergence. However, Δ cannot be chosen too small since this can make the vessel oscillate around the path.

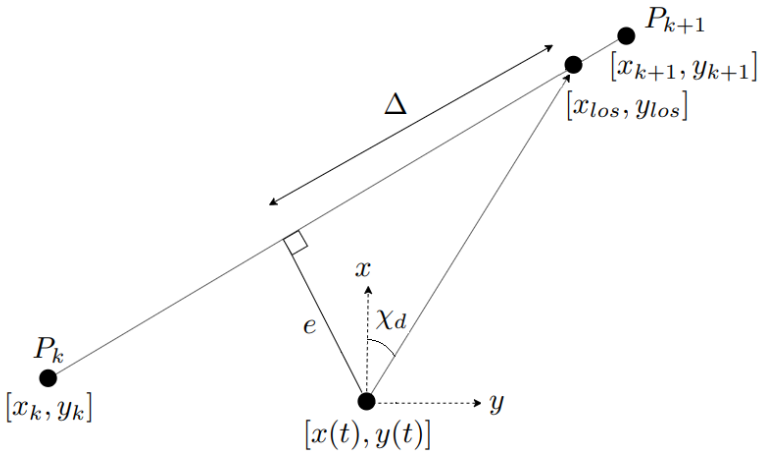

Figure 2.4: Line of sight guidance with lookahead-based LOS steering. The desired path is the straight-line path between waypoints P_k and P_{k+1}. The figure is inspired by Figure 10.10 in Fossen (2011).

The entire path from start to destination often consists of more than two waypoints. However, the lookahead-based LOS law can only follow the straight path between two waypoints. Therefore, a switching mechanism is necessary to switch between active waypoints. The switching mechanism can be explained by using an example. Consider the path in Figure 2.3 consisting of three waypoints P_1, P_2 and P_3. Assume that the vessel is currently following the straight path from P_1 to P_2, which are the two active waypoints. When the vessel is closer than R meters from waypoint P_2, the switching mechanism changes the active waypoints from P_1 and P_2 to P_2 and P_3. This makes the vessel start to move towards waypoint P_3.

The lookahead-based LOS steering law presented above have good convergence properties. However, environmental disturbances such as ocean currents and wind can give rise to convergence problems and deviation from the desired path. A solution to this problem is to include integral action, as done by Børhaug et al. (2008). Integral action helps counteract the effects of disturbances.

2.1.3 Control

The control system is responsible for generating forces and moments to make the vessel follow the path generated by the guidance system. Typically, the control system will consist of a speed controller for keeping the desired speed and a heading controller, commonly called heading autopilot, for keeping the desired heading angle. The guidance system calculates the desired speed and desired heading angle to be used as inputs to the control system.

The controllers are based on control laws such as Proportional-Integral-Derivative (PID) control or feedback linearizing control to calculate generalized control forces $\boldsymbol{\tau}$. Control allocation converts the generalized control forces into control signals $\boldsymbol{u}$ for the actuators (propellers, rudders and thrusters), which generate forces and moments that act on the vessel. Figure 2.5 illustrates the principle of control allocation.

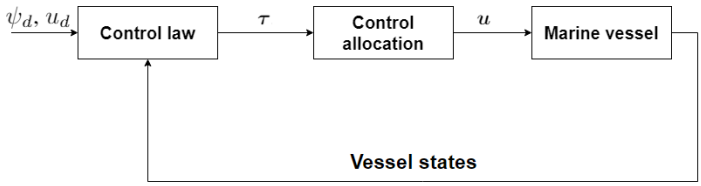

Figure 2.5: The principle of control allocation. The control law computes generalized control forces $\boldsymbol{\tau}$, which are converted into control signals $\boldsymbol{u}$ for the actuators on the marine vessel.

2.2 A 3 degrees of freedom surface vessel model

The simulator in this thesis will use a 3 degrees of freedom (DOF) surface vessel model. Figure 2.6 illustrates these three degrees of freedom: surge, sway and yaw. A 3 DOF model can only model the horizontal plane motion of the vessel. For this thesis, a 3 DOF model provides sufficient accuracy. More advanced 6 DOF models can be found in Fossen (2011).

Two different coordinate frames will be used to model the surface vessel. The North-East-Down (NED) coordinate frame $\{n\} = [x_n, y_n, z_n]$ whose x-, y- and z-axis points north, east and down towards the center of the Earth. It is assumed that the NED frame is inertial. The second coordinate frame is the body-fixed coordinate frame $\{b\} = [x_b, y_b, z_b]$

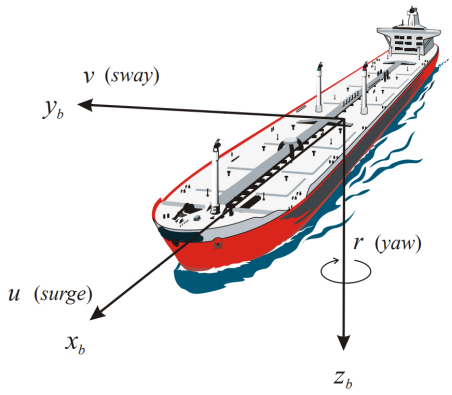

Figure 2.6: The 3 degrees of freedom for a surface vessel. The figure is taken from Fossen (2011).

whose x-, y- and z-axis points in the direction of aft to fore, right and down respectively. The origin of $\{b\}$ moves with the vessel.

Fossen (2011) uses the following vectorial representation of the 3 DOF equations of motion for a surface vessel.

$$\dot{\boldsymbol{\eta}} = \boldsymbol{R}(\psi)\boldsymbol{\nu} \tag{2.3a}$$

$$\boldsymbol{M}\dot{\boldsymbol{\nu}} + \boldsymbol{C}_{RB}(\boldsymbol{\nu})\boldsymbol{\nu} + \boldsymbol{C}_A(\boldsymbol{\nu}_r)\boldsymbol{\nu}_r + \boldsymbol{D}(\boldsymbol{\nu}_r)\boldsymbol{\nu}_r = \boldsymbol{\tau} + \boldsymbol{\tau}_{\text{wind}} + \boldsymbol{\tau}_{\text{wave}} \tag{2.3b}$$

A short explanation of the different terms in equations (2.3a) and (2.3b) will be given. For a more in-depth review of the different terms, the reader is referred to Fossen (2011).

In equation (2.3a), the vector $\boldsymbol{\eta} = [x, y, \psi]^T$ contains the position $[x, y]$ and the heading angle ψ of the vessel with respect to the NED frame $\{n\}$. The dot above $\boldsymbol{\eta}$ represents differentiation with respect to time. The velocity vector with respect to the body-fixed frame $\{b\}$ is given by $\boldsymbol{\nu} = [u, v, r]^T$, where u and v are the speeds in surge and sway direction. The yaw rate r is the angular velocity about the z-axis.

To transform between the two coordinate frames, the rotation matrix $\boldsymbol{R}(\psi)$ from the body-fixed frame $\{b\}$ to the NED frame $\{n\}$ is used. The expression for $\boldsymbol{R}(\psi)$ is given by equation (2.4).

$$\boldsymbol{R}(\psi) = \begin{bmatrix} \cos(\psi) & -\sin(\psi) & 0 \\ \sin(\psi) & \cos(\psi) & 0 \\ 0 & 0 & 1 \end{bmatrix} \tag{2.4}$$

In equation (2.3b), $\boldsymbol{M} = \boldsymbol{M}_A + \boldsymbol{M}_{RB}$ is the inertial matrix, which is the sum of the added mass matrix $\boldsymbol{M}_A$ and the rigid-body inertia matrix $\boldsymbol{M}_{RB}$. The expression for $\boldsymbol{M}_A$ is given by equation (2.5).

$$\boldsymbol{M}_A = \begin{bmatrix} -X_{\dot{u}} & 0 & 0 \\ 0 & -Y_{\dot{v}} & -Y_{\dot{r}} \\ 0 & -N_{\dot{v}} & -N_{\dot{r}} \end{bmatrix} \tag{2.5}$$

The added mass matrix $\boldsymbol{M}_A$ is included to capture the effect of added mass, a virtual mass due to the vessel moving a volume of fluid as it accelerates. In equation (2.5), the elements in the matrix $\boldsymbol{M}_A$ are called the hydrodynamic derivatives, assumed to be constants in this thesis.

The expression for $\boldsymbol{M}_{RB}$ is given by equation (2.6).

$$\boldsymbol{M}_{RB} = \begin{bmatrix} m & 0 & 0 \\ 0 & m & mx_g \\ 0 & mx_g & I_z \end{bmatrix} \tag{2.6}$$

Here, m represents the mass of the vessel, x_g is the distance along the x-axis between the center of gravity and the origin of the body-fixed frame $\{b\}$. I_z is the moment of inertia about the z-axis.

$\boldsymbol{C}_{RB}(\boldsymbol{\nu})$ represents the rigid-body Coriolis-centripetal matrix. This term is included due to the rotation of $\{b\}$ around $\{n\}$. The expression for $\boldsymbol{C}_{RB}(\boldsymbol{\nu})$ is given by equation (2.7).

$$\boldsymbol{C}_{RB}(\boldsymbol{\nu}) = \begin{bmatrix} 0 & 0 & -m(x_g r + v) \\ 0 & 0 & mu \\ m(x_g r + v) & -mu & 0 \end{bmatrix} \tag{2.7}$$

The hydrodynamic Coriolis-centripetal matrix is denoted by $\boldsymbol{C}_A(\boldsymbol{\nu}_r)$, where $\boldsymbol{\nu}_r = \boldsymbol{\nu} - \boldsymbol{\nu}_c$ is the relative velocity of the vessel compared to the velocity of the ocean currents $\boldsymbol{\nu}_c$. It will be assumed that ocean currents have zero velocity, thus $\boldsymbol{\nu}_r = \boldsymbol{\nu}$. With this assumption, the expression for $\boldsymbol{C}_A(\boldsymbol{\nu}_r)$ is given by equation (2.8).

$$\boldsymbol{C}_A(\boldsymbol{\nu}_r) = \boldsymbol{C}_A(\boldsymbol{\nu}) = \begin{bmatrix} 0 & 0 & Y_{\dot{v}} v + Y_{\dot{r}} r \\ 0 & 0 & -X_{\dot{u}} u \\ -Y_{\dot{v}} v - Y_{\dot{r}} r & X_{\dot{u}} u & 0 \end{bmatrix} \tag{2.8}$$

$\boldsymbol{D}(\boldsymbol{\nu}_r)$ is the damping matrix, given as a sum of a linear damping term $\boldsymbol{D}$ and a non-linear damping term $\boldsymbol{d}(\boldsymbol{\nu}_r)$. Thus, $\boldsymbol{D}(\boldsymbol{\nu}_r) = \boldsymbol{D} + \boldsymbol{d}(\boldsymbol{\nu}_r)$. In this thesis, the nonlinear damping term will be neglected. The expression for $\boldsymbol{D}(\boldsymbol{\nu}_r)$ is given by equation (2.9).

$$\boldsymbol{D}(\boldsymbol{\nu}_r) = \boldsymbol{D} = \begin{bmatrix} -X_u & 0 & 0 \\ 0 & -Y_v & -Y_r \\ 0 & -N_v & -N_r \end{bmatrix} \tag{2.9}$$

The elements in the linear damping matrix $\boldsymbol{D}$ are called moment coefficients. According to Fossen (2011), the diagonal elements in $\boldsymbol{D}$ can be calculated by equations (2.10a), (2.10b)

and (2.10c). The remaining non-diagonal coefficients N_v and Y_r are assumed to be zero.

$$-X_u = \frac{m - X_{\dot{u}}}{T_{\text{surge}}} \tag{2.10a}$$

$$-Y_v = \frac{m - Y_{\dot{v}}}{T_{\text{sway}}} \tag{2.10b}$$

$$-N_r = \frac{I_z - N_{\dot{r}}}{T_{\text{yaw}}} \tag{2.10c}$$

T_{surge}, T_{sway} and T_{yaw} are time constants in surge, sway and yaw respectively.

On the right-hand side of equation (2.3b), $\boldsymbol{\tau}$ is the vector of generalized forces and moment acting on the vessel. The vectors $\boldsymbol{\tau}_{\text{wind}}$ and $\boldsymbol{\tau}_{\text{wave}}$ are the forces and moments from wind and waves that affect the vessel.

2.3 Optimization and Model Predictive Control

An optimization problem is concerned with maximizing or minimizing a function of one or more variables (Nocedal and Wright, 2006). Optimization is used in many different areas, including maximizing profits (Liu et al., 2001) and minimizing electricity costs (Rao et al., 2010). Model Predictive Control (MPC) is a type of control where the control inputs are obtained by solving an optimization problem at each time step. A high-level description of the MPC principle based on Foss and Heirung (2016) will be presented.

Figure 2.7 illustrates how MPC is used to control a plant. The graph on the bottom shows the history of measured state values x_t for the plant as blue dots and the history of control inputs u_t as black bars. It is assumed that time t is a discrete variable. At each time step, an optimization problem is solved. The graph on the top in Figure 2.7 illustrates the solution of an optimization problem for the plant at the current time step t'. The optimization problem is solved in three steps:

1. Measure the current state of the plant as x'_t.
2. Solve the optimization problem on the prediction horizon from t' to $t' + N$. The solution is a set of state estimates $\hat{x}_{t'+1}$ to $\hat{x}_{t'+N}$ and a set of control inputs $u_{t'}$ to $u_{t'+N-1}$. The state estimates are found by applying the control inputs to the mathematical plant model.
3. Apply the first control input from the solution, $u_{t'}$, to the real plant.

After the optimization problem is solved, these three steps are repeated at the next time step $t' + 1$.

According to Brekke et al. (2019), MPC has historically been mostly used for process control and not so much for vehicle navigation. Using the traditional MPC approach for collision avoidance does present some challenges. Collision situations often yield complex

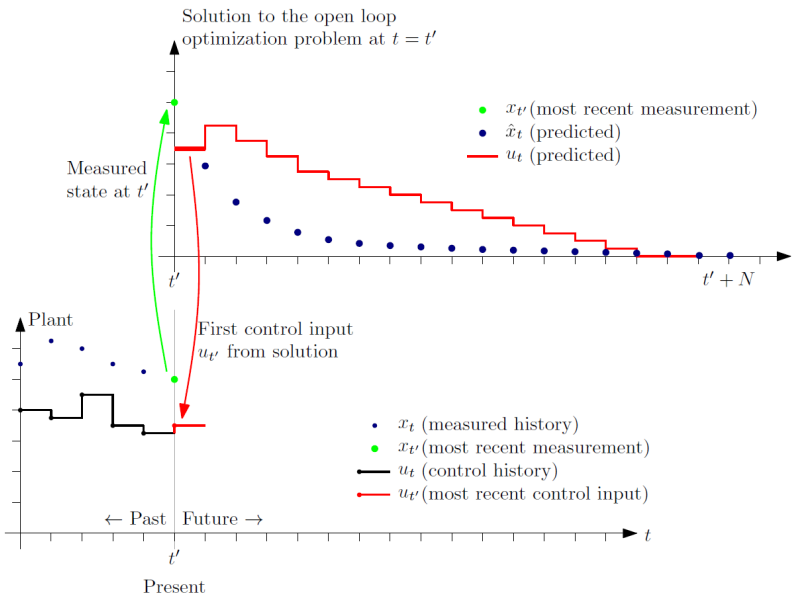

Figure 2.7: Illustration of the MPC principle. The bottom graph displays the history of states and control inputs for the plant, while the top graph displays the solution of the optimization problem as a set of estimated states and control inputs. The figure is taken from Foss and Heirung (2016).

optimization problems that are hard to solve due to high computational complexity. The approach taken by Johansen et al. (2016) in the SBMPC collision avoidance method does not solve a traditional optimization problem. Instead, a concept from the literature on robust MPC is used where optimization is done over a finite number of control behaviors. This will be further explained in chapter 5.

2.4 COLREGs

The International Regulations for Preventing Collisions at Sea (COLREGs), issued by the International Maritime Organization (1972), define a set of rules that must be followed by marine surface vessels. These rules are divided into six parts:

Part A - General (Rules 1-3)
Part B - Steering and Sailing (Rules 4-19)
Part C - Lights and Shapes (Rules 20-31)
Part D - Sound and Light Signals (Rules 23-37)
Part E - Exemptions (Rule 38)
Part F - Verification of compliance with the provisions of the Convention (Rules 39-41)

2.4.1 Relevant CORLEGs

For an automatic collision avoidance system, the rules in Part B are of primary interest. These rules contain a description of what maneuvers should be taken in different situations to prevent collisions. Part B of the COLREGs considers collision situations involving two vessels. One vessel is labeled as the stand-on vessel, which is supposed to keep a constant course, while the other vessel is labeled as the give-way vessel and is supposed to maneuver to avoid collision.

In the following, a summary of the most important rules for collision avoidance will be given. The formulation is slightly different compared to the original rules as an attempt to improve the clarity. A complete description of all the COLREGs is given in the report issued by the International Maritime Organization (1972).

Rule 6 - Safe speed

a) A vessel should at all times have a safe speed so that she can take proper and effective actions to avoid collision and be able to stop within an appropriate distance.

Rule 8 - Action to avoid collision

a) Any actions made should be taken in ample time and follow the rules given in Part B - Steering and Sailing.
b) Any alteration of course and/or speed to avoid collision should, if circumstances admit, be large enough to be readily apparent to another vessel. A series of small course and/or speed changes should be avoided.
c) If sufficient sea-room, alteration of course alone may be most effective.
d) Actions taken to avoid collision should result in passing at a safe distance.
e) If necessary, a vessel should reduce her speed, stop or reverse to allow more time to assess the situation.

Rule 13 - Overtaking

a) A vessel overtaking any other vessel should keep out of the way of the vessel being overtaken. Figure 2.8 illustrates an overtaking situation, where a vessel's current velocity is represented by a black arrow. The dashed arrows represent possible maneuvers for the overtaking vessel. The green vessel has give-way responsibility, and the red vessel has stand-on responsibility.
b) A vessel is overtaking when coming up to another vessel from a direction more than 22.5° abaft her beam.
c) When a vessel is unsure if she is overtaking another vessel, she shall assume that this is the case and act accordingly.

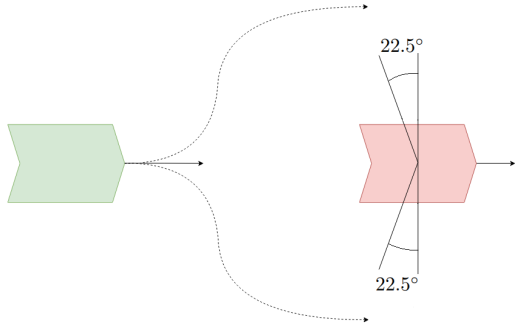

Figure 2.8: Overtaking situation. The overtaking vessel must alter her course.

Rule 14 - Head-on situation

a) When two power-driven vessels are meeting on reciprocal or nearly reciprocal courses, each vessel should alter her course to starboard. This will result in passing on the port side of each other. Figure 2.9 illustrates a head-on situation.

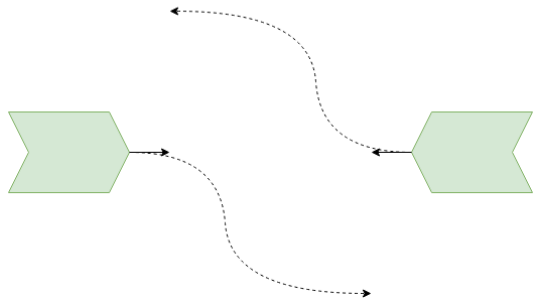

Figure 2.9: Head-on situation. Both vessels need to turn to their starboard side.

Rule 15 - Crossing situation

a) When two power-driven vessels are crossing, the vessel which has the other on her starboard side should keep out of the way, taking the role of a give-way vessel. The give-way vessel should avoid crossing ahead of the other vessel. Figure 2.10 illustrates two crossing situations.

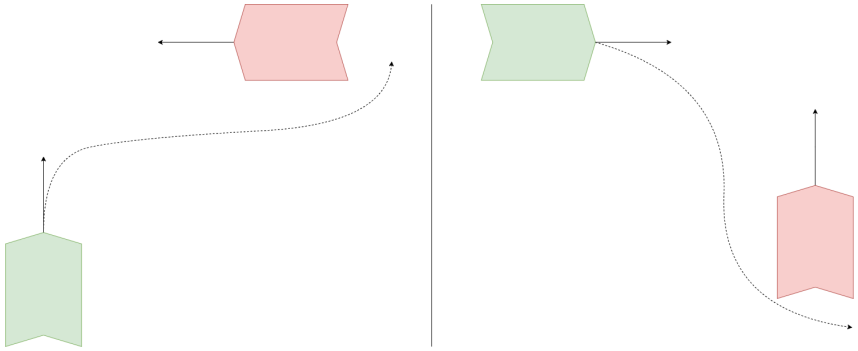

Figure 2.10: Two Crossing situations. The vessel which has the other on her starboard side must keep out of the way.

Rule 16 - Action by give-way vessel

a) Every vessel taking the role of a give-way vessel should keep out of the way of the other vessel. Also, the give-way vessel should take early and substantial actions.

Rule 17 - Action by stand-on vessel

a) While the give-way vessel should keep out of the way, the stand-on vessel should keep a constant course and speed. The stand-on vessel may take action to avoid a collision if the give-way vessel does not take appropriate action in compliance with these rules.
b) If the stand-on vessel is so close to the give-way vessel that collision cannot be avoided by the action of the give-way vessel alone, the stand-on vessel should take action to avoid collision.
c) In a crossing situation, the give-way vessel should not alter her course to her port side for a vessel on her port side.

Challenges with the COLREGs

Some studies have investigated how well human navigators understand the COLREGs. Mohović et al. (2015) found that most navigators have some difficulty with understanding the COLREGs, especially navigators with little experience. Demirel and Bayer (2015) argue that accidents related to not following the COLREGs are mainly due to insufficient training.

Even though the COLREGs are written to be followed by human navigators, the rules should also be followed by unmanned autonomous vessels. This is based on the assumption that in the near future, both manually operated ships and autonomous vessels will

occupy the same areas of the sea. Making autonomous vessels follow the COLREGs would make the autonomous vessels' behavior more predictable for human navigators.

Developing an automatic collision avoidance method that complies with the COLREGs is not a trivial task. The COLREGs are written as a legal document and have vague formulations that are open to different interpretations (Tam and Greig, 2009). This allows human navigators the flexibility of taking the most appropriate action, but is problematic when trying to implement a collision avoidance system. For instance, rule 8 uses the term "safe distance" without defining any ways to determine what a safe distance is. Another example is rule 16, which requires the give-way vessel to take "early and substantial actions". The rules do not mention how to determine what is early enough or how large the change in course angle must be before it is a "substantial action". The COLREGs have few quantitative rules, which makes it difficult for a machine to follow them.

Another difficulty with making a collision avoidance system comply with the COLREGs is that the COLREGs are designed for situations involving only two vessels. For more complicated situations involving multiple obstacle vessels, like the situation in Figure 2.11, the maneuvers required by the COLREGs may be conflicting. In this situation, vessel B is a stand-on vessel relative to vessel A by rule 15 for crossing. Thus, vessel A is a give-way vessel in this crossing situation. However, because vessel C is overtaking vessel A, the COLREGs rule 13 require vessel A to be stand-on. In this situation, the COLREGs require vessel A to be both stand-on and give-way at the same time, which is impossible. When several vessels are involved, it is often impossible to achieve 100% COLREGs compliance with all the rules.

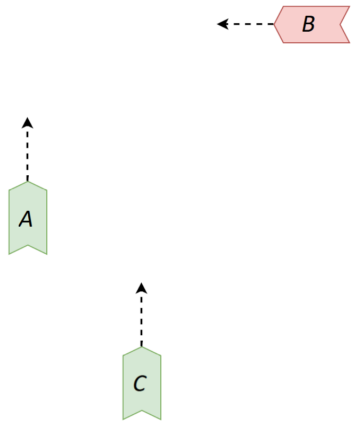

Figure 2.11: Example of a complicated collision situation. In this case, the COLREGs can be hard to interpret. Vessels A and B are in a crossing situation where A is assigned the be the give-way vessel. However, vessel C overtakes A, which makes vessel A a stand-on vessel.

Chapter 3

Manual Operation of Ships and Reasons for Collisions

This chapter explains how a manually operated ship is maneuvered to avoid collisions. Common reasons for collisions at sea and typical situations that lead to collisions will also be discussed. This chapter is partly based on chapter 3 from the specialization project by the author (Kjerstad, 2019). Compared to the specialization project, this master's thesis contains a more thorough review of how manually ships are operated and a more in-depth discussion of reasons for collisions and scenarios that often lead to collisions.

3.1 Maneuvering to avoid collisions

On manually operated ships, the Officer Of the Watch (OOW) is responsible for steering and visual monitoring of potential obstacles. However, in times with poor visibility, it is required to have an extra person on the bridge solely responsible for keeping a lookout. Autopilots are commonly used to help the OOW steer the ship, but today's vessels do not use automatic collision avoidance systems.

Statheros et al. (2008) define three different factors that influence ship collision avoidance. The first factor is the ship type, which determines the maneuverability. A small fishing boat is highly maneuverable compared to a 300-meter long oil tanker. The second factor is the type of traffic. Inside confined environments, the traffic is usually denser compared to the open sea. More dense traffic requires the OOW to pay extra close attention to potential collision situations. The final factor is weather conditions. Fog and heavy rain will reduce the visibility. Also, steering the ship can be more difficult in poor weather.

3.1.1 How navigators solve collision situations

The following text is intended to give the reader an idea of how collision avoidance is performed on a manually operated ship. The material in this section was obtained during an interview with Erlend Norstein, a consultant at DNV GL with navigation experience. A summary of this interview can be found in Appendix A.3.

The first step in avoiding collisions is to keep a proper lookout, which gives the OOW an overview of the traffic situation and makes it possible to detect potential obstacles. The main tools for keeping a proper lookout are visual monitoring and navigational equipment such as radar and ECDIS. The OOW can select ships to be tracked by the radar to display real-time information about speed, position and heading. AIS data can supplement the data from the radar tracking.

One of the most helpful tools for detecting a collision situation is alarms for Closest Point of Approach (CPA) and Time to Closest Point of Approach (TCPA). CPA is the position along the own-ship's path where the distance between the own-ship and an obstacle has its smallest value. TCPA is the time until CPA occurs. The navigation system uses information from the radar and AIS to estimate the CPA distance and TCPA using linear approximation. When the CPA distance and the TCPA value go below predefined limits, an alarm is given to the OOW. This indicates that a maneuver must be made to avoid a dangerous situation.

After a potential collision is detected, the OOW analyzes the situation and plans what maneuvers to perform. The COLREGs specify what maneuvers should be taken in different collision situations such as head-on, overtaking and crossing. When planning what maneuvers to take, it is also important to consider if this maneuver will make the ship end up in dangerous situations with any other ships in the vicinity.

For difficult collision situations, VHF radio is a useful tool for clarifying intentions. If another ship is displaying strange behavior, the OOW can ask the navigator on this ship about his intentions. VHF can be used to plan maneuvers, but this is not recommended since VHF communication often causes more confusion than it resolves, partly due to language barriers. Accidents have happened in the past because a ship used VHF to plan collision avoiding maneuvers with the wrong ship.

Ships are also equipped with other tools for communication, such as horn and lights. Different combinations of sound signals from the ship's horn can be used to communicate intentions. For instance, rule 34 in part D of the COLREGs specifies that two short sound signals indicate that "I am altering my course to port". The horn can also give warning signals. The lights on a ship are used to detect other ships in situations with poor visibility, and are also used to indicate a ship's orientation. Different colored lights are placed on different sides of the ship.

3.2 Statistics for accidents at sea

Modern navigation and communication equipment is extensively used onboard ships. Still, accidents at sea occur on a regular basis. Sormunen et al. (2016) have analyzed accident statistics for the Baltic Sea from the period 2006-2011. They found that the most common reasons for accidents were groundings and collisions. A total of 36% of the accidents were due to groundings and 34% were due to collisions.

The European Maritime Safety Agency (2019) gives a summary of more recent accident statistics from 2011-2018. In this period, a total of 25614 ships were involved in some type of accident. Figure 3.1 gives an overview of the most common types of accidents. More than half of these accidents were related to either contact, collision or grounding. In total, 26.2% of the accidents happened due to collisions. European Maritime Safety Agency (2019) Also found that collisions were the second most common cause of fatalities at sea.

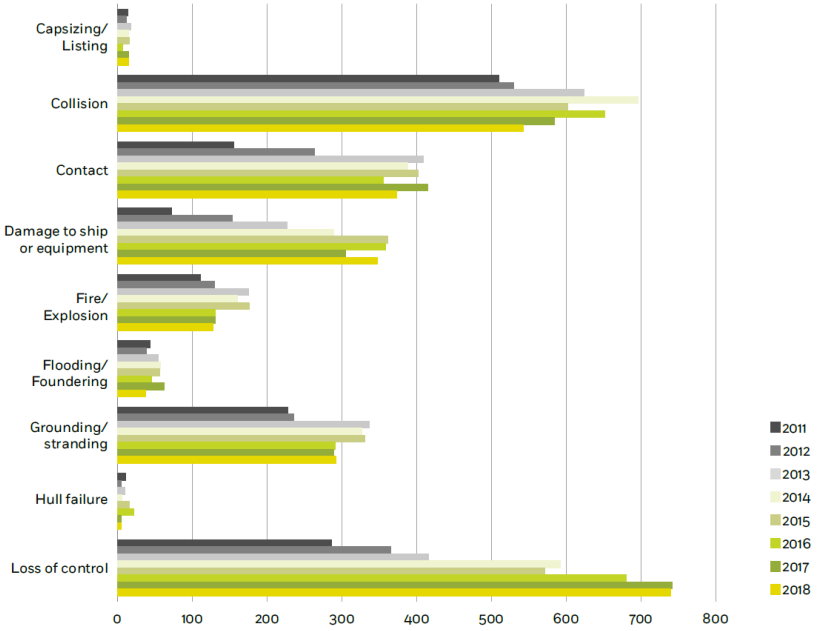

Figure 3.1: Overview of number of accidents at sea between 2011 and 2018. The figure is taken from the European Maritime Safety Agency (2019).

3.3 Collisions at sea

The accident statistics discussed in the previous section reveal that collisions and groundings are some of the most common types of accidents at sea. Unfortunately, such accidents often have disastrous consequences. A few days before Christmas in 1987, the overcrowded passenger ferry MS Doña Paz (see Figure 3.2) collided with an oil tanker in the Philippines, which led to the loss of over 4000 human lives (Mariano, 2017). In 1989, The Exxon Valdez oil tanker collided with the Bligh Reef in Alaska and caused one of the worst oil spills in history (Mambra, 2019). Both of these accidents were caused by human errors.

Figure 3.2: MS Doña Paz after the collision with an oil tanker. The figure is taken from Mariano (2017).

Statistics have shown that human errors are a common cause of accidents at sea. Allianz Global Corporate & Specialty (2017) estimates that human errors cause between 75% and 96% of all accidents in the shipping sector. When it comes to collisions, human errors also play a significant role. According to Liu and Wu (2003), over 90% of collisions are caused by human errors.

3.3.1 Common reasons for collisions

In this section, a discussion of the main reasons for collisions at sea will be given. The information is obtained primarily from accident reports and accident studies, and also from interviews conducted with experienced navigators from DNV GL as part of the specialization project Kjerstad (2019). Summaries of these interviews can be found in Appendices A.1 and A.2.

Improper lookout

The COLREGs require that every ship should keep a proper lookout for potential obstacles. Based on an investigation of all collisions and groundings in the United Kingdom between 1994 and 2003, the Marine Accident Investigation Branch (2004) found that two-thirds of the collisions were due to improper lookout. Another study by Liu and Wu (2003) also found that improper lookout was the main contributing factor to collisions.

According to Liu and Wu (2003), fatigue, lack of experience and big workloads are all contributing factors to improper lookout. In most cases, improper lookout causes actions to be taken too late or not at all. In 2017, a U.S. destroyer collided with a container ship because the crew members on the destroyer were too busy concentrating on another ship (The Japan Times, 2019). The crew on the U.S. destroyer did not notice the container ship before it was too late.

Fatigue

Fatigue is a common cause for collisions since it affects essential navigation skills such as decision making, reaction time and cognitive abilities (Strauch, 2015). In 2010, the oil tanker Eagle Otome collided with a towboat in a narrow waterway. The collision happened because the Officer Of the Watch (OOW) on the oil tanker turned too late. The OOW's error was due to decreased cognitive performance as a result of fatigue (Strauch, 2015).

Big workloads combined with bad working schedules have been shown to make crew members fatigued. A typical working schedule for the crew members is six hours on-duty followed by six hours off-duty. Research has shown that such a schedule leads to high levels of sleepiness, especially during night and morning watches (Eriksen et al., 2006). Also, it is common for the crew to work even longer shifts, sometimes up to 12-15 hours. There have been cases where collisions have happened due to the OOW falling asleep on-duty (Marine Insight, 2018).

Lack of training and experience

Ship-owners want to save as much money as possible. Therefore, the ship-owners often prefer to assign inexperienced people for watchkeeping duties (Lloyd, 2006). Experience and training play an essential role in avoiding collisions. From the 100 collision accident reports studied by Liu and Wu (2003), 54 collisions happened due to unsafe maneuvers performed by an inexperienced OOW. Inexperienced navigators might be willing to take larger risks and not keep a safe distance away from obstacles.

Lack of training for using the onboard equipment is also a common problem (Liu and Wu, 2003). Incorrect settings for the radar or misinterpreting the information from the radar can lead to dangerous situations. In 2015, a collision happened between the gas

carrier Clipper Quito and a fishing boat. The OOW on the fishing boat was supposed to give way, but did not detect the gas carrier due to improper use of the radar. In some cases, over-reliance on the technical equipment can be dangerous. For instance, if no ships appear on the radar or AIS, it might make the OOW falsely assume that no ships are nearby.

Poor weather conditions

Poor weather conditions can reduce visibility and therefore make it harder to detect obstacles. Reduced visibility due to fog is a common problem. Also, large waves and heavy winds can make the ship difficult to steer. In 2014, the small rig ship Petite lost control due to heavy wind and collided with the container ship MSC Charleston (The Maritime Executive, 2014). According to Wöhrn (2007), the effects of bad weather are often neglected by the OOW when steering a ship.

Not following the COLREGs

The COLREGs specify what maneuvers should be taken to avoid collisions. From the collisions investigated in a report by the International Maritime Organization (2017), several collisions occurred due to not following the COLREGs. In some cases, a ship turned the wrong direction, and in other cases, the turn started too late. In 2003 the bulk carriers M/V Fu Shan Hai and M/V Gdynia were in a crossing situation where M/V Gdynia was the give-way vessel. According to the COLREGs, M/V Gdynia should have made a turn to starboard, but this turn was taken too late and resulted in a collision (Danish Maritime Authority, 2003). Lack of experience and training is a contributing factor for not following the COLREGs. As mentioned in chapter 2.4, several navigators have problems with understanding the COLREGs, especially those with little navigational experience.

Equipment failure

Several collisions have happened in the past due to equipment failures. Having a well-functioning propulsion and navigation system is important for being able to steer the ship and detect obstacles. Some of the collisions investigated in the report by the International Maritime Organization (2017) happened because engine failure resulted in loss of control of the ship. Equipment failures can happen due to a lack of maintenance or lack of proper monitoring.

Bad communication

Ships can communicate via VHF radio and by using light and sound signals. In a collision situation, VHF radio can be used to communicate intended actions. However,

language barriers can make it difficult to agree on a solution. In 2017, the bulk carrier Huayang Endeavour collided with the oil tanker Seafrontier. Bad communication over VHF radio due to language issues made the ships unable to create a shared overtaking plan (Wingrove, 2018).

3.3.2 Scenarios that often lead to collisions

Based on the review of several collision accidents in the report by the International Maritime Organization (2017), several different types of scenarios lead to collisions. Collisions happen both in narrow fairways and out in the open sea, with varying weather conditions and with different types of ships involved. Even though the collision scenarios have differences, there is a common trend amongst them: the OOW was distracted in some way from keeping a proper lookout. Sometimes, collisions happen due to the OOW being too busy doing paperwork. Other times, the OOW had his attention towards a third ship that caused the OOW's ship to collide with a second ship. The distraction causes collision avoiding maneuvers to be performed too late or not at all.

In addition, situations where the obstacle ship made unexpected maneuvers that violated the COLREGs often lead to collision. In most of these cases, the OOW on the own-ship was not able to perform an evasive maneuver early enough to avoid a collision.

In summary, situations with many distractions and situations where obstacle ships behave unexpectedly are the most difficult for human navigators. This observation can be used to generate scenarios for testing collision avoidance algorithms.

Chapter 4

Simulator Development

This chapter will present the implementation details about the simulator that enables testing of the SBMPC and modified SBMPC collision avoidance algorithms. The work on the simulator started in the specialization project Kjerstad (2019). In this project, experiments were conducted to verify the performance of the simulator. The heading controller did have some problems with not being able to change the heading angle fast enough. Therefore, the controllers have been re-tuned in this master's thesis. In contrast to the specialization project, two different collision avoidance algorithms have been implemented as part of the simulator.

4.1 Simulator overview

The simulator is able to simulate the behavior of multiple ships, and consists of three different modules: the own-ship module, the passive obstacle ships module and the SBMPC obstacle ships module. Passive obstacle ships are obstacle ships without any collision avoidance system, and SBMPC obstacle ships have the same collision avoidance system as the own-ship. MATLAB and Simulink have been used for the implementation of these modules. After a simulation is completed, the log files containing all simulated states are used by an evaluation tool to evaluate the own-ship module's collision avoidance performance. An overview of the different modules and the connection between them can be seen in Figure 4.1.

The rest of this chapter will explain how the modules have been implemented. However, implementation details about the collision avoidance systems and the evaluation tool will be given in the upcoming chapters 5 and 6, respectively.

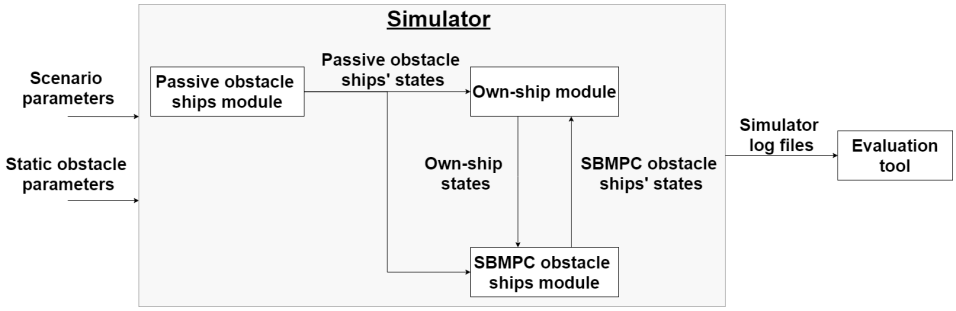

Figure 4.1: Overview of the different modules in the developed simulator.

4.2 Own-ship module

The own-ship module simulates the behavior of the own-ship by using the 3 DOF equations of motion from chapter 2.2. Figure 4.2 gives an overview of the different components in the own-ship module. The LOS guidance system in the leftmost part of the figure computes the reference velocity and reference heading angle necessary to make the own-ship follow the nominal straight path between a set of waypoints. Two different reference models convert reference velocity and heading angle into the desired velocity and heading angle. Next, a feedback linearizing controller makes the own-ship follow the desired velocity and heading. For simplicity, it is assumed that the own-ship will not be affected by environmental disturbances.

The collision avoidance algorithm is implemented as part of the own-ship module. In this thesis, two different collision avoidance algorithms will be used: the original SBMPC method proposed by Johansen et al. (2016) as well as a modified version of the SBMPC where data about intentions are included. The collision avoidance block in Figure 4.2 computes a propulsion command and a heading angle offset, making the vessel deviate from her nominal path to avoid collisions.

The choice of ship model and implementation of reference models, control and guidance systems for the own-ship module will be presented next. The implementation details of the two collision avoidance algorithms will be given in chapter 5.

4.2.1 3 DOF ship model

The own-ship is modeled as a 116-meter long Platform Supply Vessel (PSV). The 3 degrees of freedom model from chapter 2.2 is used, which only captures the horizontal plane movement of the ship. All ship parameters used are shown in Table 4.1. These parameters are provided by DNV GL, and are similar to the parameters used in the master's thesis by Minne (2017).

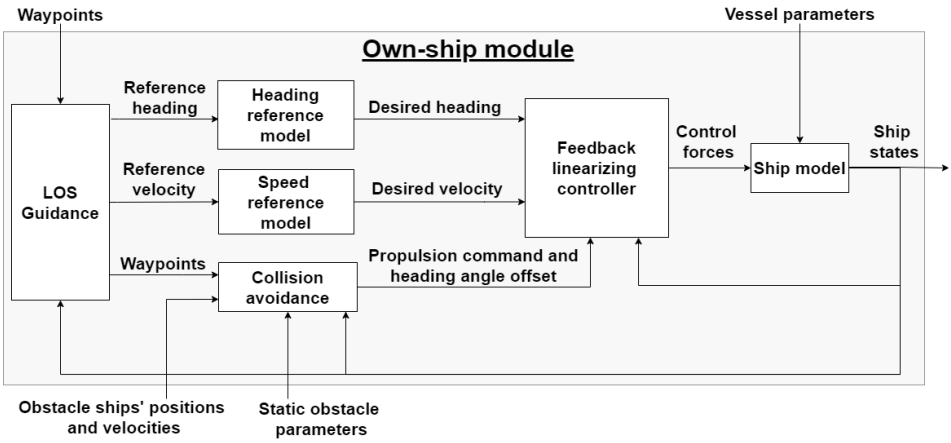

Figure 4.2: Different components of the own-ship module.

Parameter	Value	Unit
m	15524000	kg
Length	116	m
Width	25	m
I_z	$1.0437 \cdot 10^{10}$	$kg \cdot m^2$
x_g	-3.7	m
$X_{\dot{u}}$	-979290	kg
$Y_{\dot{v}}$	-10727527	kg
$Y_{\dot{r}}$	-11357800	$kg \cdot m$
$N_{\dot{r}}$	$-6.2422 \cdot 10^9$	kg/m^2
X_u	-1650	kg/s^2
Y_v	-1050060	kg/m^2
Y_r	0	$kg \cdot m/s$
N_v	0	$kg \cdot m/s$
N_r	-2452793600	$kg \cdot m^2/s$
T_{surge}	10000	s
T_{sway}	2500	s
T_{yaw}	2550	s

Table 4.1: Model parameters for the own-ship PSV.

4.2.2 LOS guidance

The lookahead-based LOS steering law from chapter 2.1.2 is implemented to make the own-ship follow the nominal straight-line path between waypoints. The steering law is repeated here for convenience.

$$\chi_d = \text{atan2}(y_{k+1} - y_k, x_{k+1} - x_k) + \text{atan}\left(\frac{-e}{\Delta}\right) \tag{4.1}$$

Equation (4.1) calculates the desired course angle χ_d necessary to make the own-ship follow the straight path between the waypoints $[x_k, y_k]^T$ and $[x_{k+1}, y_{k+1}]^T$. The closest distance between the own-ship and the path is given by the cross-track error e, and $\Delta = 1000$ m is the lookahead distance. Since this guidance law computes the desired course angle χ_d, a conversion between course angle χ and heading angle ψ is necessary. Fossen (2011) defines the course angle as $\chi = \psi + \xi$, where ξ is the sideslip angle. Because environmental disturbances are not taken into account, the sideslip angle ξ is assumed to be zero.

The switching mechanism from chapter 2.1.2 is implemented by using the condition in equation (4.2).

$$(x_{k+1} - x(t))^2 + (y_{k+1} - y(t))^2 \leq R^2 \tag{4.2}$$

When the distance between the own-ship in position $[x(t), y(t)]$ and the target waypoint in position $[x_{k+1}, y_{k+1}]$ is less than $R = 300$ m, the active waypoints will switch. Thus, when the own-ship is 300 m away from waypoint P_{k+1}, the own-ship will start to move towards the next waypoint P_{k+2}.

4.2.3 Reference models

The simulator uses reference models to compute the desired values for velocity and heading angle. Figure 4.3 illustrates the principle behind the reference models. The guidance system computes the reference heading angle necessary to make the own-ship follow the nominal path. In this example, the reference heading is a step signal. Due to slow dynamics, the own-ship is not able to change her heading angle fast enough to follow the reference heading signal. Therefore, a reference model computes a more smooth, desired heading that the own-ship can follow. The rest of this chapter will refer to reference signals as the output of the guidance system and the desired signals as the output of the reference models.

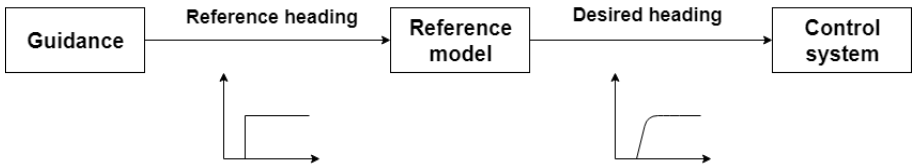

Figure 4.3: The principle behind the use of reference models. The guidance system provides the reference heading angle as a step signal and the reference model computes the desired heading angle by smoothing the input signal.

Velocity reference model

The velocity reference model computes the desired velocity vector $\boldsymbol{\nu}_d = [u_d, v_d, r_d]^T$. Using the notation from chapter 2.2, the desired speed in x- and y-direction is denoted as u_d and v_d while r_d is the desired yaw rate. The subscript d denotes a desired value.

A second-order low pass filter is used to implement the velocity reference model. This will avoid step signals in both $\boldsymbol{\nu}_d$ and $\dot{\boldsymbol{\nu}}_d$. The equation for the velocity reference model is given by equation (4.3) from Fossen (2011).

$$\dot{\boldsymbol{x}}_{\nu,d} = \boldsymbol{A}_\nu \boldsymbol{x}_{\nu,d} + \boldsymbol{B}_\nu \boldsymbol{\nu}_{\text{ref}} \tag{4.3}$$

Here, $\boldsymbol{x}_{\nu,d} = [\boldsymbol{\nu}_d, \dot{\boldsymbol{\nu}}_d]^T$ and $\boldsymbol{\nu}_{\text{ref}} = [u_{\text{ref}}, v_{\text{ref}}, r_{\text{ref}}]^T$. Subscript ref is used to denote a reference value. In the implementation, both v_{ref} and r_{ref} are set to zero. Expression for the matrices $\boldsymbol{A}_\nu$ and $\boldsymbol{B}_\nu$ are given by equations (4.4a) and (4.4b) below.

$$\boldsymbol{A}_\nu = \begin{bmatrix} \mathbf{0} & \boldsymbol{I} \\ -\boldsymbol{\Omega}^2 & -2\boldsymbol{\Delta}\boldsymbol{\Omega} \end{bmatrix} \tag{4.4a}$$

$$\boldsymbol{B}_\nu = \begin{bmatrix} \mathbf{0} \\ \boldsymbol{\Omega}^2 \end{bmatrix} \tag{4.4b}$$

The symbol $\mathbf{0}$ represents a 3x3 zero matrix and $\boldsymbol{I}$ is the 3x3 identity matrix. $\boldsymbol{\Delta}$ and $\boldsymbol{\Omega}$ are two symmetric and positive definite matrices, defined as in equations (4.5a) and (4.5b).

$$\boldsymbol{\Delta} = \begin{bmatrix} \zeta_1 & 0 & 0 \\ 0 & \zeta_2 & 0 \\ 0 & 0 & \zeta_3 \end{bmatrix} \tag{4.5a}$$

$$\boldsymbol{\Omega} = \begin{bmatrix} \omega_{n1} & 0 & 0 \\ 0 & \omega_{n2} & 0 \\ 0 & 0 & \omega_{n3} \end{bmatrix} \tag{4.5b}$$

The symbols ζ and ω_n denote relative damping ratio and natural frequency, whose values are shown in Table 4.2.

Parameter	Value
ζ_1	1
ζ_2	1
ζ_3	1
ω_{n1}	0.035
ω_{n2}	0.14
ω_{n3}	0.19

Table 4.2: Parameter values for relative damping ratios and natural frequencies.

Heading angle reference model

The heading angle reference model computes the desired heading angle ψ_d for the own-ship. It is implemented as a third-order lowpass filter, which avoids step signals in ψ_d, $\dot{\psi}_d$ and $\ddot{\psi}_d$. The heading reference model is given by equation (4.6) from Fossen (2011).

$$\dot{\boldsymbol{x}}_{\psi,d} = \boldsymbol{A}_\psi \boldsymbol{x}_{\psi,d} + \boldsymbol{B}_\psi \boldsymbol{r}_\psi \tag{4.6}$$

Here, $\boldsymbol{x}_{\psi,d} = [\boldsymbol{\eta}_d, \dot{\boldsymbol{\eta}}_d, \ddot{\boldsymbol{\eta}}_d]^T$ and $\boldsymbol{r}_\psi = [0, 0, \psi_{\text{ref}}]^T$. The desired heading angle ψ_d is extracted from the third element of $\boldsymbol{\eta}_d = [x_d, y_d, \psi_d]^T$. The expressions for the matrices $\boldsymbol{A}_\psi$ and $\boldsymbol{B}_\psi$ are given by equations (4.7a) and (4.7b).

$$\boldsymbol{A}_\psi = \begin{bmatrix} \boldsymbol{0} & \boldsymbol{I} & \boldsymbol{0} \\ \boldsymbol{0} & \boldsymbol{0} & \boldsymbol{I} \\ -\boldsymbol{\Omega}^3 & -(2\boldsymbol{\Delta} + \boldsymbol{I})\boldsymbol{\Omega}^2 & -(2\boldsymbol{\Delta} + \boldsymbol{I})\boldsymbol{\Omega} \end{bmatrix} \tag{4.7a}$$

$$\boldsymbol{B}_\psi = \begin{bmatrix} \boldsymbol{0} \\ \boldsymbol{0} \\ \boldsymbol{\Omega}^2 \end{bmatrix} \tag{4.7b}$$

The matrices $\boldsymbol{\Delta}$ and $\boldsymbol{\Omega}$ are the same as used in the velocity reference model, whose expressions are given by equations (4.4a) and (4.4b).

4.2.4 Control system

The own-ship module uses two different control systems: a speed controller and a heading controller. These control systems are responsible for making the own-ship follow the desired heading angle ψ_d and the desired speed $\boldsymbol{\nu}_d$ computed by the two reference models. Following ψ_d and $\boldsymbol{\nu}_d$ will make own-ship able to follow the nominal path defined by her waypoints.

Speed controller

The speed controller is implemented as a feedback linearizing controller. The details about this control law can be found in Fossen (2011). In short, the idea behind a feedback linearizing controller is to design the controller such that a nonlinear system is transformed into a linear system. The starting point is the equation of motion for the own-ship, which is repeated here for convenience.

$$\boldsymbol{M}\dot{\boldsymbol{\nu}} + \boldsymbol{n}(\boldsymbol{\nu}) = \boldsymbol{\tau} \tag{4.8}$$

Here, $\boldsymbol{n}(\boldsymbol{\nu}) = \boldsymbol{C}_{RB}(\boldsymbol{\nu})\boldsymbol{\nu} + \boldsymbol{C}_A(\boldsymbol{\nu})\boldsymbol{\nu} + \boldsymbol{D}\boldsymbol{\nu}$. An explanation of the different terms can be found in chapter 2.2. The force vector $\boldsymbol{\tau}$ in the feedback linearizing controller is chosen to be equal to the expression in equation (4.9).

$$\boldsymbol{\tau} = \boldsymbol{M}\boldsymbol{a}^b + \boldsymbol{n}(\boldsymbol{\nu}) \tag{4.9}$$

The symbol $\boldsymbol{a}^b$ denotes the commanded acceleration. By substituting the expression for $\boldsymbol{\tau}$ in equation (4.9) in for $\boldsymbol{\tau}$ in equation (4.8), the resulting equation of motion is given by equation (4.10).

$$\boldsymbol{M}\dot{\boldsymbol{\nu}} + \boldsymbol{n}(\boldsymbol{\nu}) = \boldsymbol{M}\boldsymbol{a}^b + \boldsymbol{n}(\boldsymbol{\nu}) \tag{4.10}$$

After simplifying equation (4.10), the own-ship dynamics can be expressed as the linear equation (4.11).

$$\dot{\boldsymbol{\nu}} = \boldsymbol{a}^b \tag{4.11}$$

The commanded acceleration $\boldsymbol{a}^b$ can be chosen as a simple proportional controller, as shown in equation (4.12).

$$\boldsymbol{a}^b = -\boldsymbol{K}_p(\boldsymbol{\nu} - \boldsymbol{\nu}_d) \tag{4.12}$$

Here, $\boldsymbol{\nu} = [u, v, r]^T$ is the speed vector, $\boldsymbol{\nu}_d = [u_d, v_d, r_d]^T$ is the desired speed vector and $\boldsymbol{K}_p$ is a design matrix, given by equation (4.13).

$$\boldsymbol{K}_p = \begin{bmatrix} k_{p,1} & 0 & 0 \\ 0 & k_{p,2} & 0 \\ 0 & 0 & k_{p,3} \end{bmatrix} \tag{4.13}$$

The speed controller gains $k_{p,1}$, $k_{p,2}$ and $k_{p,3}$ can be found in table Table 4.3.

To achieve a more realistic response, the output force vector $\boldsymbol{\tau}$ of the speed controller has been saturated. The speed controller can give a maximum force of 450 kN in the x-direction and 120 kN in the y-direction. Also, the maximum yaw torque is set to $35 \cdot 10^6$ Nm.

Heading controller

Inspired by Minne (2017), the heading controller is implemented as the proportional controller in equation (4.14). This controller calculates the desired yaw rate r_d to be used in the feedback linearizing speed controller.

$$r_d = k_{p,\psi}(\psi_d - \psi) \tag{4.14}$$

The controller gain is chosen to be $k_{p,\psi} = 0.054$.

Parameter	Value
$k_{p,1}$	0.1
$k_{p,2}$	0.1
$k_{p,3}$	0.1
$k_{p,\psi}$	0.054

Table 4.3: Parameters for the heading and velocity controllers.

4.2.5 Tuning of the control system

The speed and heading controllers were implemented as part of the specialization project Kjerstad (2019), but the heading controller has been re-tuned in this thesis to improve its performance. Tuning happened without a collision avoidance system implemented.

Heading controller tuning

In the specialization project, a maneuverability test of a 6 DOF PSV model was performed in a simulator at the DNV GL office in Trondheim. The maneuvering test showed that $45°$ and $180°$ turns could be completed in 60 and 120 seconds, respectively. However, the implemented 3 DOF PSV in the specialization project made a $180°$ turn in 250 seconds.

In this master's thesis, some parameters have been changed compared to the specialization project as an attempt to improve the performance. The heading controller gain $k_{p,\psi}$ has been increased from 0.04 to 0.054, making the heading angle converge faster towards the desired heading angle. Also, the saturation limit of yaw torque was increased from $20 \cdot 10^6$ Nm to $35 \cdot 10^6$ Nm. The last change made compared to the specialization project implementation was to increase the time constant T_{yaw} from 1700 s to 2550 s.

After re-tuning, the resulting heading and yaw torque response from a $45°$ step signal in reference heading can be seen in Figures 4.4a and 4.4b, which shows that a $45°$ turn will take approximately 75 seconds.

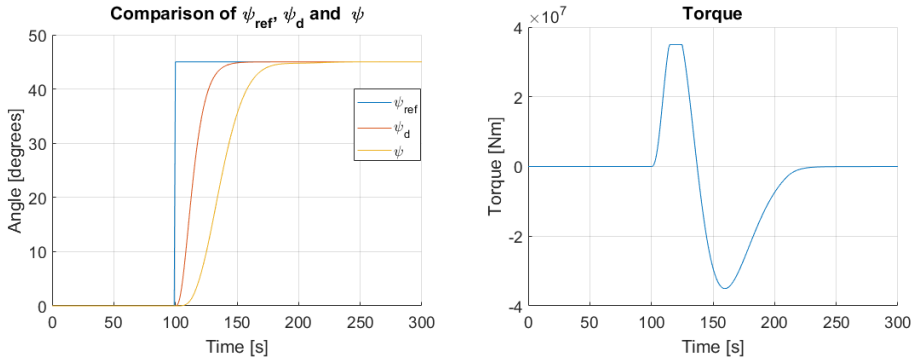

(a) Heading response

(b) Yaw torque

Figure 4.4: Simulation results for the heading controller with a step reference of $45°$.

A similar test was performed with a $180°$ step reference for heading. The simulation results in Figures 4.5a and 4.5b show that a $180°$ turn will take approximately 130 seconds.

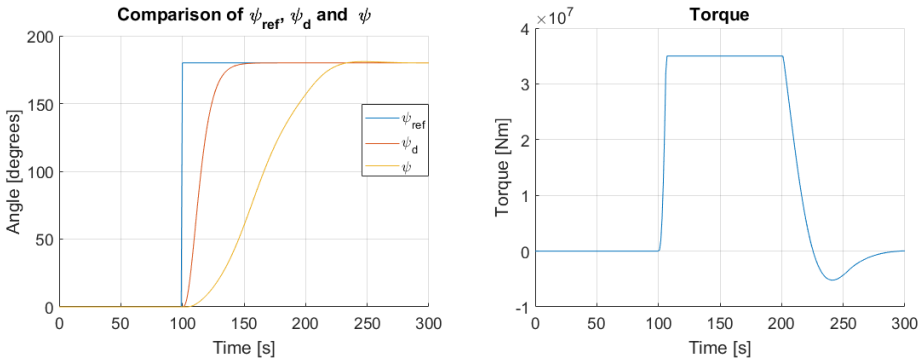

(a) Heading response

(b) Yaw torque

Figure 4.5: Simulation results for heading controller with a step reference of $180°$.

Overall, the simulation results obtained are similar to the results from the maneuverability test. However, Figure 4.4b shows that the behavior is not optimal in terms of efficiency. The yaw torque first saturates at $35 \cdot 10^6$ Nm, before it almost saturates at $-35 \cdot 10^6$ Nm to decelerate the yaw rotation. In practice, this would result in an excessive use of actuators and give a large fuel consumption. However, the primary concern when tuning has been to achieve a realistic response in terms of time used. It should also be noted that the time it takes for the rudders to physically change their angles have not been considered in the implementation.

Speed controller tuning

In the specialization project Kjerstad (2019), the speed controller was shown to give acceptable performance. Therefore, the same control parameters are used in this thesis.

4.3 Obstacle ships

The simulator has functionality for including one or more obstacle ships in the simulation. Two different types of obstacle ships will be used: passive obstacle ships without any collision avoidance system and SBMPC obstacle ships with a collision avoidance algorithm implemented.

The passive obstacle ships will only follow the straight path between waypoints. On the other hand, SBMPC obstacle ships are assumed to be autonomous with a collision avoidance algorithm implemented. Either the original SBMPC algorithm or the modified SBMPC algorithm is used on the SBMPC obstacle ships.

Both types of obstacle ships are implemented as PSVs using the exact same ship model, reference models, control systems and LOS law as the own-ship module in section 4.2. A separate list of waypoints for each obstacle ship determines where the obstacle ships will travel.

Accurate real-time data about position, speed and heading angle for all obstacle ships are assumed to be directly available to the own-ship through AIS. To detect non-AIS obstacle ships, the own-ship would need a separate tracking system. However, this is outside the scope of this thesis. Data about intentions will also be transmitted from obstacle ships to the own-ship.

4.4 Static obstacles

In the master's thesis by Otterholm (2019), an algorithm for extracting map data from electronic navigational charts is developed. A more simplistic approach is used in the developed simulator to include static obstacles.

There are two types of static obstacles that represent environmental constraints such as shorelines, shallow water zones and archipelago. The two different types of static obstacles are called boundary obstacle and circle obstacle. A collision with either of these static obstacle results in a ship grounding. An illustration of these two types of static obstacles is shown in Figure 4.6. The boundary obstacle is defined by a start and end point, while the circle obstacle is defined by the position of the circle's center and its radius.

The boundary obstacle line has two different sides. One is referred to as the legal side, while the other is called the illegal side. It is assumed that ships will always start on the legal side of the boundary obstacle. A grounding has occurred if a ship's bow crosses the boundary line and enters the illegal side. Similarly, a grounding occurs if a ship's bow crosses the edge of the circle obstacle.

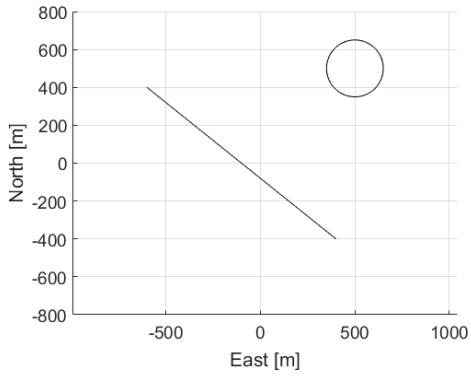

Figure 4.6: Illustration of a circle and boundary obstacle in the north-east coordinate system.

Chapter 5

Collision Avoidance Systems

The own-ship implementation discussed in the previous chapter contains a separate collision avoidance module. This chapter contains the implementation details of two different collision avoidance algorithms used in the simulator: the original SBMPC algorithm by Johansen et al. (2016) and a modified version of this algorithm, called the modified SBMPC, where data about intentions are included. These are both short-term collision avoidance algorithms responsible for immediate collision avoidance with dynamic and static obstacles. In chapter 7, the performance of these two different algorithms will be compared to determine if the inclusion of intention data can improve collision avoidance performance.

This chapter starts with a description of the implementation details of the original SBMPC algorithm, before the modified SBMPC is presented in section 5.2. A discussion of which intention data is used as well as a recommendation for a communication method to exchange intention data will be given.

5.1 Simulation-Based Model Predictive Control

Model Predictive Control (MPC) has previously been used for collision avoidance in several different areas. Bousson (2008) used the MPC principle in an algorithm to avoid collisions between aircraft, and Liu et al. (2013) used an MPC-based method to avoid collisions between unmanned ground robots. The Simulation-Based Model Predictive Control (SBMPC) algorithm is a short-term collision avoidance algorithm developed by Johansen et al. (2016). It is one of the first uses of MPC for ship collision avoidance with COLREGs compliance. According to Chiang and Tapia (2018), SBMPC is one of the current state-of-the-art methods for collision avoidance.

The SBMPC algorithm can find a collision-free and COLREGs compliant path. An explanation of how the algorithm works, in addition to implementation details, will be presented below. The SBMPC implementation in this thesis is based on the work by Johansen et al. (2016). With very few exceptions, Johansen et al. (2016) do not mention what parameter values are used. Therefore, the tuning procedure described in section 5.1.5 has been used to find appropriate parameter values.

5.1.1 System overview and scenario simulation

Figure 5.1 gives an overview of how the collision avoidance system is integrated with the GNC system in a ship model. The SBMPC method uses a modular architecture where the collision avoidance module is separated from the guidance and control system. Based on LOS guidance, the guidance system calculates the desired speed and heading angle necessary to make the own-ship follow the nominal path between a set of predefined waypoints. The collision avoidance module utilizes data about the own-ship's state and the predicted positions and velocities of the obstacle ships. This information is used to calculate a propulsion command and a heading angle offset. These two computed signals, called the control behavior, are sent to the control system to make the ship deviate from the nominal path and avoid a collision.

The positions and velocities of all obstacle ships are available through AIS or another tracking system. Also, a map provides data about the position of static obstacles. Real-time measurements of the own-ship's position, velocity and heading angle are also available. Environmental disturbances have been neglected in the implementation for this thesis, but are briefly discussed in the paper by Johansen et al. (2016).

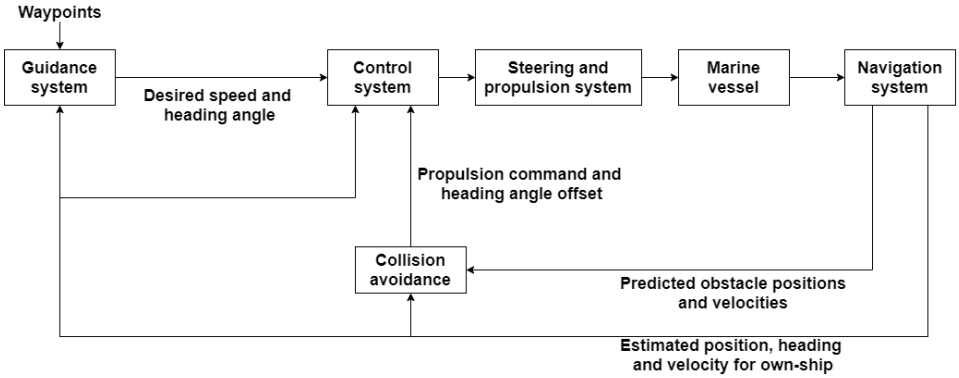

Figure 5.1: Overview of the components in a ship model. A separate collision avoidance module computes a propulsion command and a heading angle offset, referred to as the control behavior.

The SBMPC algorithm simulates several scenarios to find the best control behavior. Every 10th second, 39 different scenarios are simulated. Each scenario consists of a unique control behavior and the predicted trajectory of the own-ship resulting from this control

behavior. A scenario also consists of the predicted trajectories of all obstacle ships. The trajectories for the own-ship and obstacle ships are estimated for $T = 600$ seconds into the future. T is called the prediction horizon length.

Based on factors such as the risk of collision, COLREGs compliance, risk of grounding and deviation from the nominal path, a cost function calculates the hazard for each scenario. The scenario associated with the lowest hazard is chosen. The control behavior in the chosen scenario will be supplied to the own-ship for the next ten seconds, before a new control behavior is selected.

The scenario simulation performed by the SBMPC algorithm can be illustrated with a simple example with only three different scenarios, as shown in Figure 5.2. The green own-ship's nominal path is the straight line towards the red obstacle ship. Figure 5.2a shows the predicted trajectories of the own-ship at time t_0 for three different control behaviors: heading offsets $-30°$, $0°$ and $30°$. The propulsion command is equal in the three scenarios. Each simulation scenario contains a different control behavior. Even though the heading angle offsets stay constant during the scenario, the own-ship's true heading angle slowly converges to a heading angle of zero since the LOS guidance forces the own-ship to follow the nominal path. The predicted trajectory of the obstacle ship, shown as a black dotted line, will remain the same in all three scenarios.

Since this is a head-on situation, the control behavior with a heading offset of $30°$ is chosen for execution because it complies with the COLREGS and gives the lowest hazard. After 10 seconds, in Figure 5.2b, the three scenarios are simulated once more with the same control behaviors, and a new control behavior is chosen for execution.

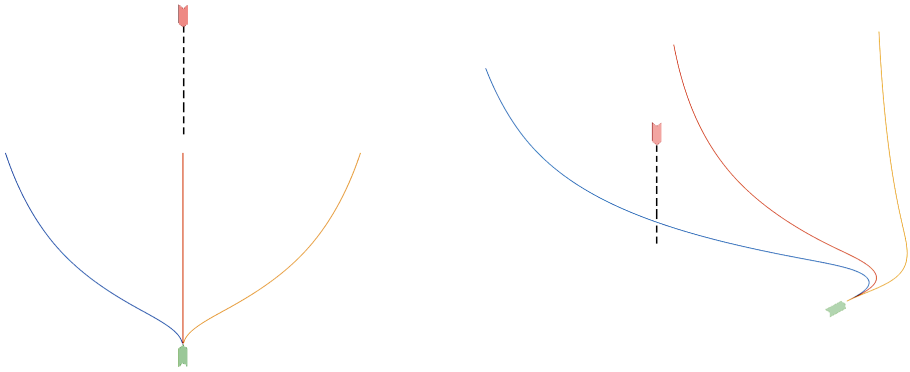

(a) Time t_0 **(b)** Time $t_0 + 10$ s

Figure 5.2: Predicted trajectories of the own-ship at t_0 and $t_0 + 10$ s for three different control behaviors.

In Johansen et al. (2016), scenarios are simulated every 5th seconds. In this thesis, the scenarios are simulated every 10th seconds to decrease the simulation time.

5.1.2 Control behaviors

A control behavior consists of a heading angle offset ψ_{ca} and a propulsion command Pr. Johansen et al. (2016) recommend a minimum set of alternative control behaviors to be:

- Heading angle offset ψ_{ca} as -90°, -75°, -60°, -45°, -30°, -15°, 0°, 15°, 30°, 45°, 60°, 75° or 90°.
- Propulsion command Pr as 1 (Keep speed), 0.5 (Slow forward), 0 (Stop) or -1 (Full reverse).

Using the recommended set of control behaviors will give $13 \cdot 4 = 52$ different scenarios. It would be desirable to have as many control behaviors as possible, but there is a trade-off between the number of scenarios and computational complexity. The implemented algorithm in this thesis uses the recommended set of heading angle offsets, but only uses the propulsion commands $Pr = \{1, 0.5, 0\}$. This gives $13 \cdot 3 = 39$ different scenarios.

5.1.3 Prediction of own-ship and obstacle ship trajectories

The SBMPC algorithm uses the 3 DOF ship model from chapter 2.2 and the control system from chapter 4 to predict the future position and heading angle of the own-ship at each time step in the prediction horizon. To include the effects of the chosen control behavior in the trajectory prediction, the heading controller makes the ship follow the heading command $\psi_c = \psi_d + \psi_{\text{ca}}$. Here, ψ_d is the desired heading angle computed by the guidance system and ψ_{ca} is the heading angle offset from the SBMPC algorithm. The speed controller makes the ship follow the speed command $u_c = u_d \cdot Pr$.

Obstacle ships are assumed to follow a straight path with a constant heading angle and constant speed throughout the prediction horizon. Therefore, the future position of obstacle ships can be predicted by using equations (5.1a) and (5.1b) from Johansen et al. (2016).

$$\hat{x}_i(t) = x_i(t_0) + \hat{U}_i(t_0) \cdot \cos\left(\psi_i(t_0)\right) \cdot (t - t_0) \tag{5.1a}$$

$$\hat{y}_i(t) = y_i(t_0) + \hat{U}_i(t_0) \cdot \sin\left(\psi_i(t_0)\right) \cdot (t - t_0) \tag{5.1b}$$

The time when the prediction horizon starts is denoted by t_0. Estimated x- and y-position of obstacle ship i after t seconds into the prediction horizon are $\hat{x}_i(t)$ and $\hat{y}_i(t)$. ψ_i is obstacle ship i's heading angle. The estimated speed is denoted as $\hat{U}(t_0)$ and is found from equation (5.2).

$$\hat{U}(t_0) = \sqrt{u_i(t_0)^2 + v_i(t_0)^2} \tag{5.2}$$

Here, u_i and v_i are the speeds in x- and y-direction for obstacle ship i.

5.1.4 Hazard computation

The control behavior for the own-ship is chosen by calculating the hazard of each scenario, and selecting the control behavior from the scenario with the smallest hazard. Equation (5.3) from Johansen et al. (2016) is used to calculate the hazard.

$$\mathcal{H}^k(t_0) = \max_i \max_{t \in D(t_0)} \left\{ \mathcal{C}_i^k(t) \mathcal{R}_i^k(t) + \kappa_i \mu_i^k(t) \right\} + f^k(Pr^k, \psi_{\text{ca}}^k) + g^k \tag{5.3}$$

The total hazard $\mathcal{H}^k(t_0)$ in scenario k is computed at time t_0. This hazard is found by using the maximum-operator to maximize over each obstacle ship i and also maximizing over each time step $t \in D(t_0)$. The set of time steps is $D(t_0) = \{t_0, t_0 + T_s, t_0 + 2T_s, ..., t_0 + T\}$ where $T_s = 0.5$ s is the discretization interval and $T = 600$ s is the prediction horizon length. The hazard computation depends on several factors:

- COLREGs compliance with obstacle i in scenario k, $\kappa_i \mu_i^k(t)$
- Cost of collision with obstacle i in scenario k, $\mathcal{C}_i^k(t)$
- Risk of collision with obstacle i in scenario k, $\mathcal{R}_i^k(t)$
- Penalty for deviation from nominal path and speed in scenario k, $f^k(Pr^k, \psi_{\text{ca}}^k)$
- Risk of grounding in scenario k, g^k

The remainder of this section is dedicated to the explanation of the different terms in the hazard computation.

COLREGs compliance

COLREGs compliance is included in the hazard computation to penalize maneuvers in violation with COLREGs rules 8 and 13-16. A binary variable $\mu_i^k(t)$ indicates a violation with the COLREGs. Like Johansen et al. (2016), the binary variables *CLOSE*, *OVERTAKEN*, *STARBOARD*, *HEAD-ON* and *CROSSED* are used for calculating $\mu_i^k(t)$.

Figure 5.3 shows the vectors used to calculate these binary variables. A green and red dot represent the position of the own-ship, $[x^k(t), y^k(t)]^T$, and obstacle ship i, $[x_i(t), y_i(t)]^T$, at time t in scenario k. The dashed green and red lines represent the predicted trajectories for the own-ship and obstacle ship, respectively. Also, the velocity vectors for the own-ship and obstacle ship i in scenario k are denoted by $\boldsymbol{V}_0^k(t)$ and $\boldsymbol{V}_i(t)$, respectively. These vectors are defined as in equations (5.4a) and (5.4b).

$$\boldsymbol{V}_0^k(t) = [u^k(t) \cdot \cos \psi^k(t), v^k(t) \cdot \sin \psi^k(t)]^T \tag{5.4a}$$

$$\boldsymbol{V}_i(t) = [u_i(t) \cdot \cos \psi_i, v_i(t) \cdot \cos \psi_i]^T \tag{5.4b}$$

The own-ship's and obstacle ship i's heading angles at time t in scenario k are $\psi^k(t)$ and ψ_i. The obstacle ship will have the same speed and heading in all scenarios.

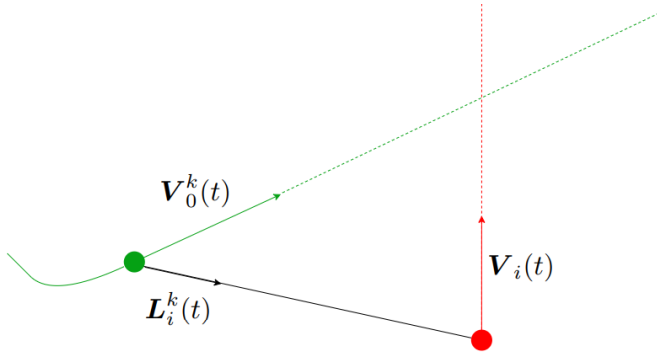

Figure 5.3: Vectors used for determining COLREGs compliance. $\boldsymbol{V}_0^k(t)$ is the own-ships' velocity vector and $\boldsymbol{V}_i(t)$ is the obstacle ship's velocity vector. $\boldsymbol{L}_i^k(t)$ is a unit vector in LOS direction from the own-ship to the obstacle ship.

In Figure 5.3, $\boldsymbol{L}_i^k(t)$ is a unit vector in the LOS direction from the own-ship to obstacle ship i in scenario k. This vector is found from equation (5.5).

$$\boldsymbol{L}_i^k(t) = \frac{[x_i(t) - x^k(t), y_i(t) - y^k(t)]^T}{|[x_i(t) - x^k(t), y_i(t) - y^k(t)]^T|} \tag{5.5}$$

The own-ship is *CLOSE* to obstacle ship i at time t in scenario k if the ships are closer than a predefined distance d_i^{cl}. The *CLOSE* variable becomes true if the condition in equation (5.6) is satisfied.

$$d_{0,i}^k(t) \leq d_i^{cl} \tag{5.6}$$

Here, $d_{0,i}^k(t)$ is the distance between the own-ship and obstacle ship i at time t in scenario k and d_i^{cl} is the distance where COLREGs start to apply. Equation (5.7) is used to find $d_{0,i}^k(t)$, and $d_i^{cl} = 2500$ m for all obstacle ships. If the own-ship is further away from obstacle ship i than d_i^{cl}, then COLREGs do not have to be considered.

$$d_{0,i}^k(t) = \sqrt{(x^k(t) - x_i(t))^2 + (y^k(t) - y_i(t))^2} \tag{5.7}$$

The own-ship is *OVERTAKEN* by obstacle ship i if the obstacle ship has a higher speed, the ships are *CLOSE* and the condition in equation (5.8) is true.

$$\boldsymbol{V}_0^k(t) \cdot \boldsymbol{V}_i(t) > \cos(\phi_{\text{overtaken}})|\boldsymbol{V}_0^k(t)||\boldsymbol{V}_i(t)| \tag{5.8}$$

The parameter $\phi_{\text{overtaken}} = 68.5°$ is tunable.

The obstacle ship i is *STARBOARD* of the own-ship at time t in scenario k if the angle of the vector $\boldsymbol{L}_i^k(t)$ is larger than the own-ship's heading angle. The angle of $\boldsymbol{L}_i^k(t)$ is found from equation (5.9).

$$\angle \boldsymbol{L}_i^k(t) = \text{atan2}\left(y_i(t) - y^k(t), x_i(t) - x^k(t)\right) \tag{5.9}$$

The obstacle ship i is *HEAD-ON* relative to the own-ship at time t in scenario k if the ships are *CLOSE*, the obstacle ship's speed is nonzero and the conditions in equations (5.10a) and (5.10b) are true.

$$\boldsymbol{V}_0^k(t) \cdot \boldsymbol{V}_i(t) < -\cos(\phi_{\text{head-on}})|\boldsymbol{V}_0^k(t)||\boldsymbol{V}_i(t)| \tag{5.10a}$$

$$\boldsymbol{V}_0^k(t) \cdot \boldsymbol{L}_i^k(t) > \cos(\phi_{\text{ahead}})|\boldsymbol{V}_0^k(t)| \tag{5.10b}$$

Here, $\phi_{\text{head-on}} = 22.5°$ and $\phi_{\text{ahead}} = 20°$ are tunable parameter.

The obstacle ship i and the own-ship are *CROSSED*, meaning that ships are in a crossing situation, at time t in scenario k if the ships are *CLOSE* and the condition in equation (5.11) is true.

$$\boldsymbol{V}_0^k(t) \cdot \boldsymbol{V}_i(t) < \cos(\phi_{\text{crossed}})|\boldsymbol{V}_0^k(t)||\boldsymbol{V}_i(t)| \tag{5.11}$$

In the implementation, the tunable parameter $\phi_{\text{crossed}} = 68.5°$.

The binary variable $\mu_i^k(t) \in \{0, 1\}$ is used to find a violation of rules 13 (overtaking), 14 (head-on) and 15 (crossing) of the COLREGs with obstacle i at time t in scenario k. A value of 1 indicates a violation of the COLREGs. To calculate $\mu_i^k(t)$, equation (5.12) is used. The parameter $\kappa_i = 25$ for all obstacle ships i is used to scale $\mu_i^k(t)$ in the total hazard computation in equation (5.3).

$$\mu_i^k(t) = RULE14 \text{ or } RULE15 \tag{5.12}$$

$RULE14$ and $RULE15$ are binary variables used to indicate a violation of rules 14 and 15 of the COLREGs. They can be found by using equations (5.13a) and (5.13b).

$$RULE14 = \textit{CLOSE} \text{ and } \textit{STARBOARD} \text{ and } \textit{HEAD-ON} \tag{5.13a}$$

$$RULE15 = \textit{CLOSE} \text{ and } \textit{STARBOARD} \text{ and } \textit{CROSSED} \text{ and NOT } \textit{OVERTAKEN} \tag{5.13b}$$

Compliance with rule 13 is implicitly taken into account in equation (5.12). Rule 8 (action to avoid collision) and 16 (action by give-way vessel) require that actions are taken early. These rules are satisfied by letting the prediction horizon length T be longer than the time it takes to make a substantial heading or speed change.

Cost of collision

The cost of collision with obstacle ship i at time t in scenario k is denoted by $\mathcal{C}_i^k(t)$, and is found from equation (5.14) from Johansen et al. (2016).

$$\mathcal{C}_i^k(t) = K_i^{coll}|\boldsymbol{V}_0^k(t) - \boldsymbol{V}_i^k(t)|^2 \tag{5.14}$$

The tunable parameter $K_i^{coll} = 0.02$ for all obstacle ships. The cost of collision increases when the relative velocity between the ships increases. Thus, a collision with a faster ship is more dangerous than a collision with a slow ship.

Risk of collision

Johansen et al. (2016) calculate the risk of collision $\mathcal{R}_i^k(t)$ between obstacle ship i and the own-ship at time t in scenario k by using equation (5.15).

$$\mathcal{R}_i^k(t) = \begin{cases} \frac{1}{|t-t_0|^p}\left(\frac{d_i^{safe}}{d_{0,i}^k(t)}\right)^q, & \text{if } d_{0,i}^k(t) \leq d_i^{safe} \\ 0, & \text{otherwise} \end{cases} \tag{5.15}$$

In this thesis, the risk of collision is calculated slightly differently by using equation (5.16).

$$\mathcal{R}_i^k(t) = \begin{cases} \frac{1}{|t-t_0|^p}\left[\left(\frac{d_i^{safe}}{d_{0,i}^k(t)}\right)^q r + k_{FC} FC_i^k(t)\right], & \text{if } d_{0,i}^k(t) \leq d_i^{safe} \\ 0, & \text{otherwise} \end{cases} \tag{5.16}$$

The difference between the two expressions for $\mathcal{R}_i^k(t)$ is the inclusion of the parameter $r = 15$ as well as the addition of the term $k_{FC} FC_i^k(t)$ in equation (5.16). The parameter $k_{FC} = 275$.

The parameter r simplifies the tuning by allowing more flexibility to scale the value of $\mathcal{R}_i^k(t)$. During testing, it was found that the original expression for $\mathcal{R}_i^k(t)$ from equation (5.15) gave too low contribution to the total hazard. In order to solve this issue, the boolean variable $FC_i^k(t)$ was added to make the own-ship prefer a greater distance between ships. If the distance between obstacle ship i and the own-ship is less than a limit $L_{FC} = 600$ m at time t in scenario k, $FC_i^k(t) = 1$. This will increase the risk $\mathcal{R}_i^k(t)$.

The exponent $p = 0.5$ in equation (5.16) determines the importance of the time until collision. Due to the first term, $1/|t-t_0|^p$, collisions close in time have a greater risk than collisions in the far future. The risk of collision will also increase as the distance between the own-ship and the obstacle ship, $d_{0,i}^k(t)$, decreases. The distance $d_i^{safe} = 1025$ m for all obstacle ships and the exponent $q = 4.65$. These values are chosen large enough to make the own-ship keep a safe distance away from the obstacle ship. The choice of d_i^{safe} depends on how maneuverable the obstacle ship is.

Penalty for deviation from nominal path and nominal speed

In the hazard computation in equation (5.3), the function $f^k(Pr^k, \psi_{\text{ca}}^k)$ is included to increase the hazard of control behaviors that make the own-ship deviate from the nominal path and nominal speed. The expression for $f^k(Pr^k, \psi_{\text{ca}}^k)$ by Johansen et al. (2016) is given by equation (5.17).

$$\begin{aligned} f^k(Pr^k, \psi_{\text{ca}}^k) = k_{Pr}(1 - Pr^k) + k_\psi(\psi_{\text{ca}}^k)^2 + \Delta_{Pr}(Pr^k - Pr_{\text{last}}^k) \\ + \Delta_\psi(\psi_{\text{ca}}^k - \psi_{\text{ca,last}}^k) \end{aligned} \tag{5.17}$$

In the implementation for this thesis, a slightly different function is used, as shown in equation (5.18).

$$f^k(Pr^k, \psi_{\text{ca}}^k) = k_{Pr}(1 - Pr^k) + k_\psi|\psi_{\text{ca}}^k| + \Delta_{Pr}|Pr^k - Pr_{\text{last}}^k| \\ +\Delta_\psi|\psi_{\text{ca}} - \psi_{\text{ca,last}}| \tag{5.18}$$

Here, Pr^k is the propulsion command in scenario k and ψ_{ca}^k is the heading angle offset in scenario k. The term $k_\psi(\psi_{\text{ca}}^k)^2$ has been substituted with $k_\psi|\psi_{\text{ca}}^k|$ in equation (5.18) to make the penalty grow slower for increasing heading angle offsets. The parameter $k_{Pr} = 33$ decides how important it is to keep the nominal speed, and k_ψ decides how important it is to keep the nominal heading angle. Any deviation from nominal values will give a penalty. Inspired by Minne (2017) and Hagen (2017), the value of k_ψ depends on whether or not the heading angle offset is a port or starboard turn, as shown in equation (5.19).

$$k_\psi = \begin{cases} k_{\psi,\text{port}} & \psi_{\text{ca}} < 0 \\ k_{\psi,\text{starboard}} & \text{otherwise} \end{cases} \tag{5.19}$$

The parameter values are chosen to be $k_{\psi,\text{port}} = 0.65$, $k_{\psi,\text{starboard}} = 0.3$. Therefore, a higher penalty will be given for port turns. This choice has been made because most COLREGs situations require a starboard turn.

In equation (5.18), Pr_{last}^k and $\psi_{\text{ca,last}}^k$ are the propulsion command and the heading angle offset that gave the lowest total hazard $\mathcal{H}^k$ at the previous time $\mathcal{H}^k$ was calculated. The parameters $\Delta_{Pr} = 13$ and Δ_ψ decide how much penalty should be given for a deviation from the previously chosen propulsion command Pr_{last}^k and the previously chosen heading angle offset $\psi_{\text{ca,last}}^k$. The expression for Δ_ψ is given by equation (5.20).

$$\Delta_\psi = \begin{cases} k_{\Delta_\psi,\text{port}} & \psi_{\text{ca}} < 0 \\ k_{\Delta_\psi,\text{starboard}} & \text{otherwise} \end{cases} \tag{5.20}$$

The parameter values are chosen to be $k_{\Delta_\psi,\text{port}} = 0.55$ and $k_{\Delta_\psi,\text{starboard}} = 0.2$. Again, port turns give higher penalty compared to starboard turns.

Risk of grounding

Johansen et al. (2016) do not specify how the risk of grounding g^k should be computed. Therefore, a suggestion for computing g^k is given in this thesis. Grounding is assumed to be a collision between the own-ship and a static obstacle, either a circle or boundary obstacle. The risk of grounding in scenario k, g^k, is computed by using equation (5.21).

$$g^k = g_{\text{circle}}^k + g_{\text{boundary}}^k \tag{5.21}$$

Two different penalty values are used to compute g^k, one for each type of static obstacle. Similarly to $\mathcal{R}_i^k(t)$, the risk g^k will increase when either time to grounding decrease or distance to static obstacles decrease.

The variable g^k_{circle} represents the risk of grounding with a circle obstacle, and is calculated by using equation (5.22). A static circle obstacle m is defined by a position $[x_m, y_m]^T$ and a radius r_m.

$$g^k_{\text{circle}} = \max_m \max_{t \in D(t_0)} \left\{ (CC^k_m(t) + 1) k_c \frac{1}{|t - t_0|^{p_c}} \left(\frac{L_c + r_m}{d^k_{0,m}(t)} \right)^{q_c} \right\} \tag{5.22}$$

The value of g^k_{circle} is found by maximizing over every circle obstacle m and maximizing over every time step t in the prediction horizon. The boolean variable $CC^k_m(t)$ denotes a crossing with a circle obstacle m. $CC^k_m(t) = 1$ when the bow of the own-ship is within a distance $r_m + 4 \cdot W$ from the center of the circle obstacle m at time t, where W is the own-ship's width. Inclusion of $CC^k_m(t) + 1$ will make sure that the own-ship receives an extra large penalty for being too close to the circle obstacle. In equation (5.22), t_0 is the time when $\mathcal{H}^k$ is computed and $k_c = 105$, $p_c = 0.2$, $L_c = 500$ m and $q_c = 3.5$ are tunable parameters. The distance between the bow of the own-ship and static circle obstacle m at time t in scenario k is $d^k_{0,m}(t)$, which can be found by using equation (5.23).

$$d^k_{0,m}(t) = \sqrt{(x_m - x^k_{\text{bow}}(t))^2 + (y_m - y^k_{\text{bow}}(t))^2} \tag{5.23}$$

Here, $[x^k_{\text{bow}}(t), y^k_{\text{bow}}(t)]^T$ is the position of the own-ship's bow at time t in scenario k. The penalty g^k_{circle} will decrease when $d^k_{0,m}(t)$ decreases.

The variable g^k_{boundary} represents the risk of grounding with a static boundary obstacle. A boundary obstacle l is defined by a straight line segment from the start point $[x_{s,l}, y_{s,l}]^T$ to the end point $[x_{e,l}, y_{e,l}]^T$. Equation (5.24) is used to calculate g^k_{boundary}.

$$g^k_{\text{boundary}} = \max_l \max_{t \in D(t_0)} \left\{ (CB^k_l(t) + 1) k_b \frac{1}{(t - t_0)^{p_b}} \left(\frac{L_b}{d^k_{0,l}(t)} \right)^{q_b} \right\} \tag{5.24}$$

The variable g^k_{boundary} is computed similarly to the variable g^k_{circle} in equation (5.22). A boolean variable $CB^k_l(t)$ has a value of 1 if the own-ship's bow crosses the line defined by the static boundary obstacle l. In this case, the tunable parameters are chosen to be $k_b = 95$, $L_b = 125$ m, $p_b = 0.25$ and $q_b = 3$. The distance between the own-ship's bow and boundary obstacle l is $d^k_{0,l}(t)$, which is found by using the algorithm for minimum distance between a point and a line by Bourke (1988).

5.1.5 Tuning of SBMPC parameters

One of the main disadvantages of the SBMPC algorithm is the complicated tuning procedure. Several different parameter values need to be chosen correctly to make the algorithm work properly. During tuning the SBMPC algorithm, the main problem encountered was finding the right balance between parameter values. Some effort was required to find parameter values that made the risk of collision, COLREGs violation, deviation from nominal path and risk of grounding have approximately equal contribution to the total hazard.

Another problem encountered was that one set of parameter values gave an acceptable response in one scenario but not an acceptable response in another scenario.

First, the algorithm was tuned until satisfactory behavior was achieved with a single obstacle ship in a head-on scenario. From here, the parameters were gradually changed to give acceptable behavior in both crossing and overtaking scenarios. Acceptable behavior was defined as keeping a distance of more than 500 m away from other obstacles and at the same time follow the COLREGs. The algorithm was only tuned with passive obstacle ships following a straight path. After acceptable performance with a single obstacle ship was achieved, the algorithm was tested in scenarios with static obstacles and scenarios with multiple obstacle ships. However, most of the tuning happened by testing scenarios with a single obstacle ship.

A summary of all tunable parameters for the hazard computation is found in Table 5.1. Tuning has been done to prioritize heading change rather than speed reduction. With this choice of parameters, the own-ship can avoid collision with both static and dynamic obstacles. However, the own-ship did have some problems with keeping a large enough distance to other ships. The choice of parameter values should not be considered as optimal, since there is still room for improvement.

5.2 The modified SBMPC algorithm

The previous section discussed the original SBMPC algorithm by Johansen et al. (2016), which does not utilize intention data. This section will suggest how the SBMPC algorithm can be modified to utilize data about other vessels' intentions. The new, modified algorithm will be referred to as the modified SBMPC. In the following, different topics such as assumptions made, data about intentions, a recommendation for a communication method and modifications made to the original SBMPC will be discussed.

The design of the modified SBMPC started in the specialization project Kjerstad (2019). Upon further inspection, this design was found to be unsuitable for implementation. Therefore, the design used in this master's thesis has been drastically changed compared to the specialization project.

5.2.1 Requirements, assumptions and scope

Data about other vessels' intentions will be used as an attempt to enhance the short-term collision-avoiding abilities of the original SBMPC algorithm. Like the original SBMPC algorithm, the modified SBMPC algorithm should also be able to avoid collisions with obstacle ships and groundings with static obstacles while being able to achieve COLREGs compliance with rules 8 and 13-16. It will be assumed that the own-ship is an unmanned autonomous ship.

Parameter	Value
T_s	0.5 s
T	600 s
K_i^{coll}	0.02
p	0.5
q	4.65
k_{FC}	275
L_{FC}	600 m
d_i^{safe}	1025 m
r	15
κ_i	25
k_{Pr}	33
$k_{\psi,\text{port}}$	0.65
$k_{\psi,\text{starboard}}$	0.3
Δ_{Pr}	13
$k_{\Delta_\psi,\text{port}}$	0.55
$k_{\Delta_\psi,\text{starboard}}$	0.2
k_c	105
p_c	0.2
q_c	3.5
L_c	500 m
k_b	95
p_b	0.25
q_b	3
L_b	125 m
d_i^{cl}	2500 m
$\phi_{\text{overtaken}}$	68.5°
ϕ_{ahead}	20°
$\phi_{\text{head-on}}$	22.5°
ϕ_{crossed}	68.5°

Table 5.1: Final choice of parameters used in the SBMPC algorithm.

The modified SBMPC algorithm is only responsible for short-term collision avoidance in a relatively small region of the sea. Waypoints that define the own-ship's nominal path are predetermined before a scenario starts. The own-ship will use LOS guidance to follow the nominal path between waypoints, and the collision avoidance algorithm will make the own-ship deviate from this nominal path to avoid collisions.

It is assumed that all data about the own-ship's state is readily available without any measurement noise or delay. In addition, the own-ship will have real-time data about the position, heading and speed of all obstacle ships from AIS data. Intention data from the obstacle ships are also available to the own-ship. The location of all static obstacles are assumed to be available to the own-ship through map data.

5.2.2 Data about intentions

Knowing other vessel's intentions would make it easier for the navigator to plan collision avoiding maneuvers. In previously published short-term collision avoidance algorithms, such as the DSSA by Kim et al. (2017) and the negotiation method by Hu et al. (2008), intention data such as planned route and intended future course angle were used. In this thesis, the modified SBMPC algorithm will use intention data about planned route, planned speed and planned role.

When following the COLREGs, a ship takes the role as either a stand-on vessel or a give-way vessel. The role that obstacle ship i plans to take relative to the own-ship can be transmitted from the obstacle ship to the own-ship as role data.

The simulator from chapter 4 contains two different types of obstacle ships: passive obstacle ships without any collision avoidance system and SBMPC obstacle ships with the SBMPC or modified SBMPC collision avoidance algorithm implemented. The two types of obstacles will transmit different kinds of intention data about their planned route and planned speed. However, intention data about the planned role will be the same for both types of obstacles.

Planned route data for passive obstacle ships

Ships are required to have a route from start to destination before departure (Porathe et al., 2013). On today's ships, the planned route is stored in the navigation system as an rtz-file. Extensible Markup Language (XML) encodes the data, as defined in the IEC 61174 standard. Information about the position of each waypoint and planned minimum and maximum speed on the leg between two waypoints is stored in the rtz-file. Currently, this information is not exchanged between ships, but there is an opportunity to utilize this stored data.

In this thesis, it will be assumed that the data about a passive obstacle ship's planned route contains the position of each waypoint, along with the planned speed on the legs between the waypoints.

Another assumption made is that the intention data is always up-to-date. Unexpected events can cause a ship to deviate from the pre-voyage planned route. For instance, a navigator can decide to change the route due to poor weather conditions. Therefore, it is fair to assume that the data stored in the rtz-file onboard ships will sometimes be outdated. However, for this thesis it will be assumed that the planned route data is always updated to contain all deviations from the pre-voyage planned route.

A problem with the proposed way of defining intention data about planned route occurs if the navigator on the obstacle ship decides to change his intentions in the middle of a maneuver. In such cases, the own-ship's SBMPC algorithm would have planned a collision

avoiding maneuver based on wrong intentions. Unfortunately, there is no way of knowing ahead in time if and when a navigator decides to change his intentions. In this thesis, it is assumed that the intention data will stay constant during the entire scenario.

Planned route data for SBMPC obstacle ships

When it comes to SBMPC obstacle ships, utilizing intention data about planned route becomes more difficult. Every 10th second, the collision avoidance algorithm on the obstacle ship chooses a new control behavior. As a result of this, the intention data about the planned route for the SBMPC obstacle ship will only be accurate for 10 seconds into the future. When considering that a collision situation can last for several minutes, this becomes problematic.

In this thesis, the intention data about the SBMPC obstacle ship's planned route will be the trajectory calculated by the obstacle ship herself. As discussed in chapter 5.1.3, a ship with SBMPC predicts her own trajectory by using the 3 DOF equations of motion. The predicted position, heading and speed of the obstacle ship for the entire prediction horizon of $T = 600$ seconds is calculated. However, the prediction will be most accurate for the first 10 seconds.

The difference between the predicted trajectory from the SBMPC and the modified SBMPC can be seen in Figure 5.4. Predictions are from the own-ship's perspective. The circles represent the position of the ships after 900 seconds. Predicted trajectories from the SBMPC and the modified SBMPC are shown as a black line and a dashed black line, respectively. The prediction using the SBMPC is always a straight line. At $t = 0$ s, the predicted trajectories are equal. After 50 seconds, the prediction from the modified SBMPC is slightly closer to the real path than the prediction from the SBMPC. After 90 seconds, the predicted trajectory from the modified SBMPC overlaps the actual trajectory. However, after 410 seconds, the modified SBMPC trajectory prediction is the least accurate.

From this example, it can be concluded that the intention data about the SBMPC obstacle ship's planned route is only correct for the first 10 seconds in general. However, if the heading angle offset computed by the modified SBMPC on the obstacle ship stays constant for an extended period of time, the prediction is relatively accurate.

Summary of planned route data

An illustration of which intention data is transmitted from both passive obstacle ships and SBMPC obstacle ships is shown in Figure 5.5. The passive obstacle ship transmits the position P of each waypoint, planned speed U on the legs between waypoints and the role the obstacle ship is planning to take relative to the own-ship. The SBMPC obstacle ship will transmit her predicted position, speed and heading for each time step in the prediction horizon in addition to the planned role.

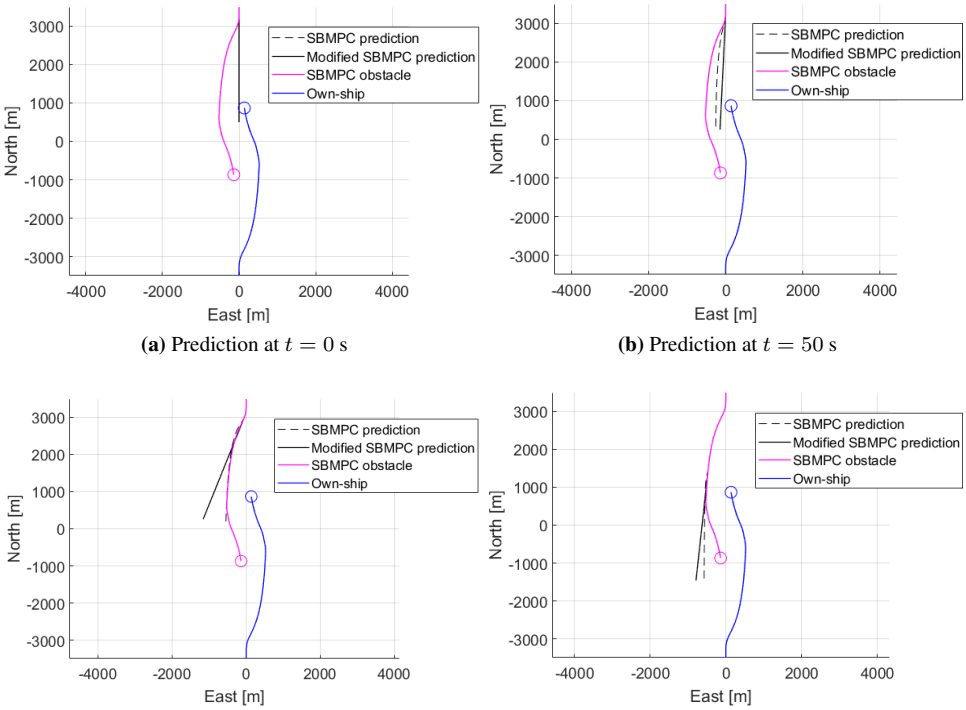

(a) Prediction at $t = 0$ s

(b) Prediction at $t = 50$ s

(c) Prediction at $t = 90$ s

(d) Prediction at $t = 410$ s

Figure 5.4: Comparison of predicted trajectories from SBMPC and modified SBMPC for a SBMPC obstacle ship in a head-on situation. The predictions are from the own-ship's perspective.

5.2.3 Communicating intention data

A ship-to-ship communication method is needed to exchange intention data. The rest of this section will discuss alternative communication technologies, and give a recommendation for which communication technology is best suited for transmitting intention data.

AIS

AIS uses Very High Frequency (VHF) radio to broadcast real-time data about the ship's state and other ship-related information, as discussed in chapter 2.1.1. It would also be possible to use AIS for exchanging intention data in addition to the real-time data. Since the SOLAS convention issued by the International Maritime Organization (IMO) (1974) requires the majority of larger ships to be equipped with AIS, most ships would not have to buy new equipment to be able to communicate data about intentions.

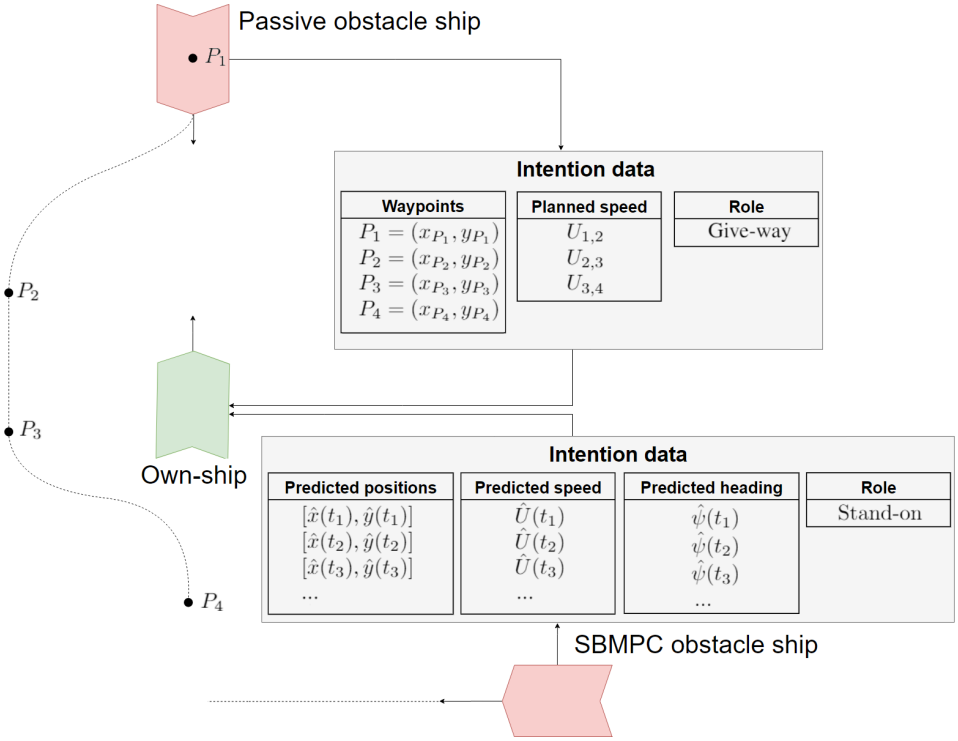

Figure 5.5: Intention data transmitted by a passive obstacle ship and a SBMPC obstacle ship in a head-on situation.

Communicating using AIS has some disadvantages. A significant drawback of AIS is the limited data capacity. Each AIS message can only contain up to 168 bits of data (Recommendation ITU-R M.1371-5). Also, the bandwidth is relatively low. Another problem with AIS is the lack of reliability. Wilthil et al. (2017) investigated the UTC timestamps of received AIS messages and discovered that around 40% of the messages from AIS arrive out of order. Harati-Mokhtari et al. (2007) reported that around 30% of messages about the ship's navigational status contained wrong information.

Balduzzi et al. (2014) have conducted a security analysis of AIS communication. Because AIS messages are broadcasted on an unsecured channel without any encryption, AIS communication is susceptible to spoofing and hijacking. Spoofing refers to broadcasting AIS data from a non-existing ship, while hijacking refers to altering of information contained in a transmitted AIS message.

VDES

VHF Data Exchange System (VDES) is a communication system consisting of three subsystems: AIS, Application Specific Messages (ASM) and VHF Data Exchange (VDE) (Lázaro et al., 2019). Each subsystem uses a different channel in the maritime VHF band. In addition to exchanging AIS data, any type of data can be transmitted using VDE. An advantage of VDES compared to AIS is the increased data capacity and higher bandwidth. According to Låg et al. (2015), VDES have 32 times higher bandwidth than AIS. VDES also increases navigation data security by adding access control and authentication features (The Maritime Executive, 2019). In addition, VDES has improved reliability over AIS with the addition of forward error correction, which allows for corrections of erroneous data (International Association of Marine Aids to Navigation and Lighthouse Authorities, 2017).

VDES is a relatively new standard defined in Recommendation ITU-R M.1371-5, and has not yet been implemented into maritime laws and regulations. However, IMO has developed a strategy for implementing e-Navigation, an initiative to achieve better maritime information sharing. Since VDES is a part of e-Navigation (IMO, 2015), VDES will most likely become a part of maritime regulations in the near future.

Mobile satellite systems

Mobile satellite systems can provide Internet access on a global scale by using a network of L-band satellites (Låg et al., 2015). Several companies are delivering mobile satellite communication systems to the maritime industry, including Inmarsat, Iridium and Thuraya. However, these systems can only deliver relatively slow bandwidth, around 400 kbps, at a relatively high price.

Maritime VSAT

Similar to mobile satellite systems, maritime very-small-aperture-terminal (VSAT) also provides global Internet access from satellite communication. However, maritime VSAT systems use C-, Ku-, and Ka-band satellites for transmitting data. This results in higher data rates and reduced cost per bit (Låg et al., 2015). A disadvantage of VSAT compared to mobile satellite systems is that VSAT installations can be relatively expensive, up to $100 000 in some cases (Låg et al., 2015). A monthly subscription is required, typically ranging from $1000 up to a few thousand dollars, depending on the bandwidth. The main reason for choosing maritime VSAT over mobile satellite systems is the increase in bandwidth.

Mobile network

The 4G mobile network allows for fast, secure and reliable communication over the Internet (Kurose and Ross, 2012). This network allows a ship to send and receive data packets by communicating with a base station. The cost is relatively low compared to satellite communication. One of the main disadvantages of mobile networks is the poor maritime network coverage. These networks will only give Internet connection up to 25 nautical miles (46.3 km) from the shore (Wireless, 2019), depending on the frequency band used and whether or not base stations are placed along the coast. Since a collision avoidance system requires communication in all parts of the sea to function correctly, using a mobile network to communicate intention data is not a practical solution.

Choice of communication technology

To summarize, there are two main ways of achieving ship-to-ship communication: using VHF to broadcast data with either AIS or VDES, or by using the Internet. Mobile satellite systems, maritime VSAT and mobile networks make it possible for a ship to connect to the Internet. With Internet access, standard Internet protocols such as Transmission Control Protocol (TCP) can be used for transferring data. These protocols have built-in functionality for achieving reliable data transfer, meaning that data is delivered from the sender to the receiver in the correct order without any message loss (Kurose and Ross, 2012). In addition, messages sent by using TCP can be encrypted when enhancing TCP with Secure Sockets Layer (SSL).

When communicating using the Internet, direct broadcasting of messages to nearby ships is not possible. Instead, a cloud server can be used. A ship connected to the Internet could upload her intention data to the cloud along with ship-related information such as a vessel identification number and current position. This ship could also be able to download the intention data for all nearby ships. Such a system could perhaps be integrated into the maritime connectivity platform, a cloud-based framework for exchanging ship information as described by Weinert et al. (2018). One of the main disadvantages of this proposed communication system is the dependency on commercially available equipment. With no requirements from any maritime authorities, it would be challenging to implement this communication system on a wide variety of ships.

VDES shows the most promising potential for exchanging intention data. Compared to AIS, VDES offers higher bandwidth and better functionality for exchanging intention data by using VDE. Even though mobile satellite systems, maritime VSAT and mobile networks can provide Internet access with a higher bandwidth compared to VDES, these communication systems are not operated nor regulated by maritime authorities. A significant advantage of VDES is that the standard is on its way to becoming a part of maritime regulations. This is important because the majority of ships will be required to have communication equipment to support VDES in the future.

5.2.4 Changes made in the modified SBMPC algorithm

The original SBMPC algorithm from section 5.1 will be modified to utilize other vessels' intentions. All proposed modifications will use intention data in some way. However, the modified SBMPC algorithm will use the same tunable parameters as the SBMPC algorithm. This will give a fair comparison of the performance of the original SBMPC and the modified SBMPC.

Modifying the obstacle trajectory prediction

The first modification made is to change the obstacle trajectory prediction. Trajectory prediction in the original SBMPC method plays a vital role in determining the correct maneuver. Almost every term in the hazard computation depends indirectly on the predicted trajectory of obstacle ships. Therefore, improving the trajectory prediction is one of the most important modifications to the SBMPC. The original SBMPC method assumes that all obstacle ships will travel along a straight line with constant speed and heading angle. In contrast, the modified SBMPC will utilize intention data about planned waypoints and planned speed to get a more accurate prediction of the obstacle's trajectory.

There are two types of obstacle ships: passive obstacle ships without a collision avoidance system and SBMPC obstacle ships with a collision avoidance system. Trajectory prediction is slightly different for these two types of obstacles.

For a passive obstacle ship i without a collision avoidance algorithm, the intention data about the planned route consist of a set of waypoints $\{P_1^i, P_2^i, ..., P_a^i, P_b^i, ...\}$. The position of waypoint P_a^i is denoted by $[x_{P_a^i}, y_{P_a^i}]^T$. In addition, data about the planned speed on the legs between the waypoints are available to the own-ship.

The proposed method for predicting the future trajectory of a passive obstacle ship i with the modified SBMPC is shown in Algorithm 1. Future position, speed and heading angle of obstacle ship i are estimated at each time step in the prediction horizon. The estimates are computed by using intention data about future waypoints and planned speed.

The trajectory prediction algorithm can be explained by using the example in Figure 5.6. In this case, the obstacle ship has three waypoints. At the time of prediction, t_0, the ship moves from P_1 towards P_2. The black line represents the predicted trajectory found by the algorithm, while the dashed line represents the actual ship trajectory. *NextWPIndex* and *StartWPIndex* will both be initialized to 2. Next, the predicted position $[\hat{x}_i(t), \hat{y}_i(t)]^T$, speed $\hat{U}_i(t)$ and heading $\hat{\psi}_i(t)$ is calculated at each time step t in the prediction horizon. The predicted trajectory is the straight line from the initial position of the ship towards the waypoint P_2. When the distance between the predicted obstacle ship position and waypoint P_2 is less than $L_d = 50$ m, the waypoints will switch and *NextWPIndex* increases by 1. This position is marked as point A. In the next iteration of the loop, the predicted trajectory will be the straight line starting at A and pointing towards the next waypoint P_3.

Algorithm 1 Algorithm for predicting a passive obstacle's planned trajectory.

NextWPIndex $\leftarrow$ Index of the waypoint (WP) the obstacle is currently moving towards.
StartWPIndex $\leftarrow$ *NextWPIndex*
EndWPIndex $\leftarrow$ Index of the final WP in the intention data.
$[x_{i,0}, y_{i,0}] \leftarrow [x_i(t_0), y_i(t_0)]$ (Start position of the obstacle ship.)
$\psi_{i,0} \leftarrow$ Current heading angle of obstacle ship.
$[x_{P_b^i}, y_{P_b^i}] \leftarrow$ Position of WP with index equal to *NextWPIndex*.
$[x_{P_a^i}, y_{P_a^i}] \leftarrow$ Position of WP with index equal to *NextWPIndex* $- 1$.
$U_{i,a,b} \leftarrow$ Speed between WPs with indexes *NextWPIndex -1* and *NextWPIndex*.
Time$_{\Delta WP} \leftarrow 0$ (Time when switching WPs)
XPosition$_{\Delta WP} \leftarrow x_{i,0}$ (Obstacle ship x-position when switching WPs)
YPosition$_{\Delta WP} \leftarrow y_{i,0}$ (Obstacle ship y-position when switching WPs)
for all time steps t in prediction horizon **do**
    $\hat{U}_i(t) \leftarrow U_{i,a,b}$
    if *StartWPIndex* $==$ *EndWPIndex* **then**
                                                ▷ Moving towards final WP.
        $\hat{\psi}(t) \leftarrow \psi_{i,0}$
        $\hat{x}_i(t) \leftarrow x_{i,0} + \hat{U}_i(t)\cos(\hat{\psi}_i(t)) \cdot t$
        $\hat{y}_i(t) \leftarrow y_{i,0} + \hat{U}_i(t)\sin(\hat{\psi}_i(t)) \cdot t$
    else if *NextWPIndex* $==$ *StartWPIndex* **then**
                                                ▷ Have not switched waypoints yet.
        $\hat{\psi}_i(t) \leftarrow \text{atan2}(y_{P_b^i} - y_{i,0}, x_{P_b^i} - x_{i,0})$
        $\hat{x}_i(t) \leftarrow x_{i,0} + \hat{U}_i(t)\cos(\hat{\psi}_i(t)) \cdot t$
        $\hat{y}_i(t) \leftarrow y_{i,0} + \hat{U}_i(t)\sin(\hat{\psi}_i(t)) \cdot t$
    else if *NextWPIndex* $>$ *StartWPIndex* and *NextWPIndex* $\leq$ *EndWPIndex* **then**
                                                ▷ Have switched WPs, but not reached final WP.
        $\hat{\psi}_i(t) \leftarrow \text{atan2}(y_{P_b^i} - \textit{YPosition}_{\Delta WP}, x_{P_b^i} - \textit{XPosition}_{\Delta WP})$
        $\hat{x}_i(t) \leftarrow \textit{XPosition}_{\Delta WP} + \hat{U}_i(t)\cos(\hat{\psi}_i(t)) \cdot (t - \textit{Time}_{\Delta WP})$
        $\hat{y}_i(t) \leftarrow \textit{YPosition}_{\Delta WP} + \hat{U}_i(t)\sin(\hat{\psi}_i(t)) \cdot (t - \textit{Time}_{\Delta WP})$
    end if
    DistanceToNextWP $\leftarrow \sqrt{(\hat{x}_i(t) - x_{P_b^i})^2 + (\hat{y}_i(t) - y_{P_b^i})^2}$
    if *DistanceToNextWP* $\leq L_d$ and *NextWPIndex* $\neq$ *EndWPIndex* **then**
                                                ▷ Switch WPs when distance to next WP is small.
        NextWPIndex $\leftarrow$ *NextWPIndex* $+ 1$
        Time$_{\Delta WP} \leftarrow t$
        XPosition$_{\Delta WP} \leftarrow \hat{x}_i(t)$
        YPosition$_{\Delta WP} \leftarrow \hat{y}_i(t)$
        $[x_{P_b^i}, y_{P_b^i}] \leftarrow$ Position of WP with index equal to *NextWPIndex*.
        $[x_{P_a^i}, y_{P_a^i}] \leftarrow$ Position of WP with index equal to *NextWPIndex* $- 1$.
    end if
end for

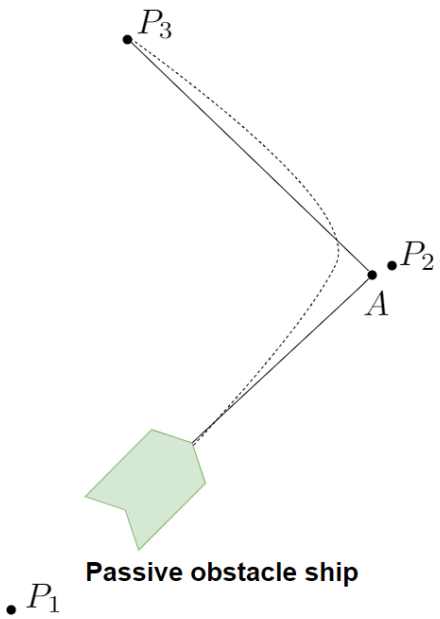

Figure 5.6: Predicted trajectory of a passive obstacle ship found by the trajectory prediction algorithm in Algorithm 1. The dashed line represents the actual ship trajectory.

For passive obstacle ships, Algorithm 1 can be used to predict the planned route based on the obstacle's transmitted intention data about planned waypoints and planned speed. For SBMPC obstacle ships, the broadcasted intention data already contain the ships' estimated position, speed and heading at each time step. Therefore, no further calculations will be necessary.

Include intended role in the hazard computation

The second modification made to the SBMPC algorithm is to add a term to the hazard function that gives a penalty for performing maneuvers while being a stand-on vessel. A problem encountered with the original SBMPC was that the algorithm did not keep a constant course and speed while assigned to be a stand-on vessel. Therefore, the hazard computation is modified to give an increased penalty for heading and speed change when the own-ship is assigned to be a stand-on vessel.

The role the obstacle ship plans to take in a collision situation is stored as a boolean variable $ROLE_i$. This variable has a value of 1 when obstacle ship i plans to be a give-way vessel relative to the own-ship. When $ROLE_i = 1$, the own-ship should be a stand-on vessel. An exception is for head-on situations where both vessels have give-way responsibility at the same time. If $ROLE_i = 1$ and vessels are not head-on, the own-ship receives a penalty for maneuvering.

The new hazard computation in the modified SBMPC becomes:

$$\mathcal{H}^k(t_0) = \max_i \max_{t \in D(t_0)} \left\{ \mathcal{C}_i^k(t) \mathcal{R}_i^k(t) + \kappa_i \mu_i^k(t) + P_{\mathrm{i,role}}^k(t) \right\} + f^k(Pr^k, \psi_{\mathrm{ca}}^k) + g^k \tag{5.25}$$

The only difference between equation (5.25) and the hazard computation expression used in the original SBMPC is the inclusion of the variable $P_{\mathrm{i,role}}^k(t)$, found by equation (5.26).

$$\mathrm{P}_{\mathrm{i,role}}^k(t) = \begin{cases} ROLE_i \cdot k_{\mathrm{role}} \cdot (1 - HO) \cdot (\sqrt{|\psi_{\mathrm{ca}}^k|} + 1 - Pr^k), & \text{if } \mathrm{L}_{\mathrm{role}} \leq \mathrm{d}_{0,i}^k(t) \leq d_i^{cl} \\ 0, & \text{otherwise} \end{cases} \tag{5.26}$$

When the own-ship and obstacle ship i are in a head-on situation or when the own-ship is a give-way vessel, $P_{\mathrm{i,role}}^k(t) = 0$. The boolean variable *HO* has a value of 1 in head-on situations. For situations where the own-ship is a stand-on vessel, the value of $P_{\mathrm{i,role}}^k(t)$ will increase when either the heading angle offset ψ_{ca}^k increases or the propulsion command Pr^k is different from 1. The tunable parameter $k_{\mathrm{role}} = 4.5$.

The penalty$P_{\mathrm{i,role}}^k(t)$ is only nonzero when the distance between ships, $d_{0,i}^k(t)$, is less than $d_i^{cl} = 2500$ m and the distance is larger than the limit $L_{\mathrm{role}} = 750$ m. When the vessels are close, the stand-on vessel is allowed by the COLREGs to perform maneuvers to avoid a collision. Therefore, no penalty is given for doing a maneuver as a stand-on vessel when the distance between the vessels is smaller than 750 m.

5.3 Challenges with the modified SBMPC algorithm

Using the modified SBMPC algorithm in a practical setting does have some challenges. First of all, the intention data used in the modified SBMPC algorithm needs to always be up to date. For manually operated obstacle ships with a human navigator, this would require the navigator to update the intentions in the onboard navigation system regularly. Since the navigator is often busy doing other tasks, there would be a high risk of having outdated intentions. It was also seen that utilizing intentions from an autonomous vessel can be problematic because the collision avoidance algorithm can change intentions during a maneuver. The implemented SBMPC algorithm changes intentions every 10th second.

Utilizing data about another vessel's intentions requires a robust communication system. In the case of communication system failure, there are some ways to deal with this problem. The first solution is to use the original SBMPC algorithm as a fallback system. Whenever the own-ship detects that intention data is no longer received or that the received intention data is erroneous, the collision algorithm could switch to the SBMPC algorithm. The second way of dealing with communication problems is to estimate the future intentions. Hexeberg et al. (2017) propose a single point neighbor search method that uses historical AIS data to predict a vessel's trajectory. The method shows promising results for the prediction of trajectories for prediction horizons up to 30 minutes.

The modified SBMPC algorithm assumes that real-time AIS data is available for all obstacle ships. It is also important to consider non-AIS vessels. Porathe et al. (2014) reported that non-AIS vessels were involved in 46% of all collisions in Korean coastal areas between 2008 and 2012. One way to handle non-AIS-vessels is to use a tracking system, like radar tracking, to obtain information about speed and heading that would typically be available through AIS.

5.4 Potential for utilizing intention data for long-term collision avoidance

Because of the challenges related to utilizing intention data for short-term collision avoidance, it is of interest to examine the potential for utilizing intentions in long-term collision avoidance algorithms. These algorithms find a path from start to destination that avoids collisions. There needs to be a balance between avoiding collisions and minimizing time to destination and fuel consumption.

Local collision avoidance is concerned with finding maneuvers when the own-ship is already close to other obstacle ships. In contrast, a long-term collision avoidance system has the potential to avoid close range encounters altogether. This is especially important in rough weather where the ship is difficult to steer. Using intention data about other vessel's future waypoints could be used to find a route that avoids close range encounters. In a practical implementation, the best performance would probably be achieved by combining both long-term and short-term collision avoidance in a hybrid architecture. Such hybrid architectures are suggested by Bitar et al. (2019) and Loe (2008).

An example of how such a long-term collision avoidance system could utilize intentions is illustrated in Figure 5.7. Assume that the vessels are a few kilometers apart such that the COLREGs do not apply yet. The green own-ship is currently following the path towards waypoint P_1. The leftmost obstacle ship intends to make a port turn, which creates a future collision situation between the three ships. A long-term collision avoidance system would be able to use intention data about the obstacle ship's planned routes, and calculate a new waypoint P_{new} for the own-ship to follow. Traveling towards this new waypoint would avoid the collision situation altogether.

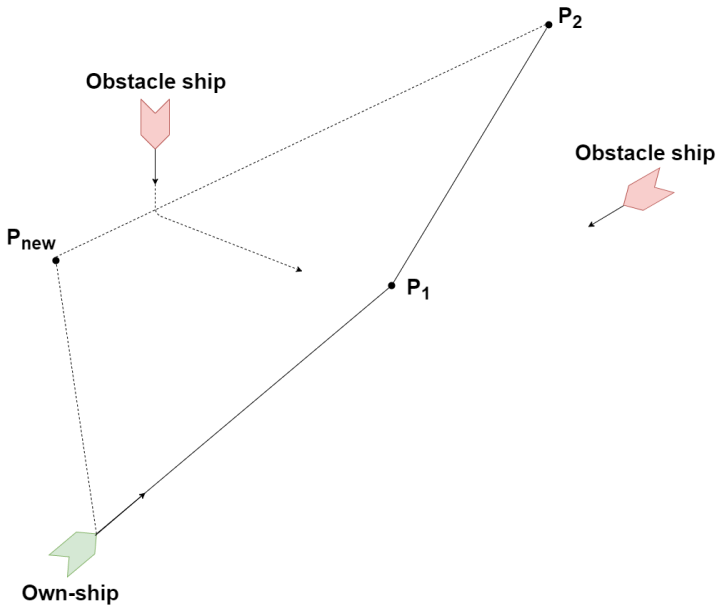

Figure 5.7: The own-ship is currently traveling towards a future collision situation. Instead of following the nominal path, the long-term collision avoidance algorithm could compute a new path that avoids the collision situation, represented by the dotted line.

Chapter 6

Collision Avoidance Performance Evaluation

The previous chapter presented implementation details about the SBMPC and modified SBMPC algorithms. This chapter will contain the details about the evaluation tool that evaluates the collision avoidance performance of the own-ship module. Several different metrics have been implemented as part of this evaluation tool. The overall evaluation process consists of the following three steps:

1. Obtain simulation data from the simulator log files.
2. Determine which COLREGs rules apply for the own-ship in each obstacle ship encounter.
3. Calculate the relevant metrics.

The metrics used are mainly based on the work by Woerner (2016), and will quantify how well the own-ship performs in terms of safety and COLREGs compliance with rules 8 and 13-17. A sparse amount of research exists on methods for evaluating collision avoidance performance and COLREGs compliance, but the work by Woerner (2016) is perhaps the most extensive on the subject. Inspiration for the metrics is also taken from the master's thesis by Minne (2017) and the article by Pedersen (2018). Minne (2017) developed a framework for automatic testing of collision avoidance algorithms, and Pedersen (2018) describes simulator-based testing of autonomous navigation systems as part of DNV GL's Revolt project. The work by Minne (2017) and Pedersen (2018) is also based on the metrics developed by Woerner (2016).

In addition to previously developed metrics, new metrics have also been developed in this master's thesis. These include metrics for avoiding static obstacles and a metric for the number of alarms given to the navigator.

6.1 Notation and definitions

In the following sections, the metrics for evaluating collision avoidance performance will be presented. The metrics are divided into four main classes: metrics for safety, metrics for avoiding static obstacles, a metric for the number of onboard alarms and metrics for COLREGs compliance. These four classes of metrics will be presented in sections 6.2, 6.3, 6.4 and 6.5, respectively.

A metric will be denoted either as a score $\mathcal{S}$ or a penalty $\mathcal{P}$. Only score metrics will be used to evaluate collision avoidance performance. However, the majority of the score metrics are functions of penalty metrics. Each metric will have a value in the range $[0, 1]$. The score metrics will have a value of 1 for best behavior and 0 for worst behavior. In contrast, the penalty metrics will have a value of 0 for best behavior and 1 for worst behavior. A superscript i will be used in cases where the metrics are related to COLREGs rule number i.

6.2 Metric for safety

The safety metric is calculated based on the distance between vessels at the Closest Point of Approach (CPA) and the pose of the vessels at CPA. In other words, both distance between vessels and orientation of the vessels will be used to determine whether a maneuver is safe or not.

6.2.1 Finding CPA and pose

By definition, CPA is the position along the own-ship's path where the distance between the own-ship and an obstacle is the shortest. This distance is denoted by r_{cpa} and is calculated by using equation (6.1) from Woerner (2016).

$$r_{\text{cpa}} = \min_{0 \leq t \leq t_{\max}} \left\{ \sqrt{(x_i(t) - x(t))^2 + (y_i(t) - y(t))^2} \right\} \tag{6.1}$$

The variable t denotes the time and $t_{\max}$ is the length of the simulation scenario. Also, $[x(t), y(t)]^T$ is the position of the own-ship and $[x_i(t), y_i(t)]^T$ is the position of obstacle ship i.

The pose of the vessels at CPA, $\Theta_{\text{cpa}} = [\alpha_{\text{cpa}}, \beta_{\text{cpa}}]^T$, is determined by the relative contact angle α and relative bearing angle β at CPA. The difference between these two angles is illustrated in Figure 6.1. Woerner (2016) defines the relative bearing angle $\beta \in [0^\circ, 360^\circ)$ as the angle between the own-ship's heading and the LOS vector from the own-ship to the obstacle ship. Positive angles have a clockwise rotation. The relative contact angle $\alpha \in [-180^\circ, 180^\circ)$ is the relative bearing angle viewed from the obstacle ship's perspective.

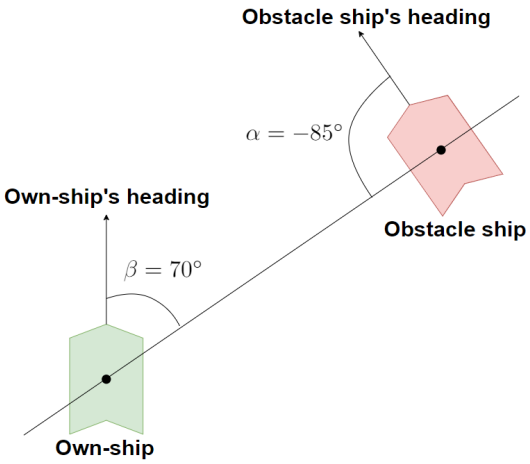

Figure 6.1: Difference between relative bearing angle β and relative contact angle α.

Similar to Woerner (2016), the relative bearing angle $\beta \in [0°, 360°)$ can be calculated using equation (6.2).

$$\beta = \begin{cases} 360° - |\mathit{bearing} - \psi| & \text{if } \mathit{bearing} - \psi < 0° \\ \mathit{bearing} - \psi - 360° & \text{if } \mathit{bearing} - \psi \geq 360° \\ \mathit{bearing} - \psi & \text{otherwise} \end{cases} \tag{6.2}$$

Here, $\psi \in (-180, 180]$ is the heading angle of the own-ship. A vessel pointing north is defined to have a heading angle of $0°$. The variable *bearing* is the absolute bearing angle, which can be calculated using equation (6.3).

$$\mathit{bearing} = \text{atan2}(y_i - y, x_i - x) \tag{6.3}$$

The atan2-function gives an output in the range $[-180°, 180°)$.

The relative contact angle $\alpha \in [-180°, 180°)$ for obstacle ship i is found by using equations (6.4) and (6.5).

$$\alpha = \begin{cases} 360° - |\mathit{contact\ angle} - \psi_i| & \text{if } \mathit{contact\ angle} - \psi_i < -180° \\ 360° - (\mathit{contact\ angle} - \psi_i) & \text{if } \mathit{contact\ angle} - \psi_i \geq 180° \\ \mathit{contact\ angle} - \psi_i & \text{otherwise} \end{cases} \tag{6.4}$$

$$\mathit{contact\ angle} = \text{atan2}(y - y_i, x - x_i) \tag{6.5}$$

6.2.2 Score metric for safety

The safety metric $\mathcal{S}_{\text{safety}}$ is a function of safety metrics for distance $\mathcal{S}_r$ and pose $\mathcal{S}_\Theta$. Minne (2017) uses a simpler approach to calculate $\mathcal{S}_{\text{safety}}$, where the safety metric only

depends on $\mathcal{S}_r$. In contrast, this thesis will use the same method as Woerner (2016) to find $\mathcal{S}_{\text{safety}}$, as shown in equation (6.6).

$$\mathcal{S}_{\text{safety}} = \gamma_\Theta \cdot \mathcal{S}_\Theta + \gamma_r \cdot \mathcal{S}_r \tag{6.6}$$

The safety metric is a weighted average of the pose safety metric $\mathcal{S}_\Theta$ and the distance safety metric $\mathcal{S}_r$. The values of the parameters are $\gamma_\Theta = 0.35$ and $\gamma_r = 0.65$, which means that the distance is more important for determining the safety metric.

The pose metric $\mathcal{S}_\Theta$ is given by equation (6.7) and will receive a high score when vessels are not facing toward each other.

$$\mathcal{S}_\Theta = \gamma_{\alpha,\Theta}\mathcal{S}_\Theta^\alpha + \gamma_{\alpha,\Theta}\mathcal{S}_\Theta^\beta \tag{6.7}$$

Two weighting parameters $\gamma_{\alpha,\Theta} = 0.5$ and $\gamma_{\alpha,\Theta} = 0.5$ are used. The expressions for $\mathcal{S}_\Theta^\alpha$ and $\mathcal{S}_\Theta^\beta$ are given by equations (6.8) and (6.9).

$$\mathcal{S}_\Theta^\alpha = \begin{cases} 1 - \cos(\alpha_{\text{cpa}}) & \text{if } |\alpha_{\text{cpa}}| < \alpha_{\text{cut}} \\ 1 & \text{if } |\alpha_{\text{cpa}}| \geq \alpha_{\text{cut}} \end{cases} \tag{6.8}$$

$$\mathcal{S}_\Theta^\beta = \begin{cases} 1 - \cos(\beta_{\text{cpa}}) & \text{if } |\beta_{\text{cpa}}| < \beta_{\text{cut}} \\ 1 & \text{if } |\beta_{\text{cpa}}| \geq \beta_{\text{cut}} \end{cases} \tag{6.9}$$

Here, α_{cpa} and β_{cpa} are relative contact angle and relative bearing angle at CPA, while α_{cut} and β_{cut} are cutoff values. These cutoffs are chosen to be $90°$, which makes equations (6.8) and (6.9) have the shape of the graph shown in Figure 6.2. When the vessels have relative contact angle $\alpha_{\text{cpa}} = 0°$ and relative bearing angle $\beta_{\text{cpa}} = 0°$, as shown in Figure 6.3a, the pose safety metric will achieve its minimum value of $\mathcal{S}_\Theta = 0$. On the other hand, the maximum score $\mathcal{S}_\Theta = 1$ will be achieved when $\alpha_{\text{cpa}} = 90°$ and $\beta_{\text{cpa}} = 90°$ as shown in Figure 6.3b.

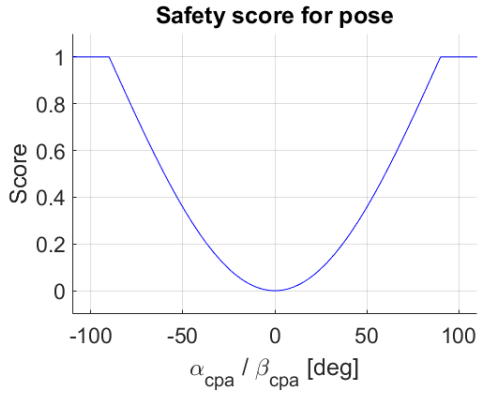

Figure 6.2: Safety score for pose, $\mathcal{S}_\Theta^\alpha$ and $\mathcal{S}_\Theta^\beta$ in equations (6.8) and (6.9), when $\beta_{\text{cut}} = \alpha_{\text{cut}} = 90°$.

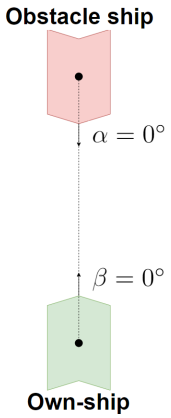

(a) Position of vessels when $\beta = \alpha = 0°$.

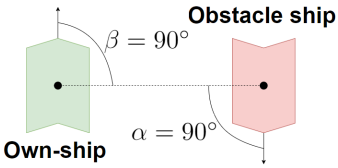

(b) Position of vessels when $\beta = \alpha = 90°$.

Figure 6.3: Pose for two different situations that achieve the minimum and maximum score for S_Θ in equation (6.7).

The second metric used to calculate the safety metric $\mathcal{S}_{\text{safety}}$ is the distance safety metric, $\mathcal{S}_r$, given by equation (6.10). This expression is also used by Minne (2017).

$$\mathcal{S}_r = \begin{cases} 1 & \text{if } r_{\text{cpa}} \geq R_{\text{pref}} \\ 1 - \gamma_{\text{nm}} \left(\frac{R_{\text{pref}} - r_{\text{cpa}}}{R_{\text{pref}} - R_{\text{nm}}} \right) & \text{if } R_{\text{nm}} \leq r_{\text{cpa}} < R_{\text{pref}} \\ 1 - \gamma_{\text{nm}} - \gamma_{\text{col}} \left(\frac{R_{\text{nm}} - r_{\text{cpa}}}{R_{\text{nm}} - R_{\text{col}}} \right) & \text{if } R_{\text{col}} \leq r_{\text{cpa}} < R_{\text{nm}} \\ 0 & \text{otherwise} \end{cases} \tag{6.10}$$

The parameters $\gamma_{\text{nm}} = 0.4$ and $\gamma_{\text{col}} = 0.6$ are weight parameters that satisfy $\gamma_{\text{nm}} + \gamma_{\text{col}} \leq 1$. Three other parameters are also used to determine the safety score:

- R_{pref}, preferred passing distance at CPA.
- R_{nm}, distance between vessels at CPA considered to be a near miss.
- R_{col}, distance between vessels at CPA considered to be a collision.

When $r_{\text{cpa}} \geq R_{\text{pref}}$, the maximum score $\mathcal{S}_r = 1$ is given. When $r_{\text{cpa}} \leq R_{\text{col}}$, the minimum score $\mathcal{S}_r = 0$ is given. Instead of using the same values for R_{pref}, R_{nm} and R_{col} in all situations, as done by Minne (2017) and Woerner (2016), a smaller CPA distance is acceptable if the obstacle ship is behind the own-ship. Therefore, the area around the own-ship is divided into two different regions. This is illustrated in Figure 6.4a. Region 1 is defined as $\beta \in [0°, 95°) \cup (265°, 360°]$, and region 2 is defined as $\beta \in [95°, 265°]$. The values of R_{pref}, R_{nm} and R_{col} for the different regions are shown in Table 6.1. Figure 6.4b illustrates how $\mathcal{S}_r$ varies in the two different regions as a function of r_{cpa}.

It is often recommended by seafarers to keep a CPA of 1 nautical mile (1.85 km) in restricted waters and 2 nautical miles (3.70 km) in open waters (Lee and Parker, 2007). However, acceptable CPA distance is highly dependant on the type of obstacle ship. From

the interview in Appendix A.3 it became clear that high CPA distances are required when facing large tankers with little maneuverability. In situations with small, maneuverable vessels, smaller CPA distances can be accepted. Since the obstacle ships in this thesis will be PSVs with high maneuverability, the preferred CPA distances are chosen somewhat smaller than the recommendation by Lee and Parker (2007).

Parameter	Value
$R_{\text{pref},1}$	1000 [m]
$R_{\text{nm},1}$	600 [m]
$R_{\text{col},1}$	200 [m]
$R_{\text{pref},2}$	750 [m]
$R_{\text{nm},2}$	400 [m]
$R_{\text{col},2}$	100 [m]
γ_{nm}	0.4
γ_{col}	0.6

Table 6.1: Parameters used in the distance safety metric $\mathcal{S}_r$ in equation (6.10).

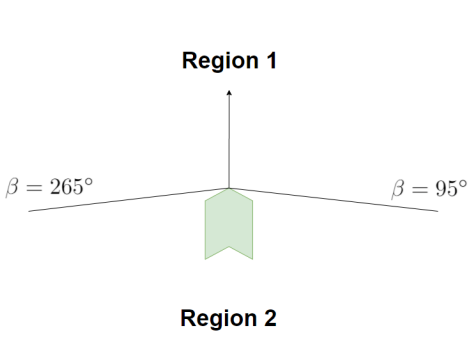

(a) Different regions defined by the value of β

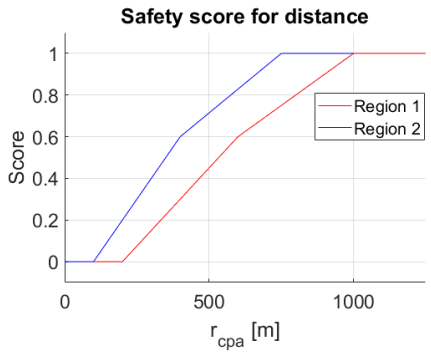

(b) Score for distance safety metric $\mathcal{S}_r$ in equation (6.10) for different values of r_{cpa} in different regions.

Figure 6.4: The safety score for distance depends on where the obstacle ship is relative to the own-ship. When the obstacle ship is in region 2, a smaller CPA distance is accepted.

6.3 Metrics for avoiding static obstacles

Minne (2017) and Woerner (2016) did not consider static obstacles in their implementations. For this thesis, two new metrics have been implemented to give a score for how well static obstacles are avoided. Both of these metrics are based on the distance between the own-ship's bow and the static obstacle.

For static circle obstacles, the metric $\mathcal{S}_{\text{circle}}$ is calculated by using equation (6.11). This

calculation is very similar to equation (6.10) for calculating the distance safety metric $\mathcal{S}_r$. The metric $\mathcal{S}_{\text{circle}}$ will be calculated for each circle obstacle in the scenario. In the case of multiple circle obstacles, the smallest score metric $\mathcal{S}_{\text{circle}}$ is chosen.

$$\mathcal{S}_{\text{circle}} = \begin{cases} 1 & \text{if } r_{\text{c,cpa}} \geq R_{\text{c,pref}} \\ 1 - \gamma_{\text{c,nm}} \left(\frac{R_{\text{c,pref}} - r_{\text{c,cpa}}}{R_{\text{c,pref}} - R_{\text{c,nm}}} \right) & \text{if } R_{\text{c,nm}} \leq r_{\text{c,cpa}} < R_{\text{c,pref}} \\ 1 - \gamma_{\text{c,nm}} - \gamma_{\text{c,col}} \left(\frac{R_{\text{c,nm}} - r_{\text{c,cpa}}}{R_{\text{c,nm}} - R_{\text{c,col}}} \right) & \text{if } R_{\text{c,col}} \leq r_{\text{c,cpa}} < R_{\text{c,nm}} \\ 0 & \text{otherwise} \end{cases} \tag{6.11}$$

A summary of the parameters used is given in Table 6.2. The variable $r_{\text{c,cpa}}$ represents the CPA distance from the own-ship's bow to the circle obstacle's boundary. This distance is calculated by using equation (6.12).

$$r_{\text{c,cpa}} = \min_{0 \leq t \leq t_{\max}} \left\{ \sqrt{(x_c - x_{\text{bow}}(t))^2 + (y_c - y_{\text{bow}}(t))^2} - r_c \right\} \tag{6.12}$$

Here, $[x_{\text{bow}}(t), y_{\text{bow}}(t)]^T$ represents the position of the own-ship's bow and $[x_c, y_c]^T$ is the circle obstacle's center. The radius of the circle obstacle is r_c.

The metric for static boundary obstacles is calculated similarly to the circle obstacle metric. The computation of $\mathcal{S}_{\text{boundary}}$ is shown in equation (6.13). The metric $\mathcal{S}_{\text{boundary}}$ is calculated for each boundary obstacle in the scenario. In the case of multiple boundary obstacles, the smallest score metric $\mathcal{S}_{\text{boundary}}$ is chosen.

$$\text{S}_{\text{boundary}} = \begin{cases} 1 & \text{if } r_{\text{b,cpa}} \geq R_{\text{b,pref}} \\ 1 - \gamma_{\text{b,nm}} \left(\frac{R_{\text{b,pref}} - r_{\text{b,cpa}}}{R_{\text{b,pref}} - R_{\text{b,nm}}} \right) & \text{if } R_{\text{b,nm}} \leq r_{\text{b,cpa}} < R_{\text{b,pref}} \\ 1 - \gamma_{\text{b,nm}} - \gamma_{\text{b,col}} \left(\frac{R_{\text{b,nm}} - r_{\text{b,cpa}}}{R_{\text{b,nm}} - R_{\text{b,col}}} \right) & \text{if } R_{\text{b,col}} \leq r_{\text{b,cpa}} < R_{\text{b,nm}} \\ 0 & \text{otherwise} \end{cases} \tag{6.13}$$

The same notation is used, where $r_{\text{b,cpa}}$ is the CPA distance from the own-ship's bow to the line defined by the boundary obstacle. This distance is found by using the algorithm for distance from a point to a line segment by Bourke (1988). A summary of the other parameters in equation (6.13) is shown in Table 6.2.

6.4 Metrics based on CPA/TCPA alarms

As discussed in chapter 3.1.1, the use of CPA/TCPA alarms is one of the primary methods for detecting collision situations. The OOW can select obstacles to be tracked on the radar, and the navigation system will calculate CPA and TCPA values for the tracked obstacles. This calculation is based on a linear approach and assumes that all vessels will keep a constant speed and heading angle. When either the CPA or TCPA value for the tracked obstacle goes below a chosen limit, an alarm is given (IEC 62388).

Parameter	Value
$R_{\mathrm{c,pref}}$	200 m
$R_{\mathrm{c,nm}}$	100 m
$R_{\mathrm{c,col}}$	50 m
$\gamma_{\mathrm{c,nm}}$	0.4
$\gamma_{\mathrm{c,col}}$	0.6
$R_{\mathrm{b,pref}}$	200 m
$R_{\mathrm{b,nm}}$	100 m
$R_{\mathrm{b,col}}$	50 m
$\gamma_{\mathrm{b,nm}}$	0.4
$\gamma_{\mathrm{b,col}}$	0.6

Table 6.2: Parameters for calculating $\mathcal{S}_{\mathrm{circle}}$ and $\mathcal{S}_{\mathrm{boundary}}$ in equations (6.11) and (6.13).

CPA/TCPA alarms can go off quite frequently. Too frequent alarms are often a burden on the OOW (Fukuto and Imazu, 2013). Unlike Minne (2017) and Woerner (2016), a metric based on CPA/TCPA alarms has been implemented. This metric is a function of the number of alarms received and the duration of the alarms. Few and short alarms during a simulation scenario would suggest good performance.

The metric for CPA/TCPA alarms, $\mathcal{S}_{\mathrm{alarms}}$, is found by equation (6.14).

$$\mathcal{S}_{\mathrm{alarms}} = \mathrm{sat}_0^1 \left\{ 1 - \gamma_{\mathrm{N,alarms}} N_{\mathrm{alarms}} - \gamma_{\mathrm{D,alarms}} \frac{D_{\mathrm{alarms}}}{t_{\max}} \right\} \tag{6.14}$$

Here, N_{alarms} is the number of alarms given during the scenario and D_{alarms} is the duration of the longest CPA/TCPA alarm. The weight parameters are chosen to be $\gamma_{\mathrm{N,alarms}} = 0.25$ and $\gamma_{\mathrm{D,alarms}} = 0.4$. The simulation scenario length is $t_{\max}$ seconds, and $\mathcal{S}_{\mathrm{alarms}}$ is saturated to have a value between 0 and 1.

The procedure of finding N_{alarms} and D_{alarms} is given in Algorithm 2. A loop runs through all time steps t from the start of the scenario, t_0, to the time of the true CPA, t_{cpa}. Next, the future positions of the obstacle ship and own-ship are estimated at each future time step $\hat{t} \in [t+1, t_{\mathrm{cpa}}]$ by using equations (6.15a) - (6.15d).

$$\hat{x}_i(\hat{t}) = x_i(t) + U_i(t) \cdot \cos\left(\psi_i(t)\right) \cdot (\hat{t} - t) \tag{6.15a}$$

$$\hat{y}_i(\hat{t}) = y_i(t) + U_i(t) \cdot \sin\left(\psi_i(t)\right) \cdot (\hat{t} - t) \tag{6.15b}$$

$$\hat{x}(\hat{t}) = x(t) + U(t) \cdot \cos\left(\psi(t)\right) \cdot (\hat{t} - t) \tag{6.15c}$$

$$\hat{y}(\hat{t}) = y(t) + U(t) \cdot \sin\left(\psi(t)\right) \cdot (\hat{t} - t) \tag{6.15d}$$

Here, $[\hat{x}(\hat{t}), \hat{y}(\hat{t})]^T$ and $[\hat{x}_i(\hat{t}), \hat{y}_i(\hat{t})]^T$ are the estimated future positions of the own-ship and obstacle ship i. This prediction assumes that the vessels will travel along straight lines with constant speed and constant heading angle. The CPA and TCPA values calculated based on these predicted positions are denoted as $\hat{r}_{\mathrm{cpa}}$ and $\hat{t}_{\mathrm{cpa}}$.

Next, a variable *isTargetTracked* determines if the obstacle requires the OOW's attention. This variable becomes $True$ if $\hat{r}_{\text{cpa}} < L_{\text{cpa,max}} = 3000$ m and $\hat{t}_{\text{cpa}} < L_{\text{tcpa,max}} = 600$ s.

When either $\hat{r}_{\text{cpa}} < L_{\text{cpa}} = 400$ m or $\hat{t}_{\text{cpa}} < L_{\text{tcpa}} = 400$ s, the alarm turns on and N_{alarms} will increase by 1. The alarm turns off when $\hat{r}_{\text{cpa}} > L_{\text{cpa}}$ and $\hat{t}_{\text{cpa}} > L_{\text{tcpa}}$, and the duration of the alarm is calculated.

Algorithm 2 Algorithm for calculating $\mathcal{S}_{\text{alarms}}$.

$N_{\text{alarms}} \leftarrow 0$
$D_{\text{alarms}} \leftarrow 0$
$t_{\text{alarmStart}} \leftarrow 0$
$t_{\text{alarmEnd}} \leftarrow -1$
alarmOn $\leftarrow False$
isTargetTracked $\leftarrow False$
for $t \in [t_0, t_{\text{cpa}}]$ **do**
    for $\hat{t} \in [t+1, t_{\max}]$ **do**
        $[\hat{x}_i(\hat{t}), \hat{y}_i(\hat{t})]^T \leftarrow$ Predicted obstacle position (equation (6.15a) - (6.15b))
        $[\hat{x}(\hat{t}), \hat{y}(\hat{t})]^T \leftarrow$ Predicted own-ship position (equation (6.15c) - (6.15d))
    end for
    $\hat{r}_{\text{cpa}} \leftarrow$ CPA distance using predicted positions
    $\hat{t}_{\text{cpa}} \leftarrow$ Time until $\hat{r}_{\text{cpa}}$ occurs
    if $\hat{r}_{\text{cpa}} \leq L_{\text{cpa,max}}$ and $\hat{t}_{\text{cpa}} \leq L_{\text{tcpa,max}}$ **then**
        isTargetTracked $\leftarrow True$
    else
        isTargetTracked $\leftarrow False$
    end if
    if ($\hat{r}_{\text{cpa}} < L_{\text{cpa}}$ or $\hat{t}_{\text{cpa}} < L_{\text{tcpa}}$) and *alarmOn* $== False$ and *isTargetTracked* $== True$ **then**
        $t_{\text{alarmStart}} \leftarrow t$
        alarmOn $= True$
        $N_{\text{alarms}} \leftarrow N_{\text{alarms}} + 1$
    end if
    if $\hat{r}_{\text{cpa}} > L_{\text{cpa}}$ and $\hat{t}_{\text{cpa}} > L_{\text{tcpa}}$ and *alarmOn* $== True$ **then**
        alarmOn $\leftarrow False$
        $t_{\text{alarmEnd}} \leftarrow t$
        $D_{\text{alarms}} \leftarrow \max\{D_{\text{alarms}}, t_{\text{alarmEnd}} - t_{\text{alarmStart}}\}$
    end if
end for
$\mathcal{S}_{\text{alarms}} = \text{sat}_0^1 \left\{ 1 - \gamma_{\text{N,alarms}} N_{\text{alarms}} - \gamma_{\text{D,alarms}} \frac{D_{\text{alarms}}}{t_{\max}} \right\}$

6.5 Metrics for COLREGs compliance

This thesis will use metrics to quantify compliance with COLREGs rules 8 and 13-17. Before these metrics are calculated, the evaluation tool must determine which rules apply in a particular scenario. Woerner (2016) developed an algorithm to determine what collision situation the own-ship and obstacle ship are in (overtaking, crossing or head-on), and what role the own-ship has (give-way or stand-on). The algorithm by Woerner (2016) will also be used in this thesis.

The algorithm from Woerner (2016) is presented with pseudocode in Algorithm 3. The pose, consisting of the initial relative bearing angle β_0 and the initial relative contact angle α_0, determines the type of collision situation and the role of the own-ship. The parameters $\alpha^{13}_{\text{crit}}$, $\alpha^{14}_{\text{crit}}$ and $\alpha^{15}_{\text{crit}}$ in the algorithm are tolerances for determining if the situation can be categorized as overtaking (rule 13), head-on (rule 14) or crossing (rule 15). The default values suggested by Woerner (2016) are used: $\alpha^{13}_{\text{crit}} = 45°$, $\alpha^{14}_{\text{crit}} = 13°$ and $\alpha^{15}_{\text{crit}} = 10°$.

The variables $\beta^{180^\circ} \in [-180°, 180°)$ and $\alpha^{360^\circ} \in [0°, 360°)$ in Algorithm 3 are defined in equations (6.16a) and (6.16b).

$$\beta^{180^\circ} = \begin{cases} -360° + \beta & \text{if } \beta \geq 180° \\ \beta & \text{otherwise} \end{cases} \tag{6.16a}$$

$$\alpha^{360^\circ} = \begin{cases} 360° - |\alpha| & \text{if } \alpha < 0 \\ \alpha & \text{otherwise} \end{cases} \tag{6.16b}$$

The following sections will present the metrics for determining compliance with COLREGs rules 8 and 13-17.

6.5.1 Rule 8 - Action to avoid collision

Rule 8 requires the own-ship to perform maneuvers in ample time to give passing at a safe distance. Also, the own-ship's maneuver is required to be readily apparent. The total score metric for rule 8 is a function of the following penalty metrics:

1. $\mathcal{P}^8_{\text{delay}}$, penalty for not taking actions in ample time.
2. $\mathcal{P}^8_{\Delta\psi_{\text{app}}}$, penalty for non-apparent heading change.
3. $\mathcal{P}^8_{\Delta U_{\text{app}}}$, penalty for non-apparent speed change.
4. $\mathcal{P}^8_{\Delta_{\text{app}}}$, penalty for non-apparent maneuver.
5. $\mathcal{P}^8_r$, penalty for non-safe maneuver.

Each of these five penalty metrics will be discussed before the final score metric for rule 8 is presented.

Algorithm 3 Algorithm for determining collision situation and role of own-ship. Algorithm is taken from Woerner (2016).

$\alpha_{\text{crit}}^{13} \leftarrow$ Overtaking tolerance
$\alpha_{\text{crit}}^{14} \leftarrow$ Head-on tolerance
$\alpha_{\text{crit}}^{15} \leftarrow$ Crossing aspect limit
$\alpha_0 \leftarrow$ Initial relative contact angle ($\alpha_0 \in [-180°, 180°)$)
$\beta_0 \leftarrow$ Initial relative bearing angle ($\beta_0 \in [0°, 360°)$)
if ($\beta_0 > 112.5°$) and ($\beta_0 < 247.5°$) and ($|\alpha_0| < \alpha_{\text{crit}}^{13}$) and $U_{\text{own-ship}} < U_i$ **then**
    Own-ship is overtaken and takes the role as a stand-on vessel.
    (Rules 13 and 17)
else if ($\alpha_0^{360°} > 112.5°$) and ($\alpha_0^{360°} < 247.5°$) and ($|\beta_0^{180°}| < \alpha_{\text{crit}}^{13}$) and $U_{\text{own-ship}} > U_i$ **then**
    Own-ship overtakes obstacle and takes the role as a give-way vessel.
    (Rules 8, 13 and 16)
else if ($|\beta_0^{180°}| < \alpha_{\text{crit}}^{14}$) and ($|\alpha_0| < \alpha_{\text{crit}}^{14}$) **then**
    Own-ship is in head-on situation.
    (Rules 8 and 14)
else if ($\beta_0 > 0°$) and ($\beta_0 < 112.5°$) and ($\alpha_0 > -112.5°$) and ($\alpha_0 < \alpha_{\text{crit}}^{15}$) **then**
    Own-ship is in crossing situation and takes the role as a give-way vessel.
    (Rules 8, 15 and 16)
else if ($\alpha_0^{360°} > 0°$) and ($\alpha_0^{360°} < 112.5°$) and ($\beta_0^{180°} > -112.5°$) and ($\beta_0^{180°} < \alpha_{\text{crit}}^{15}$) **then**
    Own-ship is in crossing situation and takes the role as a stand-on vessel.
    (Rules 15 and 17)
else
    No collision situation.
end if

Penalty for not taking actions in ample time

According to rule 8, the give-way vessel must perform actions in ample time. Ideally, actions should be taken as soon as the obstacle is detected. Therefore, the penalty metric $\mathcal{P}^8_{\text{delay}}$ gives a penalty when the own-ship starts to maneuver too late. Woerner (2016) and Minne (2017) suggest calculating the penalty metric by using equation (6.17).

$$\mathcal{P}^{8'}_{\text{delay}} = \begin{cases} \frac{r_{\text{detect}} - r_{\text{maneuver}}}{r_{\text{detect}} - r_{\text{cpa}}} & \text{if } r_{\text{maneuver}} < r_{\text{detect}} \\ 0 & \text{otherwise} \end{cases} \tag{6.17}$$

The variable r_{detect} is the distance from the own-ship to the obstacle when the own-ship detects the obstacle ship. A variable r_{maneuver} denotes the distance from the own-ship to the obstacle ship when the own-ship starts to maneuver. The disadvantage with this approach is that the penalty will decrease with decreasing r_{cpa}. Because of this problem, another penalty metric is used for this thesis, as shown in equation (6.18).

$$\mathcal{P}^{8}_{\text{delay}} = \begin{cases} \frac{r_{\text{detect}} - r_{\text{maneuver}}}{r_{\text{detect}}} & \text{if } r_{\text{maneuver}} < r_{\text{detect}} \\ 0 & \text{otherwise} \end{cases} \tag{6.18}$$

Here, r_{cpa} has been removed. The penalty metric $\mathcal{P}^8_{\text{delay}}$ is illustrated in Figure 6.5.

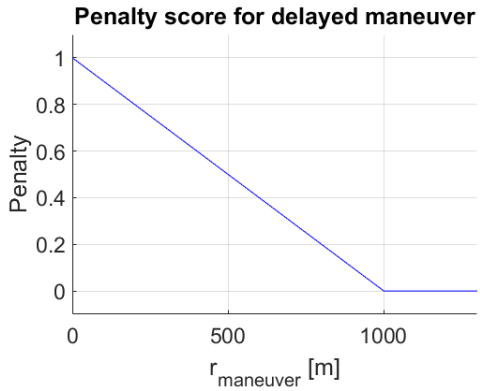

Figure 6.5: Penalty metric $\mathcal{P}^8_{\text{delay}}$ from equation (6.18) for delayed maneuvers. In this case, $r_{\text{detect}} = 1000$ m. A penalty is given when r_{maneuver} is too small.

Woerner (2016) uses the constant value $r_{\text{detect}} = 1.8 \cdot R_{\text{pref}}$. In contrast, the implementation in this thesis stores the time when the obstacle is detected as t_{detect}. Since the position of the vessels at each time step is also stored, the distance r_{detect} can be found.

The variable r_{maneuver} is found by using the same approach as Minne (2017). It is assumed that a maneuver starts when either the heading angle or speed of the own-ship changes by more than some predefined amount. To find out when a maneuver starts, equations (6.19a) and (6.19b) are used.

$$|\psi(t_{\text{detect}}) - \psi(t)| \geq \epsilon_\psi \tag{6.19a}$$

$$|U(t_{\text{detect}}) - U(t)| \geq \epsilon_U \tag{6.19b}$$

If either of these two conditions evaluates to true at time t, then $t_{\text{maneuver}} = t$. According to Allen (2005), any alterations of heading angle larger than 3° is detectable by the radar. Therefore, $\epsilon_\psi = 3^\circ$. For speed changes, $\epsilon_U = 1$ m/s.

Penalty for non-apparent heading change

Rule 8 of the COLREGs requires actions by the give-way vessel to be readily apparent for other vessels. Cockcroft and Lameijer (2012) argue that heading changes should be at least 30° before they are readily apparent for other vessels.

The penalty metric for non-apparent heading changes is given by equation (6.20). The same equation is also used by Woerner (2016).

$$\mathcal{P}^8_{\Delta\psi_{\text{app}}} = \begin{cases} 1 & \text{if } |\Delta\psi| \leq \Delta\psi_{\text{md}} \\ \frac{\Delta\psi_{\text{app}} - |\Delta\psi|}{\Delta\psi_{\text{app}} - \Delta\psi_{\text{md}}} & \text{if } \Delta\psi_{\text{md}} < |\Delta\psi| < \Delta\psi_{\text{app}} \\ 0 & \text{if } |\Delta\psi| \geq \Delta\psi_{\text{app}} \end{cases} \tag{6.20}$$

In this equation, $\Delta\psi_{\text{app}} = 30^\circ$ is a threshold value. Heading changes larger than $\Delta\psi_{\text{app}}$ are considered to be apparent for other vessels. The parameter $\Delta\psi_{\text{md}} = 4^\circ$ defines the smallest detectable heading change. The variable $|\Delta\psi|$ is the absolute value of the maximum heading change during the maneuver, and is found by using equation (6.21). Minne (2017) uses the same approach to find $|\Delta\psi|$.

$$\begin{aligned} |\Delta\psi| = \max \{ & |\psi(t_{\text{maneuver}}) - \psi(t_{\text{maneuver}})|, |\psi(t_{\text{maneuver}} + 1) - \psi(t_{\text{maneuver}})|, \\ & |\psi(t_{\text{maneuver}} + 2) - \psi(t_{\text{maneuver}})|, ..., |\psi(t_{\text{cpa}}) - \psi(t_{\text{maneuver}})| \} \end{aligned} \tag{6.21}$$

Here, t_{maneuver} is the time when the maneuver starts. The penalty metric $\mathcal{P}^8_{\Delta\psi_{\text{app}}}$ from equation (6.20) is illustrated in Figure 6.6. Apparent heading changes larger than 30° will not give any penalty.

Penalty metric for non-apparent speed change

The metric for penalizing non-apparent speed change, $\mathcal{P}^8_{\Delta U_{\text{app}}}$, is given by equation (6.22). The same approach as Woerner (2016) is used.

$$\mathcal{P}^8_{\Delta U_{\text{app}}} = \begin{cases} 0 & \text{if } \Delta U \geq \Delta U_{\text{app}} \\ \frac{\Delta U_{\text{app}} - \Delta U}{\Delta U_{\text{app}}} & \text{otherwise} \end{cases} \tag{6.22}$$

Here, ΔU_{app} is the threshold for what is considered as an apparent speed reduction. This value is set to 50%. The variable ΔU is the reduction in speed during a maneuver, also given as a percentage, and is found by using equation (6.23).

$$\Delta U = \frac{U_{\text{maneuver}} - U_{\min}}{U_{\text{maneuver}}} \tag{6.23}$$

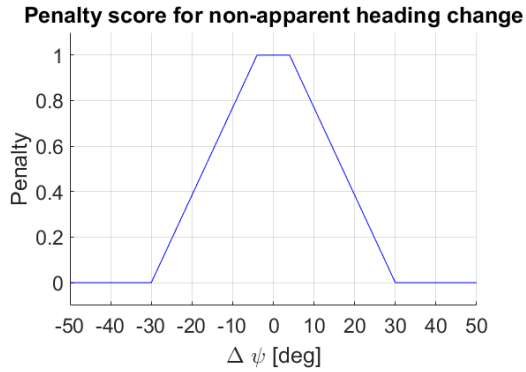

Figure 6.6: Penalty metric $\mathcal{P}^8_{\Delta\psi_{\text{app}}}$ from equation (6.20) for non-apparent changes in heading. A penalty will be given when the maximum heading change during the maneuver, $|\Delta\psi|$, is smaller than $\Delta\psi_{\text{app}} = 30°$.

Here, U_{maneuver} is the speed of the own-ship when she starts to maneuver, and $U_{\min}$ is the lowest own-ship speed during the maneuver. It must be assumed that the own-ship will only decrease her speed during the maneuver, such that $U_{\min} < U_{\text{maneuver}}$. The penalty metric $\mathcal{P}^8_{\Delta U_{\text{app}}}$ is illustrated in Figure 6.7. If the own-ship does not decrease her speed by more than 50% during a maneuver, a penalty for non-apparent speed change is given.

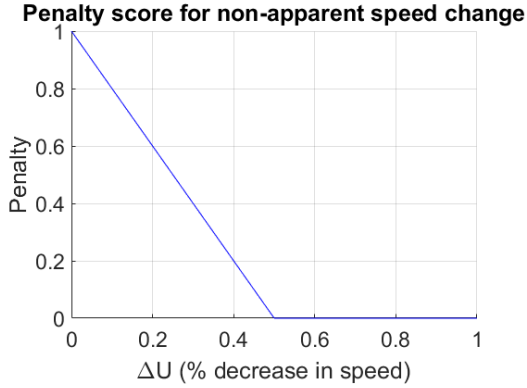

Figure 6.7: Penalty metric $\mathcal{P}^8_{\Delta U_{\text{app}}}$ from equation (6.22) for non-apparent speed change. If the speed is reduced by more than the threshold $\Delta U_{\text{app}} = 50\%$, no penalty is given.

Penalty metric for non-apparent maneuvers

A penalty metric for non-apparent maneuvers combines the penalty metrics for non-apparent heading change in equation (6.20) and the penalty metric for non-apparent speed change in equation (6.22). The resulting penalty metric for non-apparent maneuvers is

shown in equation (6.24). This metric is also used by Minne (2017).

$$\mathcal{P}^8_{\Delta_{\text{app}}} = \mathcal{P}^8_{\Delta U_{\text{app}}} \cdot \mathcal{P}^8_{\Delta \psi_{\text{app}}} \tag{6.24}$$

When either an apparent change in speed or an apparent change in heading occurs, the penalty metric $\mathcal{P}^8_{\Delta_{\text{app}}}$ will become zero.

Penalty metric for non-safe maneuver

Part d) of rule 8 requires that the vessels shall pass at a safe distance from each other. Woerner (2016) and Minne (2017) have not taken this into account for rule 8. However, in this thesis there is a penalty metric for penalizing non-safe distances, given by equation (6.25). The same metric is used by Pedersen (2018).

$$\mathcal{P}^8_r = 1 - \mathcal{S}_r \tag{6.25}$$

Here, $\mathcal{S}_r$ is the metric for safe distance from equation (6.10) in section 6.2.2.

Total score metric for rule 8

Inspired by Pedersen (2018), the total score metric for rule 8 can be constructed as shown in equation (6.26).

$$\mathcal{S}^8 = \text{sat}^1_0 \left\{ 1 - \gamma^8_{\text{app}} \mathcal{P}^8_{\Delta_{\text{app}}} - \gamma^8_r \mathcal{P}^8_r - \gamma^8_{\text{delay}} \mathcal{P}^8_{\text{delay}} \right\} \tag{6.26}$$

The parameters $\gamma^8_{\text{app}} = 0.33$, $\gamma^8_r = 0.33$ and $\gamma^8_{\text{delay}} = 0.33$ are tunable. $\mathcal{S}^8$ will be reduced when the own-ship does not perform safe, apparent maneuvers in ample time.

6.5.2 Rule 13 - Overtaking situation

In overtaking situations, rule 13 says that the give-way vessel can overtake the stand-on vessel on either side. Compliance with rule 13 depends on which role the own-ship takes. If the own-ship is a stand-on vessel, the metric for rule 16 is used. On the other hand, if the own-ship is a give-way vessel, the metric for rule 17 is used. Woerner (2016) points out that the overtaking vessel should avoid passing ahead of the stand-on vessel. Therefore, a penalty metric $\mathcal{P}^{13}_{\text{ahead}}$ penalizes passing ahead of the stand-on vessel. This metric is given by equation (6.27).

$$\mathcal{P}^{13}_{\text{ahead}} = \begin{cases} 1 & \text{if } -45^\circ < \alpha_{\text{cpa}} < 45^\circ \\ 0 & \text{else} \end{cases} \tag{6.27}$$

The score metric for rule 13 then becomes $\mathcal{S}^{13}$, given by equation (6.28). This is the same equation as used by Minne (2017).

$$\mathcal{S}^{13} = \begin{cases} \text{sat}_0^1 \left\{ \mathcal{S}^{16} - \gamma_{\text{ahead}}^{13} \mathcal{P}_{\text{ahead}}^{13} \right\} & \text{if own-ship is give-way vessel} \\ \mathcal{S}^{17} & \text{if own-ship is stand-on vessel} \end{cases} \tag{6.28}$$

Here, $\gamma_{\text{ahead}}^{13} = 0.3$ is a tunable weight to specify how much passing ahead contributes to $\mathcal{S}^{13}$. $\mathcal{S}^{16}$ and $\mathcal{S}^{17}$ are score metrics for rules 16 and 17, respectively. They will be discussed in more detail in the upcoming sections 6.5.5 and 6.5.6.

6.5.3 Rule 14 - Head-on situation

Rule 14 for head-on situations requires the two vessels involved to make a starboard turn such that the vessels pass each other on the port side. Both vessels are required to perform a maneuver, and they both take the role as a give-way vessel. Therefore, keeping a constant heading or turning to port should result in a failure of compliance with the rule. The score metric for rule 14 depends on four different penalty metrics:

1. $\mathcal{S}_{\Theta_{\text{cpa}}}^{14}$, score for passing port-to-port.
2. $\mathcal{P}_{\text{nst}}^{14}$, penalty for non-starboard turns.
3. $\mathcal{P}_{\text{delay}}^{8}$, penalty for not doing actions in ample time.
4. $\mathcal{P}_{\Delta\psi_{\text{app}}}^{8}$, penalty for non-apparent heading changes.

The metrics $\mathcal{S}_{\Theta_{\text{cpa}}}^{14}$ and $\mathcal{P}_{\text{nst}}^{14}$ will be discussed, before the final score metric for rule 14 is presented. $\mathcal{P}_{\text{delay}}^{8}$ and $\mathcal{P}_{\Delta\psi_{\text{app}}}^{8}$ are the penalty metrics from section 6.5.1.

Score metric for passing port-to-port

Woerner (2016) suggests the following score metric for passing port-to-port:

$$\mathcal{S}_{\Theta_{\text{cpa}}}^{14} = \left(\frac{\sin\left(\alpha_{\text{cpa}}\right) - 1}{2} \right)^2 \left(\frac{\sin\left(\beta_{\text{cpa}}\right) - 1}{2} \right)^2 \tag{6.29}$$

where α_{cpa} is the relative contact angle at CPA and β_{cpa} is the relative bearing angle at CPA.

A plot of the score metric $\mathcal{S}_{\Theta_{\text{cpa}}}^{14}$ is shown in Figure 6.8. The maximum score $\mathcal{S}_{\Theta_{\text{cpa}}}^{14} = 1$ is obtained when the vessels pass each other with $\beta_{\text{cpa}} = 270^\circ$ and $\alpha_{\text{cpa}} = -90^\circ$, in which case the vessels pass each other on the port side.

Penalty metric for non-starboard turns

Woerner (2016) does not mention how to find the penalty for non-starboard turns.

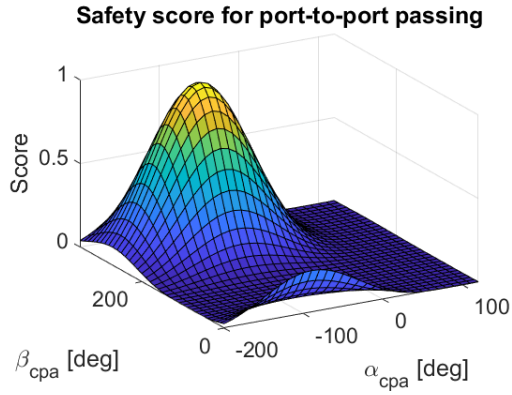

Figure 6.8: Score metric $\mathcal{S}^{14}_{\Theta_{\text{cpa}}}$ in equation (6.29) for passing port-to-port. The maximum score of 1 is achieved for $\beta_{\text{cpa}} = 270^\circ$ and $\alpha_{\text{cpa}} = -90^\circ$, when the vessels pass each other on the port side.

Therefore, a suggestion for a penalty metric to penalize port turns is given in equation (6.30).

$$\mathcal{P}^{14}_{\text{nst}} = \begin{cases} 1 & \text{if } d \geq d_T \text{ and } e > 0 \\ 1 - \left(\frac{2(d_T - d)}{d_T}\right)^4 & \text{if } \frac{d_T}{2} < d < d_T \text{ and } e > 0 \\ 0 & \text{if } e \leq 0 \text{ or } d \leq \frac{d_T}{2} \end{cases} \tag{6.30}$$

To calculate $\mathcal{P}^{14}_{\text{nst}}$, three different positions are defined:

1. $\boldsymbol{P}_0 = [x(t_0), y(t_0)]^T$
2. $\boldsymbol{P}_2 = [\hat{x}(t_{\max}), \hat{y}(t_{\max})]^T$
3. $\boldsymbol{P} = [x(t_2), y(t_2)]^T$

These three positions are illustrated in Figure 6.9. $\boldsymbol{P}_0$ is the initial start position of the own-ship, $\boldsymbol{P}_2$ is the estimated own-ship position at the end of the scenario, calculated by assuming the own-ship will follow a straight path. Finally, $\boldsymbol{P}$ is the true own-ship position at a time $t_2 > t_0$. In addition to the threshold $d_T = 100$ m, two variables are used to compute $\mathcal{P}^{14}_{\text{nst}}$. The distance between the position $\boldsymbol{P}$ and the line from $\boldsymbol{P}_0$ to $\boldsymbol{P}_2$ is denoted by d. This distance is calculated by using equation (6.31).

$$d = \frac{|[\hat{y}(t_{\max}) - y(t_0)] \cdot x(t_2) - [\hat{x}(t_{\max}) - x(t_0)] \cdot y(t_2) + \hat{x}(t_{\max}) y(t_0) - \hat{y}(t_{\max}) x(t_0)|}{\sqrt{[\hat{y}(t_{\max}) - y(t_0)]^2 + [\hat{x}(t_{\max}) - x(t_0)]^2}} \tag{6.31}$$

Also, e in equation (6.30) is a number whose value is negative if the point $\boldsymbol{P}$ is on the right side of the line from $\boldsymbol{P}_0$ to $\boldsymbol{P}_2$. The variable e is positive if $\boldsymbol{P}$ is on the left side of this line. Thus, $e > 0$ for port turns. To calculate e, equation (6.32) is used.

$$e = [x(t_2) - x(t_0)] \cdot [\hat{y}(t_{\max}) - y(t_0)] - [\hat{y}(t_{\max}) - y(t_0)] \cdot [\hat{x}(t_{\max}) - x(t_0)] \tag{6.32}$$

In the implemented evaluation tool, d, e and $\mathcal{P}_{\text{nst}}^{14}$ are computed every 10th second between t_0 and t_{cpa}. The final value for $\mathcal{P}_{\text{nst}}^{14}$ is found by maximizing over the computed values of $\mathcal{P}_{\text{nst}}^{14}$.

The penalty metric $\mathcal{P}_{\text{nst}}^{14}$ is illustrated in Figure 6.10. If the true position of the own-ship at time t_2, $\boldsymbol{P}$, is on the left side the line from $\boldsymbol{P}_0$ to $\boldsymbol{P}_2$, and at the same time the distance $d > \frac{d_T}{2}$, then a port turn is detected and a penalty is given.

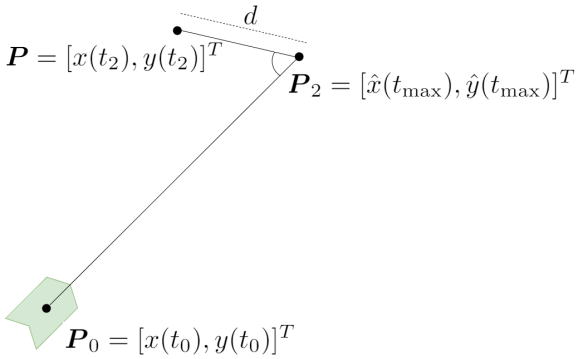

Figure 6.9: Definition of the three positions for determining the penalty metric $\mathcal{P}_{\text{nst}}^{14}$ in equation (6.30) for penalizing non-starboard turns. In this example, $e > 0$ since $\boldsymbol{P}$ is on the left side of the line from $\boldsymbol{P}_0$ to $\boldsymbol{P}_2$.

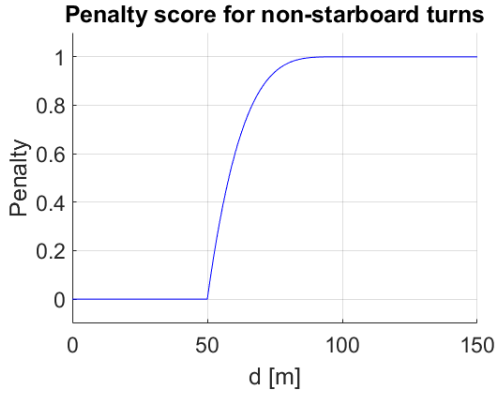

Figure 6.10: Penalty metric $\mathcal{P}_{\text{nst}}^{14}$ from equation (6.30) for penalizing non-starboard turns. In this case, $e > 0$ and $d > d_T = 100$ m.

Total score metric for rule 14

Similar to Pedersen (2018), the total metric for rule 14 is found by combining the previously discussed metrics, as shown in equation (6.33).

$$\mathcal{S}^{14} = \text{sat}_0^1 \left\{ \left(1 - \gamma_{\text{nst}}^{14} \mathcal{P}_{\text{nst}}^{14} - \gamma_{\text{delay}}^{8} \mathcal{P}_{\text{delay}}^{8} - \gamma_{\psi_{\text{app}}}^{8} \mathcal{P}_{\Delta\psi_{\text{app}}}^{8} \right) \cdot \mathcal{S}_{\Theta_{\text{cpa}}}^{14} \right\} \tag{6.33}$$

$\mathcal{P}_{\text{nst}}^{14}$ is the penalty for turning to port side, $\mathcal{P}_{\text{delay}}^{8}$ is the penalty for not performing a maneuver in ample time, $\mathcal{P}_{\Delta\psi_{\text{app}}}^{8}$ is the penalty for non-apparent heading changes and $\mathcal{S}_{\Theta_{\text{cpa}}}^{14}$ is the score for port-to-port passing. The values for the tunable weight parameters are $\gamma_{\text{nst}}^{14} = 0.4$, $\gamma_{\text{delay}}^{8} = 0.33$ and $\gamma_{\psi_{\text{app}}}^{8} = 0.27$.

6.5.4 Rule 15 - Crossing situation

Rule 15 tells what responsibilities the give-way and stand-on vessels have in a crossing situation. The give-way vessel is required to turn starboard and pass behind the stand-on vessel. Because passing ahead should be avoided, Woerner (2016) developed a penalty metric that penalizes passing ahead of the stand-on vessel, given in equation (6.34).

$$\mathcal{P}_{\text{ahead}}^{15} = \begin{cases} 1 & \text{if } T_{\text{ahead,low}} < \alpha_{\text{cpa}} < T_{\text{ahead,high}} \\ 0 & \text{else} \end{cases} \tag{6.34}$$

From equation (6.34), it is clear that $\mathcal{P}_{\text{ahead}}^{15}$ gives a penalty of 1 only if the relative contact angle α_{cpa} is between the thresholds $T_{\text{ahead,low}} = -25°$ and $T_{\text{ahead,high}} = 165°$.

Similarly to the score metric for rule 13 in section 6.5.2, the score metric for rule 15, $\mathcal{S}^{15}$, depends on which role the own-ship has. $\mathcal{S}^{15}$ is calculated using equation (6.35) from Woerner (2016). If the own-ship is a give-way vessel, the requirements for rule 16 applies. If the own-ship is a stand-on vessel, the requirements for rule 17 applies.

$$\mathcal{S}^{15} = \begin{cases} \text{sat}_0^1 \left\{ \mathcal{S}^{16} - \gamma_{\text{ahead}}^{15} \mathcal{P}_{\text{ahead}}^{15} \right\} & \text{if own-ship is give-way vessel} \\ \mathcal{S}^{17} & \text{if own-ship is stand-on vessel} \end{cases} \tag{6.35}$$

The parameter $\gamma_{\text{ahead}} = 0.5$ is tunable.

6.5.5 Rule 16 - Action by give-way vessel

Rule 16 requires the give-way vessel to take early action and keep out of the way of the stand-on vessel. The score metric to measure compliance with rule 16 is a function of three different metrics:

1. $\mathcal{S}_{\text{safety}}$, score for safe maneuvers.

2. $\mathcal{P}^8_{\text{delay}}$, penalty for not doing actions in ample time.
3. $\mathcal{P}^8_{\Delta_{\text{app}}}$, penalty for non-apparent maneuvers.

The score metric for rule 16 is given by equation (6.36), which is the same as the metric used by Minne (2017) and Woerner (2016).

$$\mathcal{S}^{16} = \mathcal{S}_{\text{safety}}(1 - \mathcal{P}^8_{\text{delay}})(1 - \mathcal{P}^8_{\Delta_{\text{app}}}) \tag{6.36}$$

The score metric $\mathcal{S}^{16}$ increases with the safety score $\mathcal{S}_{\text{safety}}$. Also, $\mathcal{S}^{16}$ is reduced when the own-ship does not take action in ample time and does not perform an apparent maneuver.

6.5.6 Rule 17 - Action by stand-on vessel

Rule 17 requires the stand-on vessel to keep a constant heading angle and speed. However, the stand-on vessel is required to maneuver in situations where the give-way vessel does not take action to avoid collision. Such situations are called *in extremis* and require special attention when developing the score metric for rule 17. The total score metric for rule 17 is a function of five different penalty metrics:

1. $\mathcal{P}^{17}_{\Delta\psi}$, penalty for heading changes.
2. $\mathcal{P}^{17}_{\Delta U}$, penalty for speed changes.
3. $\mathcal{P}^{14}_{\text{nst}}$, penalty for port turns in crossing situations.
4. $\mathcal{P}^{17}_{\Delta}$, penalty for maneuvering when not in extremis.
5. $\mathcal{S}_{\text{safety}}$, score for safe maneuvers.

Each of these five penalty metrics will be explained before the total score metric for rule 17 is presented.

Penalty metric for heading changes

The penalty metric used by Woerner (2016) to penalize heading changes is shown in equation (6.37).

$$\mathcal{P}^{17}_{\Delta\psi} = \begin{cases} 0 & \text{if } |\Delta\psi| < \Delta\psi_{\text{md}} \\ \frac{|\Delta\psi| - \Delta\psi_{\text{md}}}{\Delta\psi_{\text{app}} - \Delta\psi_{\text{md}}} & \Delta\psi_{\text{md}} \leq |\Delta\psi| \leq \Delta\psi_{\text{app}} \\ 1 & \text{if } |\Delta\psi| > \Delta\psi_{\text{app}} \end{cases} \tag{6.37}$$

Here, $|\Delta\psi|$ is the absolute value of the maximum heading change during the maneuver, which can be found by using equation (6.21). $\Delta\psi_{\text{app}} = 30^\circ$ is a threshold for what is considered to be an apparent change in heading, and $\Delta\psi_{\text{md}} = 4^\circ$ is the smallest detectable heading change. A plot of $\mathcal{P}^{17}_{\Delta\psi}$ is shown in Figure 6.11. As long as the change in heading angle, $|\Delta\psi|$, is larger than the threshold $\Delta\psi_{\text{md}}$, the penalty increases for increasing heading change.

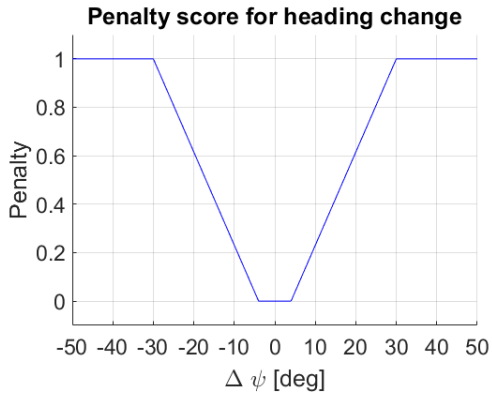

Figure 6.11: Penalty metric $\mathcal{P}^{17}_{\Delta\psi}$ in equation (6.37) for penalizing heading changes.

Penalty metric for speed changes

The penalty metric for penalizing speed changes in this thesis differs from the penalty metric by Woerner (2016) and Minne (2017). Instead of differentiating between penalizing speeding up and speeding down in two separate ways, both types of speed changes are penalized the same way. The penalty metric for this thesis is shown in equation (6.38).

$$\mathcal{P}^{17}_{\Delta U} = \begin{cases} 0 & \text{if } |\Delta U_{\max}| < \Delta U_{\text{md}} \\ \frac{|\Delta U_{\max}| - \Delta U_{\text{md}}}{\Delta U_{\text{app}} - \Delta U_{\text{md}}} & \text{if } \Delta U_{\text{md}} \leq |\Delta U_{\max}| \leq \Delta U_{\text{app}} \\ 1 & \text{if } |\Delta U_{\max}| > \Delta U_{\text{app}} \end{cases} \tag{6.38}$$

This penalty metric has the same shape as $\mathcal{P}^{17}_{\Delta\psi}$ in Figure 6.11. A penalty is given when the own-ship changes her speed during a maneuver. If the speed either increase or decrease by more than $\Delta U_{\text{app}} = 50\%$ of U_{maneuver}, the maximum penalty is given. U_{maneuver} is the speed at the start of the maneuver. $\Delta U_{\text{md}} = 0.2$ m/s is the smallest detectable speed change and $\Delta U_{\text{app}} = 50\%$ is a threshold for what is considered as an apparent speed change. $\Delta U_{\max}$ is the largest deviation in speed from U_{maneuver}.

Penalty metric for port turns in crossing situations

Rule 17 requires the stand-on vessel to avoid turning port while in a crossing situation. The penalty metric $\mathcal{P}^{14}_{\text{nst}}$ from equation (6.30) penalizes port turns.

Penalty metric for maneuvering when not in extremis

The score metric for rule 17 must take into account that the stand-on vessel is allowed to maneuver in extremis when the give-way vessel does not take appropriate actions. The

following penalty metric is used:

$$\mathcal{P}_{\Delta}^{17} = \begin{cases} 0 & r_{\text{maneuver}} < L_{\min} \\ 1 - \left(\frac{r_{\text{maneuver}} - L_{\max}}{L_{\max} - L_{\min}} \right)^2 & L_{\min} \leq r_{\text{maneuver}} \leq L_{\max} \\ 1 & r_{\text{maneuver}} > L_{\max} \end{cases} \tag{6.39}$$

This penalty metric gives a penalty when the own-ship with stand-on responsibility maneuvers when being far away from the obstacle ship. However, no penalty is given if the own-ship maneuvers when being close to the obstacle ship. In equation (6.39), r_{maneuver} is the distance from the own-ship to the obstacle when the own-ship starts maneuvering. $L_{\min} = 300$ m and $L_{\max} = 750$ m. If $r_{\text{maneuver}} < L_{\min}$, then the stand-on vessel does not get a penalty for making a maneuver. The maximum penalty is received when $r_{\text{maneuver}} > L_{\max}$. The Penalty metric $\mathcal{P}_{\Delta}^{17}$ is illustrated in Figure 6.12.

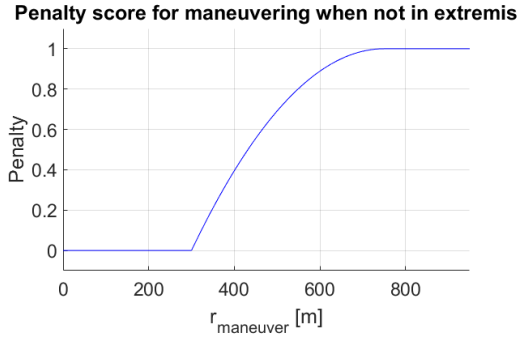

Figure 6.12: Penalty metric $\mathcal{P}_{\Delta}^{17}$ in equation (6.39) for maneuvering when not in extremis.

Total score metric for rule 17

Finally, the score metric for rule 17 can be constructed. The expression is given in equation (6.40), inspired by the score metric from Minne (2017).

$$\mathcal{S}^{17} = \text{sat}_0^1 \left\{ 1 - \gamma_{\text{safety}}^{17}(1 - \mathcal{S}_{\text{safety}}) - \gamma_{\Delta}^{17}\mathcal{P}_{\Delta}^{17} \left(\gamma_{\Delta U}^{17}\mathcal{P}_{\Delta U}^{17} + \gamma_{\Delta\psi}^{17}\mathcal{P}_{\Delta\psi}^{17} \right) - C\gamma_{\text{nst}}^{17}\mathcal{P}_{\text{nst}}^{14} \right\} \tag{6.40}$$

The score is reduced when the safety score $\mathcal{S}_{\text{safety}}$ is small. Also, the inclusion of the term $-\gamma_{\Delta}^{17}\mathcal{P}_{\Delta}^{17}(\gamma_{\Delta U}^{17}\mathcal{P}_{\Delta U}^{17} + \gamma_{\Delta\psi}^{17}\mathcal{P}_{\Delta\psi}^{17})$ makes sure that $\mathcal{S}^{17}$ is reduced if the stand-on vessel either changes her speed or heading while being far away from the obstacle vessel. Heading changes will give larger penalty than speed changes, since $\gamma_{\Delta\psi}^{17} = 1.5 > \gamma_{\Delta U}^{17} = 0.25$. If the stand-on vessel is close to the give-way vessel, $\mathcal{P}_{\Delta}^{17} = 0$ and the stand-on vessel is allowed to perform maneuvers without reducing $\mathcal{S}^{17}$. C is a boolean variable with a value of 1 if the stand-on vessel is in a crossing situation, in which case a penalty $\mathcal{P}_{\text{nst}}^{14}$ is given for any port turns. The parameters $\gamma_{\text{safety}}^{17} = 0.7$, $\gamma_{\Delta}^{17} = 0.5$ and $\gamma_{\text{nst}}^{17} = 0.5$ are tunable.

Chapter 7

Simulation Results

The design of the SBMPC and modified SBMPC algorithms were introduced in chapter 5. In this chapter, the performance of these algorithms will be compared in a wide range of scenarios. The goal is to determine if the inclusion of intentions positively impacts the collision avoidance performance. The metrics introduced in the previous chapter will be used to quantify the performance of the two collision avoidance algorithms.

7.1 Explanation of plots

The simulation results in this chapter will consist of trajectory, speed and heading plots as shown in Figure 7.1. The trajectory plots consist of three different snapshots. The leftmost plot shows the situation near the start of the scenario, the middle plot shows the situation at the time when Closest Point of Approach (CPA) occurs and the rightmost plot shows the situation at the end of the scenario. The blue line in the trajectory plot represents the own-ship's trajectory, and the blue circle represents the position of the own-ship. The trajectories of the SBMPC obstacle ship and the passive obstacle ship are shown with the colors magenta and red, respectively. The obstacle ships are also numbered.

In the bottom part of Figure 7.1, the own-ship's speed and heading angle resulting from both algorithms are displayed. The speed plot displays the real speed u of the own-ship in blue, and $u_c = u_d \cdot Pr$ is the speed the own-ship's speed controller is trying to follow. In the heading plot, the blue line represents the true heading angle ψ of the own-ship. The black, dashed line is the heading angle offset ψ_{ca} computed by the collision avoidance algorithm. A red, dashed line represents ψ_d, the desired heading angle computed by the LOS guidance and the heading reference model. The own-ship's heading controller tries to follow $\psi_d + \psi_{\mathrm{ca}}$.

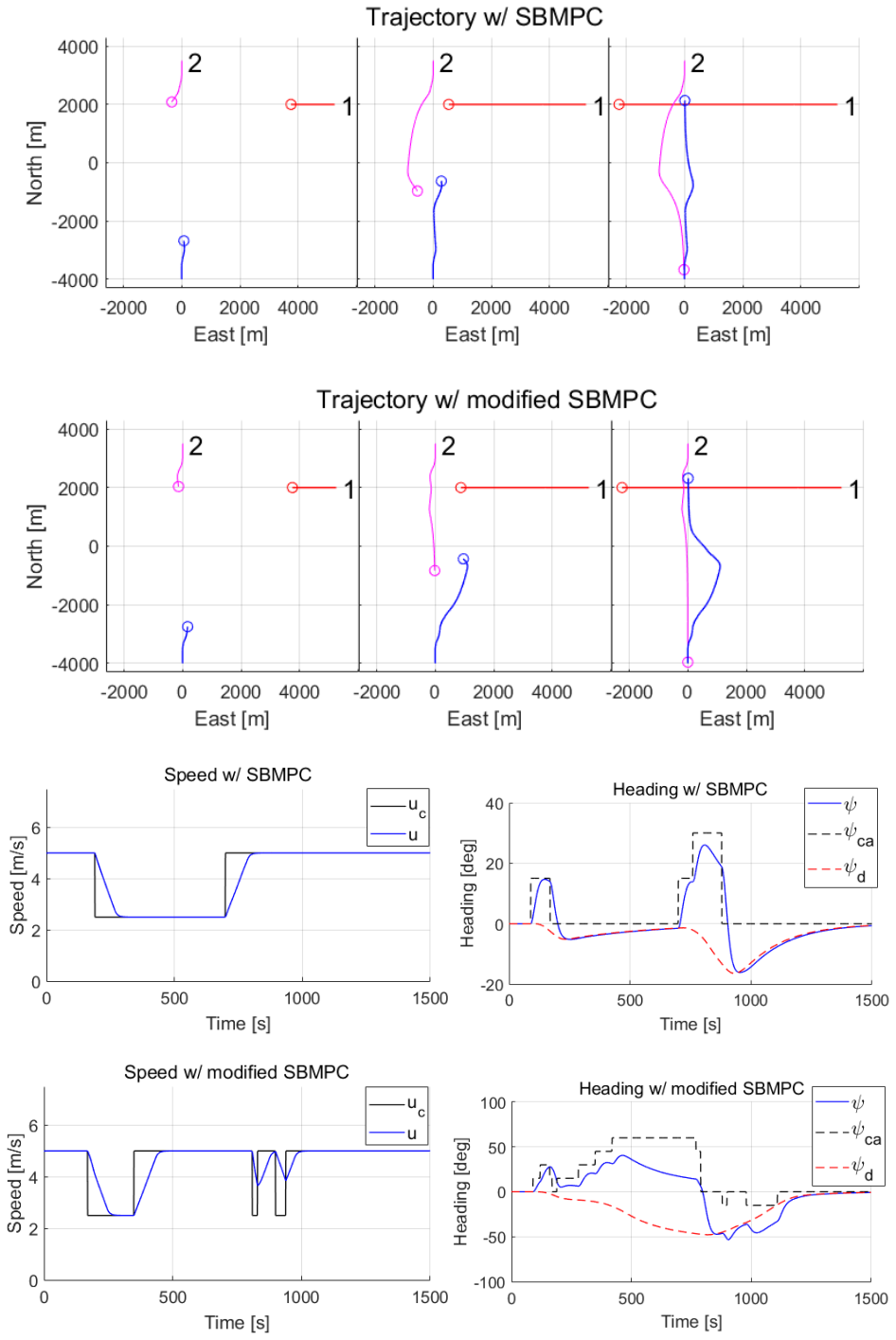

Figure 7.1: Example of simulation results from a scenario with one SBMPC obstacle ship and one passive obstacle ship.

7.2 Simulation study

The scenarios in the simulation study have been manually designed to cover a wide range of collision situations with varying difficulty. In each scenario, the vessels are approaching a collision situation. If no maneuvers are made, a collision will occur. Each scenario will be simulated two times. One time in which the own-ship and any SBMPC obstacle ship is equipped with the original SBMPC algorithm, and one more time in which these vessels are equipped with the modified SBMPC algorithm. Unless otherwise stated, all vessels have a speed of 5 m/s.

The scenarios will include passive obstacle ships, SBMPC obstacle ships as well as static obstacles. Passive obstacle ships represent manually operated ships without any collision avoidance system. They will only follow the path between waypoints, and are sometimes used to represent ships that have unpredictable behavior. SBMPC obstacle ships represent autonomous ships steered by LOS guidance and a collision avoidance system. Using SBMPC obstacle ships will give more realistic scenarios compared to using passive obstacle ships, since the SBMPC obstacle ships respond to the movements made by the own-ship. Static obstacles are included to represent environmental constraints such as shallow water zones and archipelago.

The first scenarios will be common collision situations such as head-on, crossing and overtaking with only a single obstacle ship. The simulation study will continue with more challenging scenarios where the own-ship is facing two, three and four obstacle ships. The scenarios with multiple obstacle ships are designed to test the collision avoidance algorithms' performance in scenarios that often lead to collision for manually operated vessels. In chapter 3 it was concluded that collisions for manually operated ships are most likely to happen in situations where the obstacle ships behave unexpectedly, for instance, making sudden maneuvers that violate the COLREGs. Also, situations with many distractions are likely to cause collisions.

A summary of the metrics from chapter 6 for quantifying collision avoidance performance is given in Table 7.1. The superscript refers to the COLREGs rule number, and every metric gives a value between 0 and 1. A value of 1 represents the best behavior. However, any score over 0.5 should be considered acceptable.

Metric	Description
$\mathcal{S}_{\text{safety}}$	Score metric for safety. High score for large CPA distance and good pose at CPA.
$\mathcal{S}_{\text{alarms}}$	Score metric for CPA/TCPA alarms. High score for few and short alarms.
$\mathcal{S}_{\text{circle}}$	Score metric for avoiding a static circle obstacle. High score when the distance from the obstacle is large.
$\mathcal{S}_{\text{boundary}}$	Score metric for avoiding a static boundary obstacle. High score when the distance from the obstacle is large.
$\mathcal{S}^{8}$	Score metric for rule 8. High score for readily apparent maneuvers taken in ample time.
$\mathcal{S}^{13}$	Score metric for overtaking. Score depends on whether the own-ship is give-way or stand-on.
$\mathcal{S}^{14}$	Score metric for head-on. High score when turning starboard and performing an apparent maneuver in ample time.
$\mathcal{S}^{15}$	Score metric for a crossing situation. Score depends on whether the own-ship is give-way or stand-on.
$\mathcal{S}^{16}$	Score metric for following give-way vessel responsibilities. High score when keeping a safe distance and taking early and apparent maneuvers.
$\mathcal{S}^{17}$	Score metric for following stand-on vessel responsibilities. High score when no speed or heading change occurs when vessels are far apart.

Table 7.1: Summary of the metrics for quantifying collision avoidance performance. More details about each metric can be found in chapter 6.

7.2.1 Scenarios with one obstacle ship

Head-on with a SBMPC obstacle ship

In head-on scenarios, rule 14 of the COLREGs require both vessels to make a starboard turn, resulting in a port side passing. The maneuvers should be performed in ample time and also be readily apparent for the other ship. Figure 7.2 and Table 7.2 show the simulation results and metric scores from a head-on situation between the own-ship and a SBMPC obstacle ship. Both vessels were able to turn in the correct direction and avoid the other obstacle with an acceptable safety margin. Therefore, the COLREGs are satisfied.

At first sight, the algorithms do have quite similar behavior, but there are some differences. The heading plot illustrates that the modified SBMPC kept a larger heading angle offset ψ_{ca} for a longer period of time compared to the SBMPC. However, the LOS guidance system caused the true own-ship heading angle ψ to decrease faster with the modified SBMPC compared to the SBMPC. The desired heading angle ψ_d computed by the LOS guidance system computed is fighting against the heading angle offset. This caused a lower CPA distance, r_{cpa}, and a lower safety score, $\mathcal{S}_{\text{safety}}$, for the modified SBMPC. The other metric scores for $\mathcal{S}_{\text{alarms}}$, $\mathcal{S}^8$, $\mathcal{S}^{14}$ and $\mathcal{S}^{16}$ were relatively similar for both algorithms. Overall, the modified SBMPC did not have any improvement in performance compared to the SBMPC.

The modified SBMPC decided to have a larger heading angle offset for a longer period because of a different trajectory prediction. The SBMPC algorithm on the own-ship predicted that the obstacle would travel in a straight line. In contrast, the modified SBMPC algorithm used intention data from the SBMPC obstacle to get a different prediction.

With SBMPC	With modified SBMPC
Active COLREGs: 8,14,16	Active COLREGs: 8,14,16
$r_{\text{cpa}} = 833$ m	$r_{\text{cpa}} = 732$ m
$\mathcal{S}_{\text{safety}} = 0.89$	$\mathcal{S}_{\text{safety}} = 0.83$
$\mathcal{S}_{\text{alarms}} = 0.56$	$\mathcal{S}_{\text{alarms}} = 0.56$
$\mathcal{S}^8 = 0.87$	$\mathcal{S}^8 = 0.86$
$\mathcal{S}^{14} = 0.93$	$\mathcal{S}^{14} = 0.96$
$\mathcal{S}^{16} = 0.70$	$\mathcal{S}^{16} = 0.71$

Table 7.2: Metric scores for the scenario with a head-on situation with a SBMPC obstacle ship.

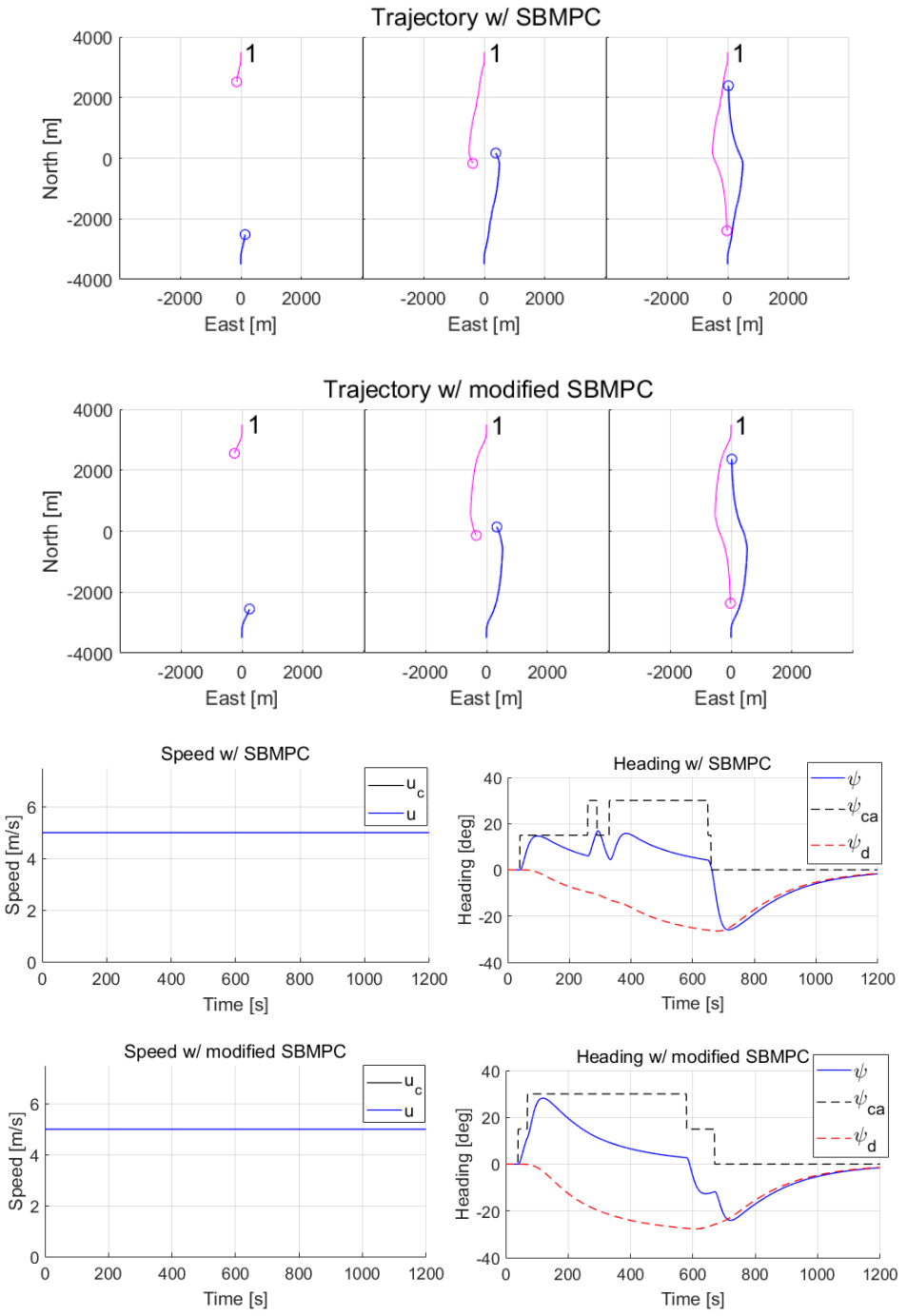

Figure 7.2: Simulation results from the scenario with a head-on situation with a SBMPC obstacle ship.

Head-on with a passive obstacle ship changing course

In this scenario, the own-ship was head-on with a passive obstacle ship that was breaking the COLREGs by turning to her port side. Figure 7.3 and Table 7.3 show the simulation results and metric scores obtained from this scenario.

The two algorithms did have different performance. By using intention data about the passive obstacle ship's planned waypoints, the own-ship with the modified SBMPC knew that the obstacle ship was going to turn. Therefore, the modified SBMPC started to maneuver earlier compared to the own-ship with the SBMPC. This resulted in a CPA distance increase of more than 300 m, which in return gave a higher safety score $\mathcal{S}_{\text{safety}}$. The modified SBMPC was also able to improve the COLREGs metrics $\mathcal{S}^8$, $\mathcal{S}^{14}$ and $\mathcal{S}^{16}$ compared to the SBMPC. This increase in COLREGs metrics scores happened because the modified SBMPC own-ship started to maneuver earlier, and also because of the increase in CPA distance. The metric for CPA/TCPA alarms $\mathcal{S}_{\text{alarms}}$ did not increase because the earlier maneuver did not increase the time until CPA. Overall, the modified SBMPC performed better in this scenario.

The speed plot in Figure 7.3 illustrates that the own-ship's speed dropped after about 850 seconds due to an abrupt change in the heading angle. The own-ship was not able to keep her full speed when making a sharp turn.

With SBMPC	With modified SBMPC
Active COLREGs: 8,14,16	Active COLREGs: 8,14,16
$r_{\text{cpa}} = 510$ m	$r_{\text{cpa}} = 830$ m
$\mathcal{S}_{\text{safety}} = 0.65$	$\mathcal{S}_{\text{safety}} = 0.89$
$\mathcal{S}_{\text{alarms}} = 0.55$	$\mathcal{S}_{\text{alarms}} = 0.53$
$\mathcal{S}^8 = 0.76$	$\mathcal{S}^8 = 0.94$
$\mathcal{S}^{14} = 0.89$	$\mathcal{S}^{14} = 0.93$
$\mathcal{S}^{16} = 0.53$	$\mathcal{S}^{16} = 0.88$

Table 7.3: Metric scores for the scenario with a head-on situation with a passive obstacle ship that changes course.

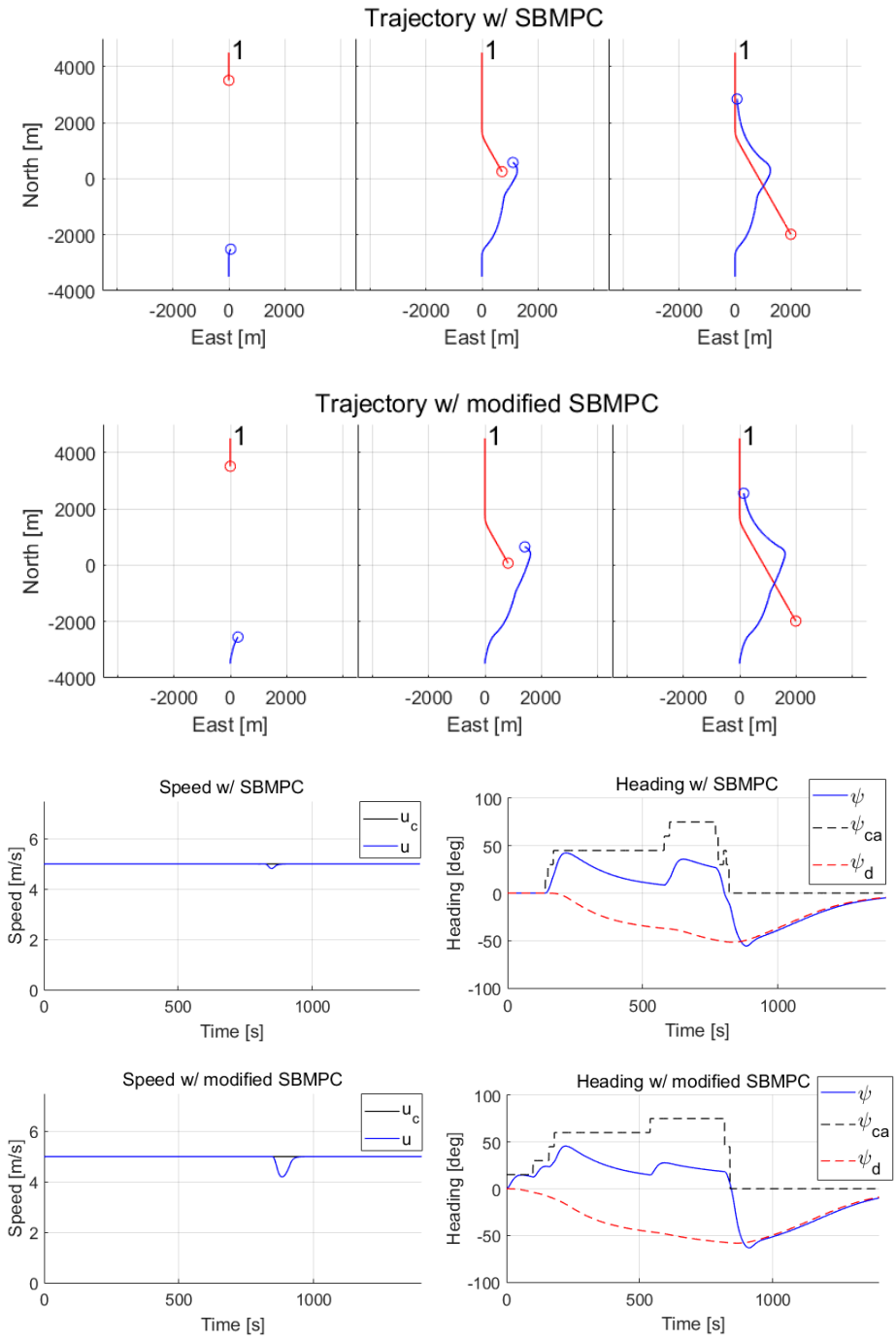

Figure 7.3: Simulation results from the scenario with a head-on situation with a passive obstacle ship that changes course.

Crossing with a SBMPC obstacle ship on the starboard side

The next scenario is a crossing situation between the own-ship and a SBMPC obstacle ship on the starboard side. According to COLREGs rule 15, the own-ship was give-way and was required to make an apparent starboard turn and avoid the SBMPC obstacle. Also, the SBMPC obstacle was the stand-on vessel and was required to keep a constant heading and speed. The simulation results and metric scores are shown in Figure 7.4 and Table 7.4.

In this scenario, there is a clear difference between the behavior from the SBMPC and the modified SBMPC. The own-ship with the SBMPC had an unfortunate back and forth motion that occurred when the own-ship was trying to compensate for the movement by the SBMPC obstacle ship. This behavior would be very confusing for a human navigator observing the situation, and it would make the situation difficult to interpret. The back and forth movement of the own-ship with SBMPC did result in a significantly lower score for $\mathcal{S}_{\text{alarms}}$ because the CPA/TCPA alarm was turned on and off several times.

The reason why the own-ship with the SBMPC turned back and forth several times was because the obstacle ship did not keep her stand-on role. In the modified SBMPC, the inclusion of intention data about the own-ship's planned role as a give-way vessel made the SBMPC obstacle ship keep a constant heading and speed. Thus, the SBMPC obstacle ship kept her stand-on role. Constant heading and speed were kept because the modified SBMPC algorithm in the obstacle ship gives a penalty for changing course or speed while being a stand-on vessel.

When the obstacle ship kept her stand-on role, the own-ship had a more smooth path and achieved a higher CPA distance. The modified SBMPC was in fact able to increase all metric scores, partly due to having a larger CPA distance. Therefore, the modified SBMPC performed better than the SBMPC in this scenario.

With SBMPC	With modified SBMPC
Active COLREGs: 8,15,16	Active COLREGs: 8,15,16
$r_{\text{cpa}} = 815$ m	$r_{\text{cpa}} = 947$ m
$\mathcal{S}_{\text{safety}} = 0.88$	$\mathcal{S}_{\text{safety}} = 0.97$
$\mathcal{S}_{\text{alarms}} = 0.07$	$\mathcal{S}_{\text{alarms}} = 0.33$
$\mathcal{S}^{8} = 0.93$	$\mathcal{S}^{8} = 0.97$
$\mathcal{S}^{15} = 0.84$	$\mathcal{S}^{15} = 0.93$
$\mathcal{S}^{16} = 0.84$	$\mathcal{S}^{16} = 0.93$

Table 7.4: Metric scores for the scenario with a crossing situation with a SBMPC obstacle ship on the starboard side.

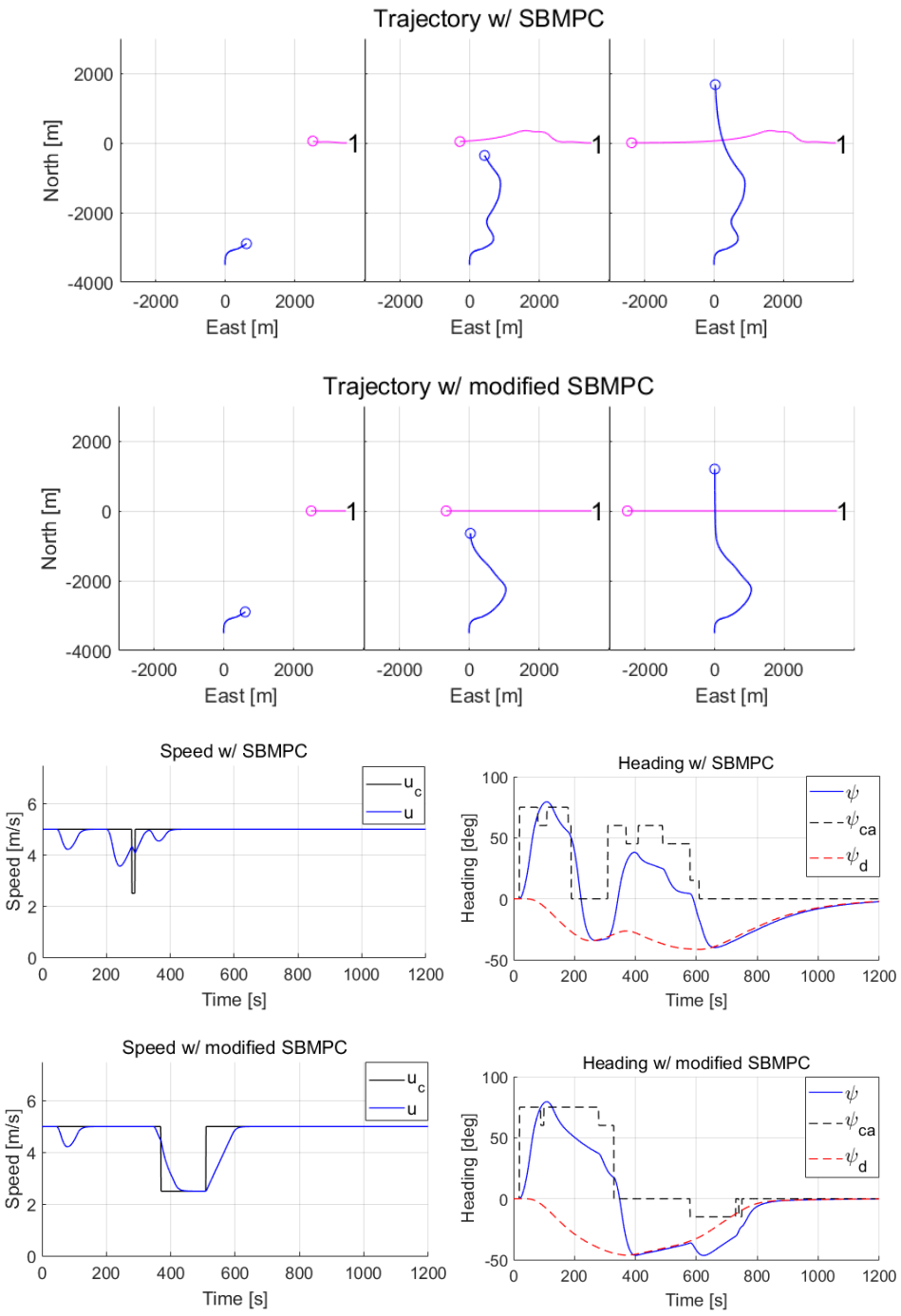

Figure 7.4: Simulation results from the scenario with a crossing situation with a SBMPC obstacle ship on the starboard side.

Crossing with a passive obstacle ship on the port side that changes course

This scenario contains a crossing situation with a passive obstacle ship on the port side. A static circle obstacle is also included. The simulation results and metric scores are shown in Figure 7.5 and Table 7.5. In this situation, COLREGs rule 15 required the own-ship to be a stand-on vessel and the passive obstacle ship to be a give-way vessel. The obstacle ship intended to follow the COLREGs and turned starboard to avoid collision.

In this scenario, both algorithms were able to avoid grounding with the circle obstacle with high safety margins. Also, both algorithms were able to avoid collision with the obstacle ship. However, the modified SBMPC algorithm did a better job of following the stand-on requirement from the COLREGs. Therefore, high scores for $\mathcal{S}^{15}$ and $\mathcal{S}^{17}$ were achieved with the modified SBMPC. In contrast, the SBMPC algorithm made the own-ship turn to starboard and did not follow her stand-on responsibility. Thus, the metric scores for $\mathcal{S}^{15}$ and $\mathcal{S}^{17}$ from the SBMPC were relatively low.

The reason why the modified SBMPC was able to keep the stand-on responsibility was due to the utilization of intention data. The modified SBMPC own-ship knew that the obstacle ship was going to turn, and decided that keeping a constant heading and speed would result in an acceptable CPA distance. The intention data about the obstacle's planned role to be a give-way vessel also helped with keeping the own-ship on a straight course, because a penalty is given to the own-ship when trying to turn while being the stand-on vessel.

Keeping a straight course did reduce $\mathcal{S}_{\text{alarms}}$ with the modified SBMPC because the own-ship did not try to steer away from the obstacle. However, the original SBMPC achieved a higher CPA distance, which gave a higher safety score than the modified SBMPC. Overall, the modified SBMPC did perform better in this scenario because an acceptable safety score was achieved along with higher COLREGs compliance compared to the SBMPC.

With SBMPC	With modified SBMPC
Active COLREGs: 15,17	Active COLREGs: 15,17
$r_{\text{cpa}} = 1353$ m	$r_{\text{cpa}} = 586$ m
$\mathcal{S}_{\text{safety}} = 0.92$	$\mathcal{S}_{\text{safety}} = 0.81$
$\mathcal{S}_{\text{circle}} = 1.00$	$\mathcal{S}_{\text{circle}} = 1.00$
$\mathcal{S}_{\text{alarms}} = 0.67$	$\mathcal{S}_{\text{alarms}} = 0.61$
$\mathcal{S}^{15} = 0.19$	$\mathcal{S}^{15} = 0.80$
$\mathcal{S}^{17} = 0.19$	$\mathcal{S}^{17} = 0.80$

Table 7.5: Metric scores for the scenario with a crossing situation with a passive obstacle ship on the port side that changes course.

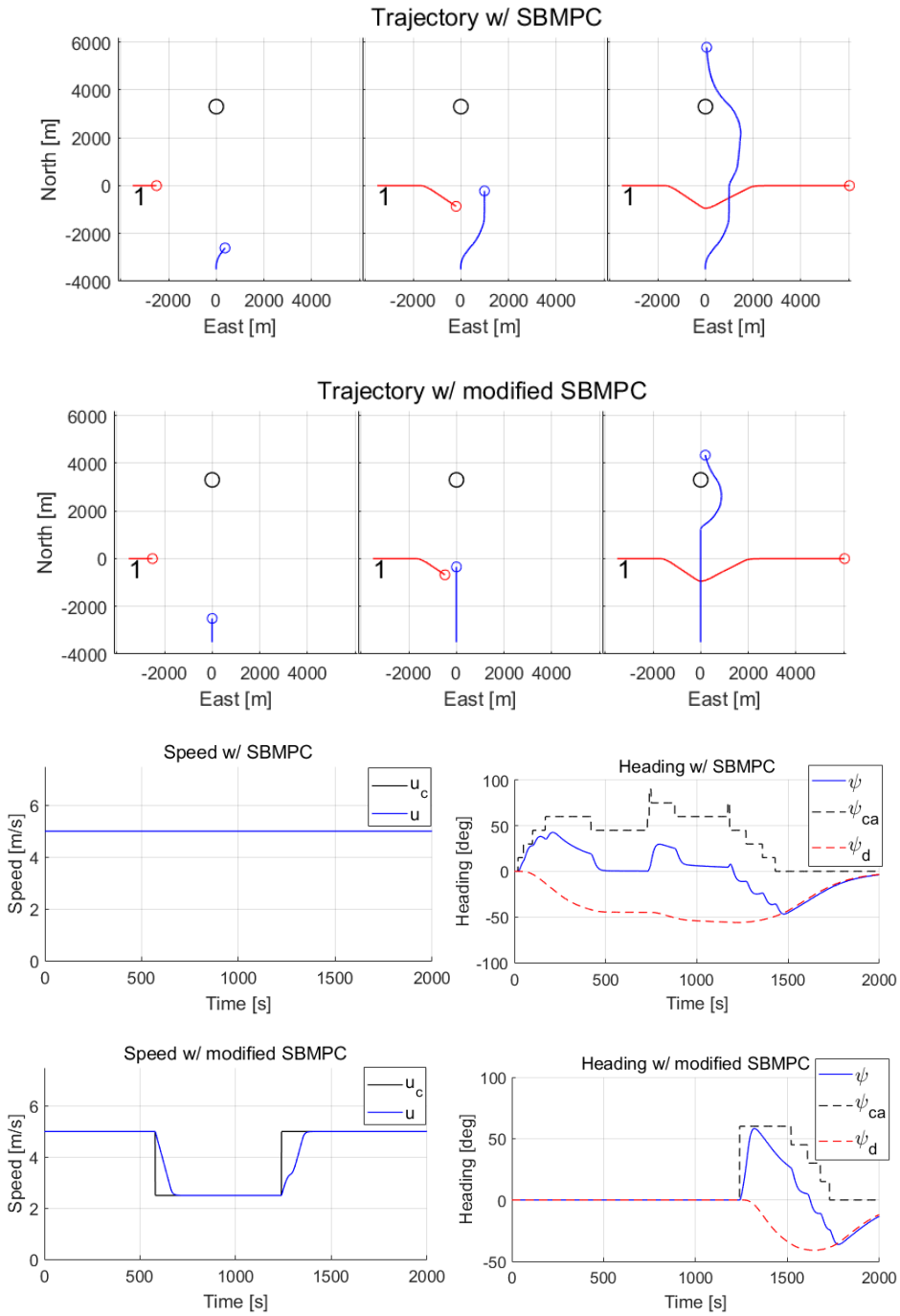

Figure 7.5: Simulation results from the scenario with a crossing situation with a passive obstacle ship on the port side that changes course.

Own-ship overtakes a passive obstacle ship

In this scenario, the own-ship was traveling with a speed of 5 m/s and planned to overtake a passive obstacle ship traveling in the same direction with a speed of 1 m/s. The simulation results and metric scores can be seen in Figure 7.6 and Table 7.6. COLREGs rule 13 required the own-ship to be a give-way vessel and the obstacle ship to be a stand-on vessel. In overtaking situations, the give-way vessel is allowed to overtake the stand-on vessel on either side.

Both the SBMPC and the modified SBMPC had the exact same behavior with the exact same metric scores. The use of intentions did not improve the trajectory prediction when the obstacle ship followed a straight path. $\mathcal{S}^8$ is quite high, which indicates that the maneuver was apparent and taken in ample time. The scores for $\mathcal{S}^{13}$ and $\mathcal{S}^{16}$ were somewhat lower, primarily because of a low CPA distance. With both algorithms, the own-ship preferred to overtake the obstacle ship on the starboard side. This happened because the algorithms are tuned to prefer a starboard turn over a port turn.

When inspecting the trajectory plots in Figure 7.6, it becomes clear that both algorithms decided to turn back to the nominal path too early. This caused a low CPA distance and was not optimal in terms of safety. A better behavior would be achieved if the own-ship kept the heading angle offset of 45° for a longer period of time and started to turn back after being ahead of the obstacle ship. This behavior could be achieved with a different set of tuning parameters, for instance by increasing the risk of collision.

With SBMPC	With modified SBMPC
Active COLREGs: 8,13,16	Active COLREGs: 8,13,16
$r_{\text{cpa}} = 382$ m	$r_{\text{cpa}} = 382$ m
$\mathcal{S}_{\text{safety}} = 0.63$	$\mathcal{S}_{\text{safety}} = 0.63$
$\mathcal{S}_{\text{alarms}} = 0.54$	$\mathcal{S}_{\text{alarms}} = 0.54$
$\mathcal{S}^8 = 0.83$	$\mathcal{S}^8 = 0.83$
$\mathcal{S}^{13} = 0.58$	$\mathcal{S}^{13} = 0.58$
$\mathcal{S}^{16} = 0.58$	$\mathcal{S}^{16} = 0.58$

Table 7.6: Metric scores for the scenario where the own-ship overtakes a passive obstacle ship.

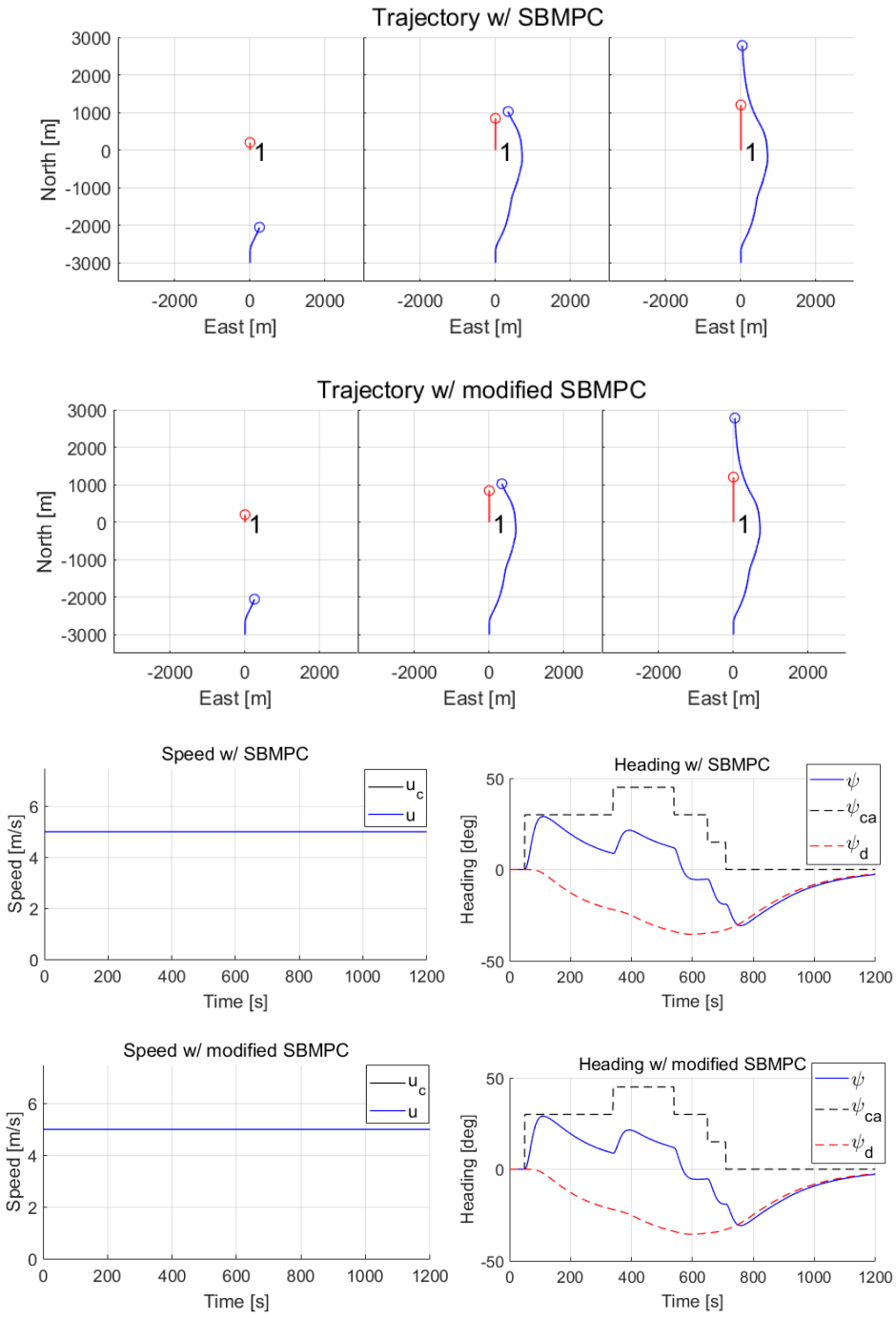

Figure 7.6: Simulation results from the scenario where the own-ship overtakes a passive obstacle ship.

The same scenario is simulated once more with a static boundary obstacle on the starboard side of the own-ship. The simulation results and metric scores for this scenario are shown in Figure 7.7 and Table 7.7. Here, the own-ship decided to pass the obstacle ship on the port side instead of the starboard side. Once again, the SBMPC and modified SBMPC had the same behavior with the same metric scores. Both collision avoidance algorithms were able to handle the presence of a static boundary obstacle, and they achieved a maximum boundary safety score $\mathcal{S}_{\text{boundary}} = 1.00$.

With the presence of a boundary obstacle, the CPA distance was more than 100 m smaller compared to the scenario without any boundary obstacle. As a result, very low metric scores for $\mathcal{S}_{\text{safety}}$, $\mathcal{S}^{13}$ and $\mathcal{S}^{16}$ were given. The reason for having a lower CPA distance comes from the choice of tuning parameters. Turning to the port side gives a higher penalty compared to starboard turns, which made the own-ship prefer a smaller heading offset compared to the previous scenario. With this in mind, it would be beneficial to reduce the penalty for port turns. This would result in higher CPA distances for this particular scenario.

It should also be noted that the propulsion command was set to 0.5 for almost the entire scenario. Intuitively, reducing the speed should not give any advantage in an overtaking situation. This indicates that the tuning parameters could be changed to give a higher penalty for speed reductions. It is also strange that the algorithms had a short, positive heading angle offset before the heading angle offset became negative. This probably happened because port turns have too high penalty.

With SBMPC	With modified SBMPC
Active COLREGs: 8,13,16	Active COLREGs: 8,13,16
$r_{\text{cpa}} = 252$ m	$r_{\text{cpa}} = 252$ m
$\mathcal{S}_{\text{safety}} = 0.35$	$\mathcal{S}_{\text{safety}} = 0.35$
$\mathcal{S}_{\text{alarms}} = 0.08$	$\mathcal{S}_{\text{alarms}} = 0.08$
$\mathcal{S}_{\text{boundary}} = 1.00$	$\mathcal{S}_{\text{boundary}} = 1.00$
$\mathcal{S}^{8} = 0.68$	$\mathcal{S}^{8} = 0.68$
$\mathcal{S}^{13} = 0.33$	$\mathcal{S}^{13} = 0.33$
$\mathcal{S}^{16} = 0.33$	$\mathcal{S}^{16} = 0.33$

Table 7.7: Metric scores for the scenario where the own-ship overtakes a passive obstacle ship with a static boundary obstacle on the starboard side.

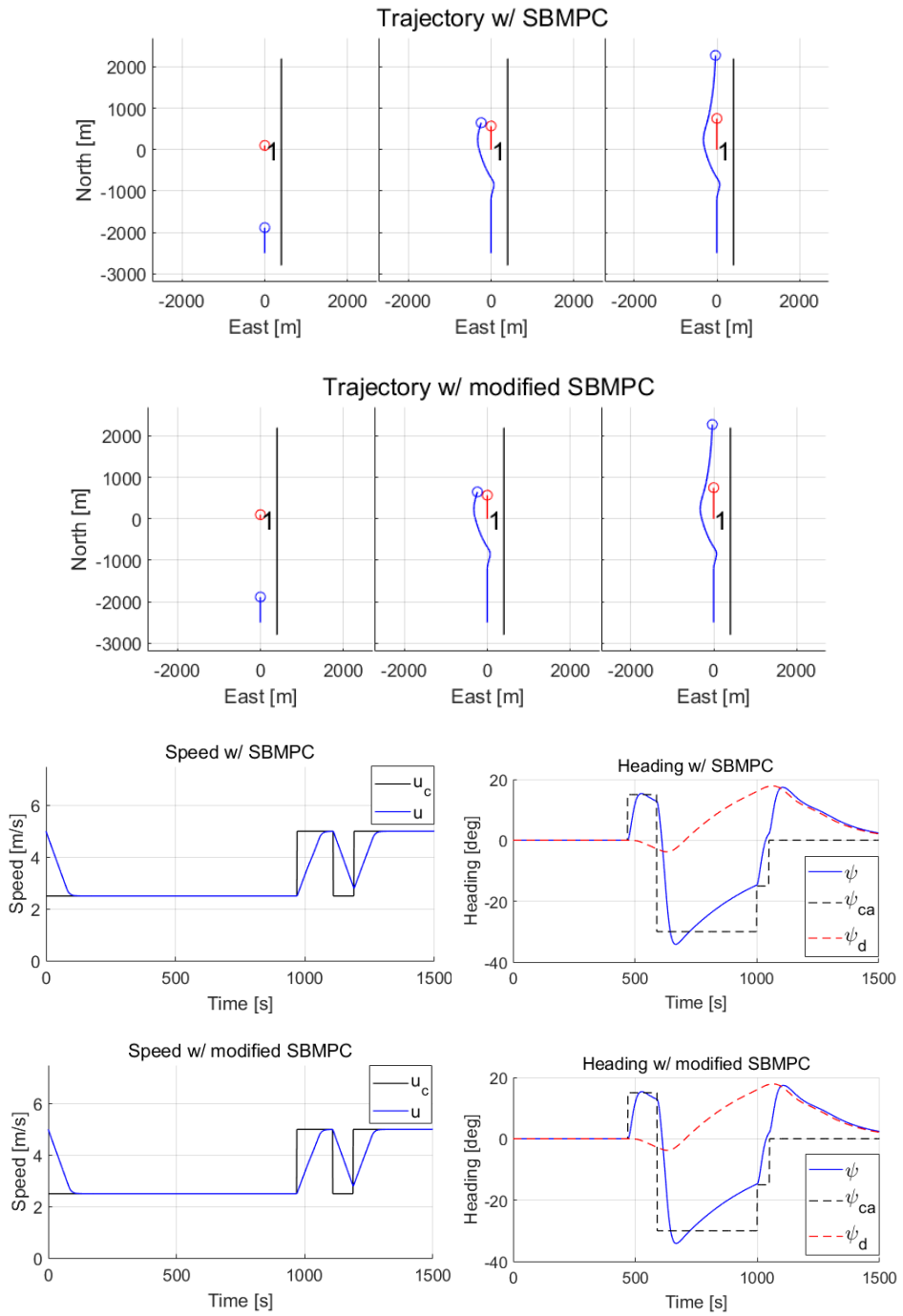

Figure 7.7: Simulation results from the scenario where the own-ship overtakes a passive obstacle ship with a static boundary obstacle on the starboard side.

Own-ship overtaken by a passive obstacle ship

In this scenario, the own-ship was traveling north with a speed of 1 m/s, and a passive obstacle ship was overtaking the own-ship with a speed of 5 m/s. The simulation results and the metric scores can be seen in Figures 7.8 and Table 7.8. The obstacle ship was assigned the give-way role by COLREGs rule 13, but did not intend to steer out of the way. Therefore, the own-ship needed to perform a maneuver to avoid collision.

Both the SBMPC and modified SBMPC had the same behavior with the same metric scores. When the obstacle ship traveled along a straight path, the trajectory prediction of the obstacle ship was equal in both algorithms. Both $\mathcal{S}^{13}$ and $\mathcal{S}^{17}$ had a score of zero because the own-ship decided to perform an apparent heading change. However, these scores did not take into account that the own-ship had to perform a maneuver because the obstacle ship was breaking COLREGs. Therefore, the metric scores are not representative of the behavior. Even though low scores were achieved, the own-ship did have acceptable behavior since she was able to perform an evasive maneuver that avoided collision. However, it would be preferred to have a higher safety score.

With SBMPC	With modified SBMPC
Active COLREGs: 8,13,17	Active COLREGs: 8,13,17
$r_{\text{cpa}} = 336$ m $\mathcal{S}_{\text{safety}} = 0.48$ $\mathcal{S}_{\text{alarms}} = 0.32$ $\mathcal{S}^{13} = 0.00$ $\mathcal{S}^{17} = 0.00$	$r_{\text{cpa}} = 336$ m $\mathcal{S}_{\text{safety}} = 0.48$ $\mathcal{S}_{\text{alarms}} = 0.32$ $\mathcal{S}^{13} = 0.00$ $\mathcal{S}^{17} = 0.00$

Table 7.8: Metric scores for the scenario where a passive obstacle ship overtakes the own-ship.

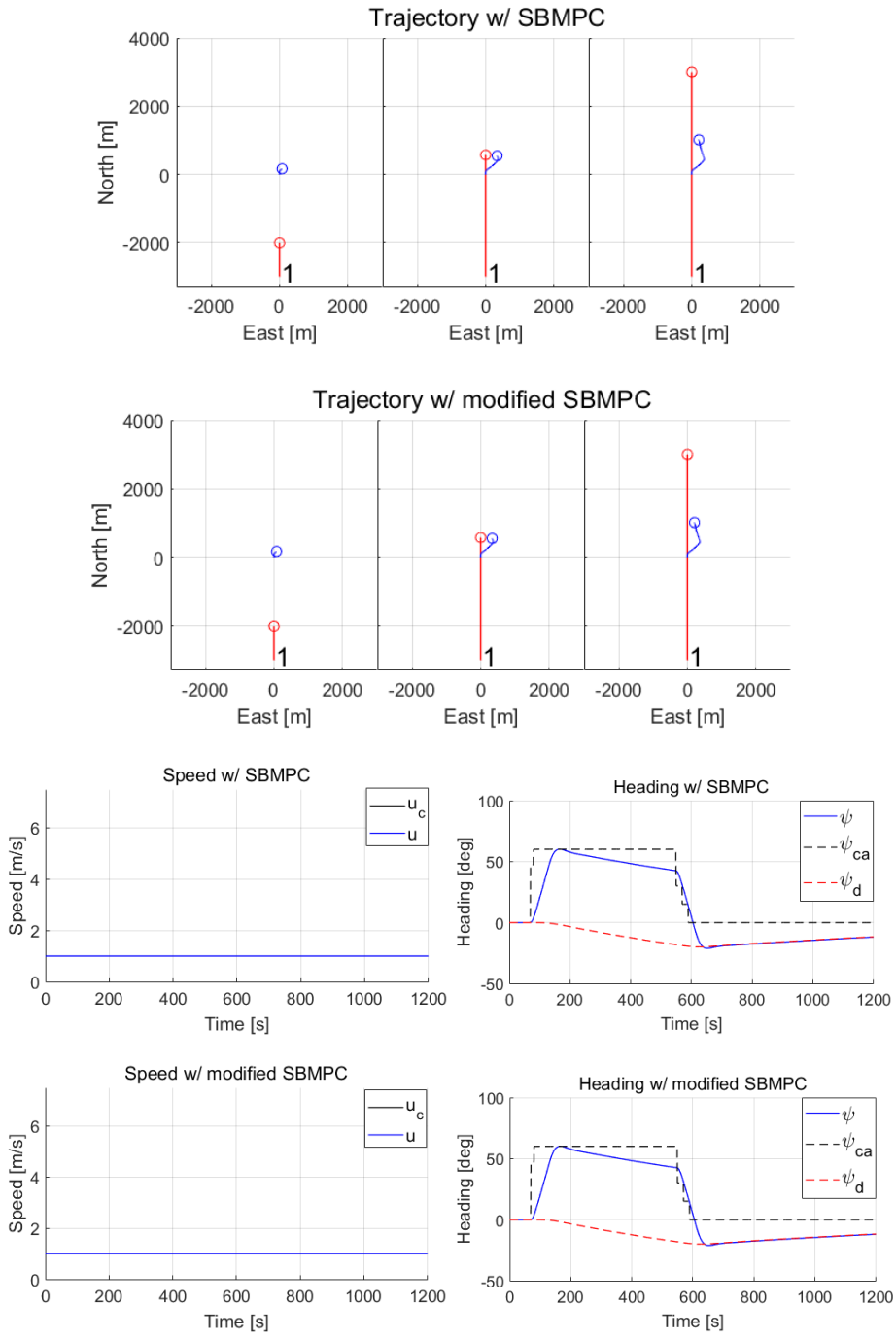

Figure 7.8: Simulation results from the scenario where a passive obstacle ship overtakes the own-ship.

7.2.2 Choice of metrics in scenarios with multiple obstacle ships

The previous section presented simulation results from scenarios with a single obstacle ship where metrics for COLREGs compliance with rules 8 and 13-17 were computed. The rest of the simulation study is concerned with scenarios with two, three and four obstacle ships. When in a complicated collision situation with several obstacle ships, the COLREGs can sometimes give conflicting requirements. For instance, when two obstacle ships are crossing ahead of the own-ship on both sides, the own-ship has both stand-on role relative to the obstacle ship on the port side and give-way role relative to the obstacle ship on the starboard side. In complicated scenarios, it can be impossible to comply 100% with all COLREGs rules.

Because of the problem with conflicting COLREGs, different metrics will be used in different multi-obstacle scenarios. In scenarios where the own-ship only has give-way responsibility at the start of the scenario, the metrics for the relevant COLREGs rules will be computed. However, in situations where the own-ship has stand-on and give-way responsibility at the same time, the metrics for COLREGs rules will not be used. Instead, only the safety metric $\mathcal{S}_{\text{safety}}$ will be used. The CPA/TCPA alarms metric $\mathcal{S}_{\text{alarms}}$ will not be calculated for the scenarios with multiple obstacles, since other ships will always be close.

In addition to using metrics, the performance of the two algorithms in multi-obstacle scenarios have been discussed with an experienced navigator from DNV GL. A summary of this discussion can be found in Appendix A.4. From this discussion, it became clear that passing ahead of obstacle ships is dangerous and should be avoided. Also, in complicated situations it is preferred to avoid unnecessary turning whenever it is safe. Too much turning can cause human navigators to misinterpret the situation and make bad decisions.

7.2.3 Scenarios with two obstacle ships

Two crossing obstacle ships

Next, a scenario where the own-ship was in a crossing situation with a passive obstacle ship and a SBMPC obstacle ship will be discussed. The simulation results and metric scores can be seen in Figure 7.9 and Table 7.9. This table shows which rules apply for the own-ship relative to the encounters with obstacles 1 and 2. The CPA distance, r_{cpa}, and safety score, $\mathcal{S}_{\text{safety}}$, achieved by the own-ship relative to both obstacles are also displayed. From COLREGs rule 15 for crossing situations, the own-ship had stand-on responsibility relative to the SBMPC obstacle ship 2 and give-way responsibility relative to the passive obstacle ship 1. Because of conflicting roles for the own-ship, COLREGs metrics are not calculated. This situation was extra challenging due to the presence of two circle obstacles.

Both algorithms had acceptable behavior, and they both avoided collision and grounding with acceptable safety margins. Because the SBMPC algorithm kept a distance of 44 m

further away from the circle obstacle, a higher score for $\mathcal{S}_{\text{circle}}$ was achieved with the SBMPC. Both algorithms reduced the own-ship's speed at the start of the scenario to increase the CPA distance relative to obstacle ship 1.

There were some differences in the behavior with the SBMPC and the modified SBMPC for obstacle ship 2. First of all, with the SBMPC algorithm, obstacle ship 2 decided to turn around both circle obstacles. In contrast, the modified SBMPC made obstacle ship 2 travel between the circle obstacles. The difference in behavior occurred due to different trajectory prediction with the two algorithms.

The own-ship also behaved differently with the two algorithms. With the modified SBMPC, the own-ship decided to keep a relatively straight course until after 400 seconds when the own-ship made a sharper starboard turn compared to the SBMPC. This caused the modified SBMPC to have a higher CPA distance relative to obstacle ship 1 compared to the SBMPC algorithm. Overall, the values for $\mathcal{S}_{\text{safety}}$ show that the use of intentions did make the own-ship's maneuver safer relative to obstacle ship 1, but at the same time, the maneuver was less safe relative to obstacle ship 2. Even though it is preferred that obstacle ship 2 avoids large maneuvers, since this will make the situation harder to interpret, the use of intentions did not give an increase in performance.

With SBMPC			With modified SBMPC		
	Obs. 1	Obs. 2		Obs. 1	Obs. 2
Rules	8,15,16	15,17	Rules	8,15,16	15,17
r_{cpa}	545 m	1676 m	r_{cpa}	617 m	1152 m
$\mathcal{S}_{\text{safety}}$	0.69	0.89	$\mathcal{S}_{\text{safety}}$	0.75	0.87
$\mathcal{S}_{\text{circle}} = 1.00$			$\mathcal{S}_{\text{circle}} = 0.81$		

Table 7.9: Metric scores for the scenario where the own-ship is in a crossing situation with a SBMPC obstacle ship on the port side and a passive obstacle ship on the starboard side.

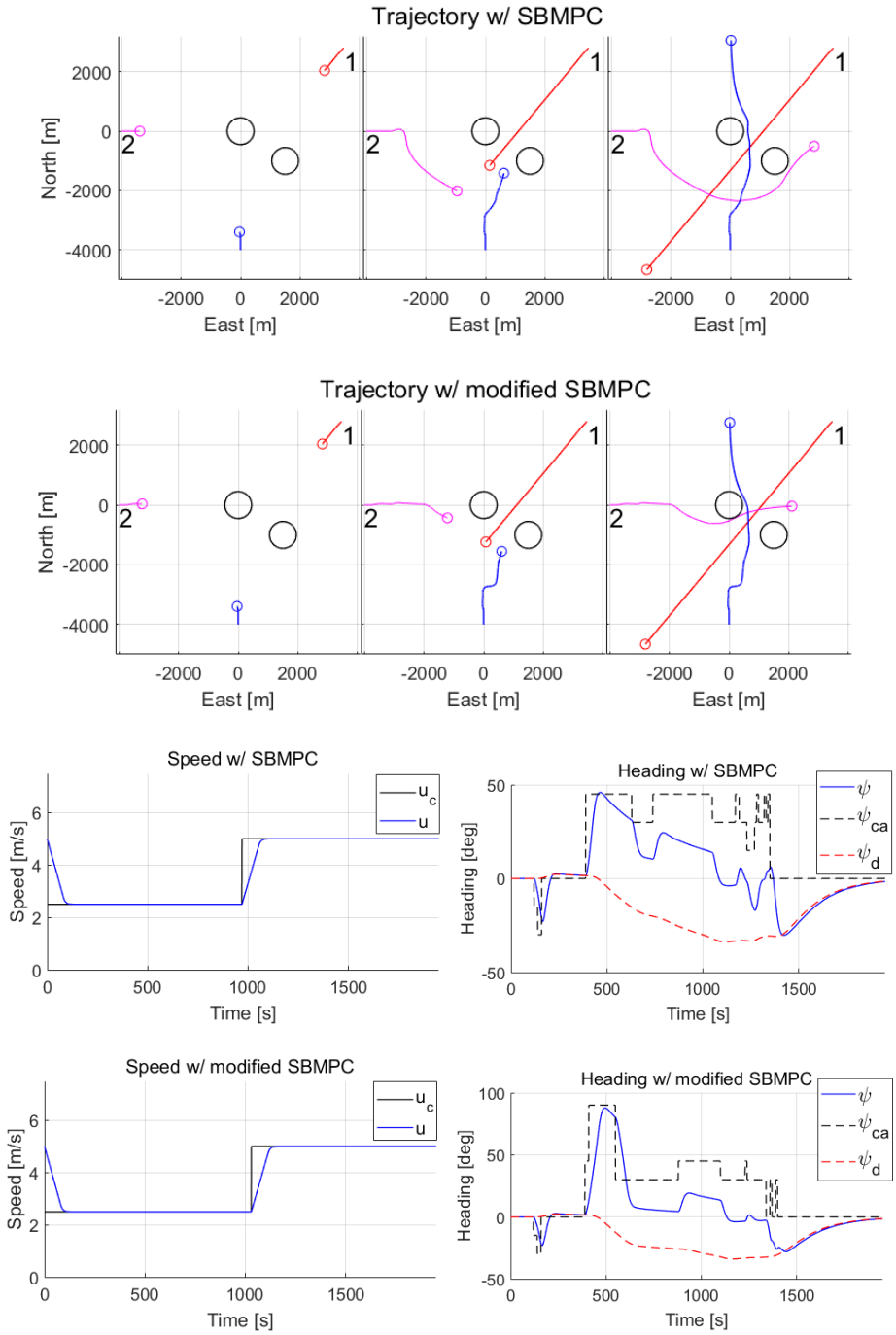

Figure 7.9: Simulation results from the scenario where the own-ship is in a crossing situation with a SBMPC obstacle ship on the port side and a passive obstacle ship on the starboard side.

Own-ship overtakes and is head-on with SBMPC obstacle ships

Simulation results and metric scores from a scenario where the own-ship was overtaking SBMPC obstacle ship 1 and was head-on with SBMPC obstacle ship 2 can be found in Figure 7.10 and Table 7.10. In this scenario, the own-ship was traveling north with a speed of 4.5 m/s and was overtaking SBMPC obstacle ship 1 traveling with a speed of 1 m/s. The own-ship had give-responsibility relative to both obstacle ships according to COLREGs rules 13 and 14. Thus, the own-ship should turn to starboard to satisfy the requirements from the head-on situation.

The SBMPC and modified SBMPC algorithms gave different results in this scenario. With the SBMPC, the own-ship and obstacle ship 2 passed obstacle ship 1 on opposite sides. In contrast, the modified SBMPC made the own-ship and obstacle ship 2 pass obstacle ship 1 on the same side. This difference in behavior occurred because the own-ship intended to be a give-way vessel relative to obstacle ship 1. Thus, the modified SBMPC on obstacle ship 1 decided to keep a constant heading and speed because of the intention data received from the own-ship.

From the metric scores in Table 7.10 it can be observed that the modified SBMPC did have the lowest scores for all metrics relative to obstacle 2 because the CPA distance was reduced. However, the modified SBMPC did have a higher safety score and COLREGs score relative to obstacle ship 1. The fact that the SBMPC caused all vessels to perform substantial turns made the situation very complicated. The back and forth motion of the own-ship is especially bad. This makes the situation difficult to interpret for any human navigators. Overall, the modified SBMPC gave better in this scenario because it avoided excessive turning and still had acceptable safety.

With SBMPC			With modified SBMPC		
	Obs. 1	Obs. 2		Obs. 1	Obs. 2
Rules	8,13,16	8,14,16	Rules	8,13,16	8,14,16
r_{cpa}	334 m	684 m	r_{cpa}	376 m	548 m
$\mathcal{S}_{\text{safety}}$	0.59	0.79	$\mathcal{S}_{\text{safety}}$	0.63	0.69
$\mathcal{S}^8$	0.82	0.89	$\mathcal{S}^8$	0.84	0.84
$\mathcal{S}^{13}$	0.57	-	$\mathcal{S}^{13}$	0.60	-
$\mathcal{S}^{14}$	-	0.99	$\mathcal{S}^{14}$	-	0.84
$\mathcal{S}^{16}$	0.57	0.79	$\mathcal{S}^{16}$	0.60	0.69

Table 7.10: Metric scores for the scenario where the own-ship is overtaking a SBMPC obstacle ship while being in a head-on situation with another SBMPC obstacle ship.

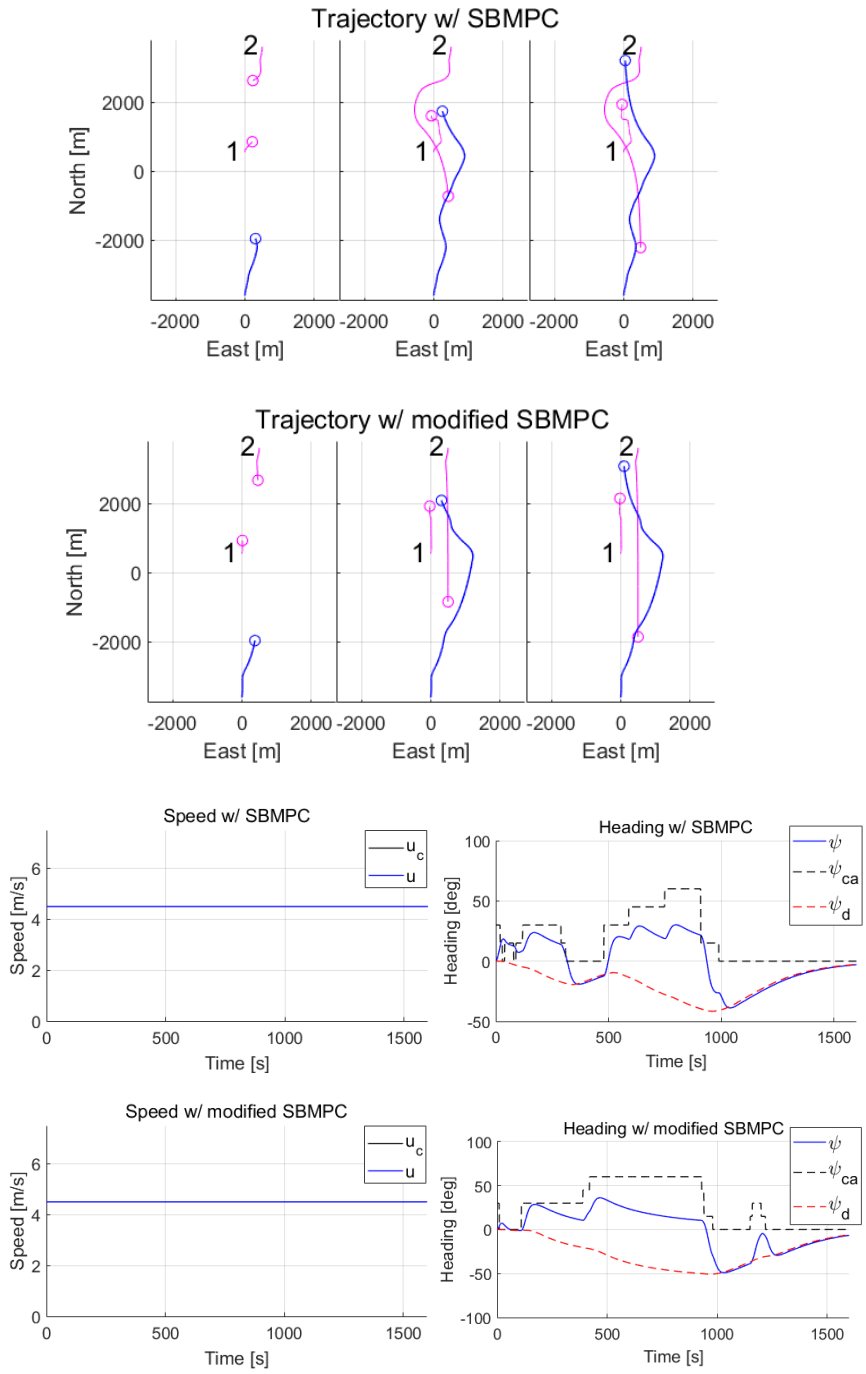

Figure 7.10: Simulation results from the scenario where the own-ship is overtaking a SBMPC obstacle ship while being in a head-on situation with another SBMPC obstacle ship.

7.2.4 Scenarios with three obstacle ships

Own-ship traveling towards a shallow water zone and facing three obstacle ships

In this scenario, the own-ship was facing two SBMPC obstacle ships and a passive obstacle ship. The speed of the own-ship, obstacle ship 1 and 2 were 4 m/s and obstacle ship 3's speed was 2 m/s. Also, two static obstacles enclosed a region with shallow water that the vessels must avoid. The simulation results and metric scores can be seen in Figure 7.11 and Table 7.11. The own-ship was initially in no COLREGs situation with obstacle ships 1 and 2, but in a crossing situation with obstacle ship 3 where the own-ship had stand-on responsibility according to rule 15. The COLREGs metrics are not calculated in this scenario because the own-ship was stand-on, but was still required to maneuver because of the static obstacles.

The collision avoidance algorithms did have different results in this scenario. For the own-ship, the SBMPC algorithm decided to have a sizeable heading offset of 75° at the start of the scenario. On the other hand, the modified SBMPC slowly increased the heading offset over time, which resulted in a more smooth path.

The most crucial difference between the SBMPC and the modified SBMPC was the behavior of SBMPC obstacle ship 3. With the SBMPC algorithm, obstacle ship 3 kept a constant heading angle and therefore broke COLREGs rule 15 that required obstacle ship 3 to give way for the own-ship. In contrast, the modified SBMPC made obstacle ship 3 perform a starboard turn to avoid the own-ship. The difference between the algorithms occurred primarily because of better trajectory prediction with the modified SBMPC.

Both collision avoidance algorithms were able to make the own-ship keep well clear of the boundary obstacle, as reflected with metrics score for $\mathcal{S}_{\text{boundary}}$ of 1 and 0.97. Compared to the SBMPC own-ship, the modified SBMPC own-ship was able to achieve a better safety score $\mathcal{S}_{\text{safety}}$ relative to obstacle ship 3, but had worse safety score relative to the two other obstacle ships. Overall, the modified SBMPC did perform better since it made obstacle ship 3 perform a starboard turn to follow rule 15 of the COLREGs. The difference in safety scores for obstacles 1 and 2 is not of vital importance. Generally, it is most important to increase the safety of the least safe encounter.

With SBMPC			
	Obs. 1	Obs. 2	Obs. 3
Rules	-	-	15,17
r_{cpa}	636 m	836 m	258 m
$\mathcal{S}_{\text{safety}}$	0.73	0.95	0.51
$\mathcal{S}_{\text{boundary}} = 1.00$			

With modified SBMPC			
	Obs. 1	Obs. 2	Obs. 3
Rules	-	-	15,17
r_{cpa}	624 m	688 m	418 m
$\mathcal{S}_{\text{safety}}$	0.70	0.81	0.67
$\mathcal{S}_{\text{boundary}} = 0.97$			

Table 7.11: Metric scores for the scenario where the own-ship is traveling towards a shallow water zone and facing three obstacle ships.

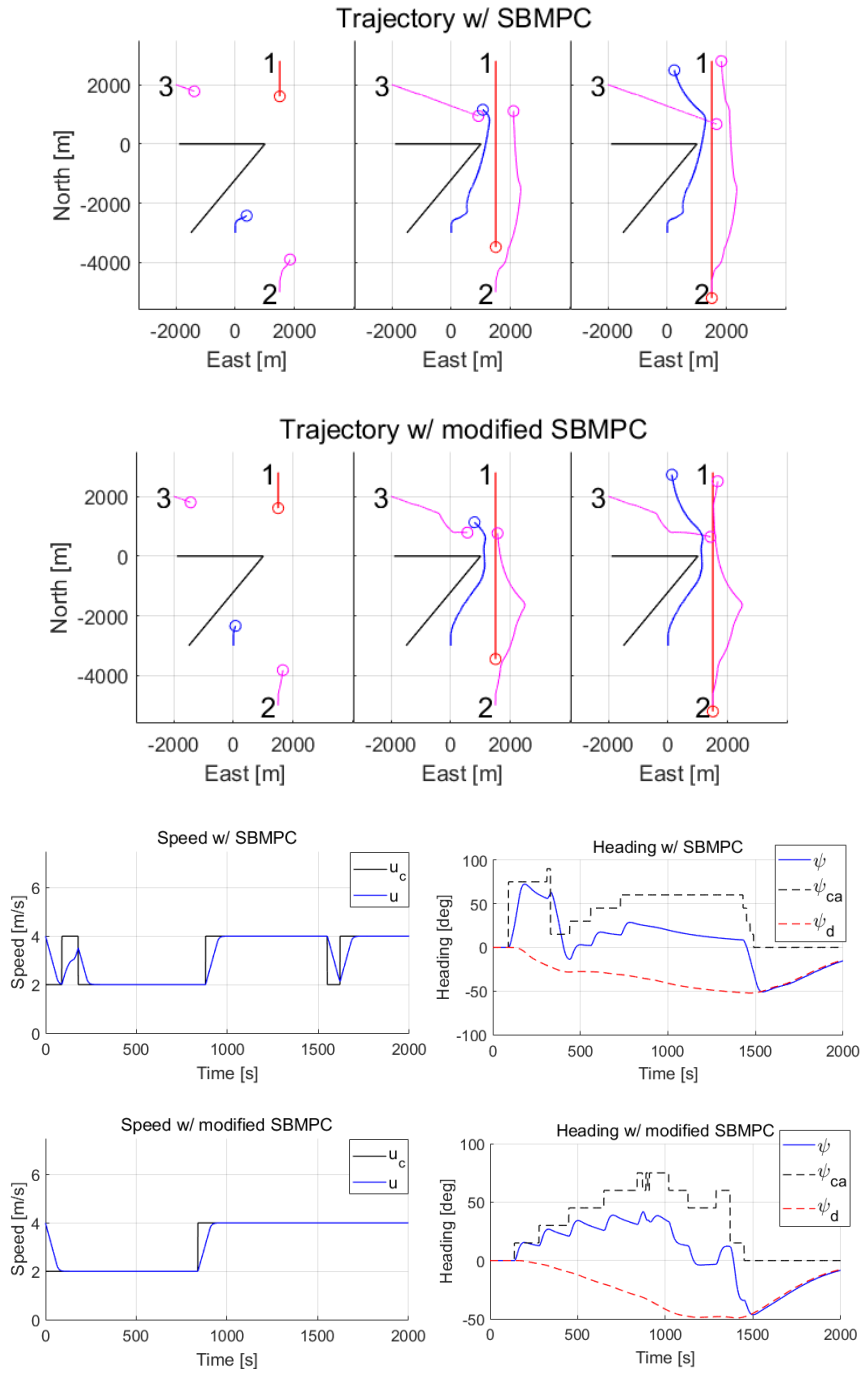

Figure 7.11: Simulation results from the scenario where the own-ship is traveling towards a shallow water zone and facing three obstacle ships.

Own-ship is overtaking, head-on and in a crossing situation with three obstacle ships

Simulation results and metric scores from this scenario are shown in Figure 7.12 and Table 7.12. The own-ship overtook SBMPC obstacle ship 3 traveling at 2 m/s. Initially, the own-ship was also in a head-on situation with passive obstacle ship 1 and in a crossing situation with passive obstacle ship 2. The own-ship had give-way responsibility relative to all obstacle ships, and the own-ship needed to perform a starboard turn to comply with the COLREGs.

There are some differences between the SBMPC and modified SBMPC. Both algorithms decided to perform a starboard turn and pass ahead of obstacle ship 1, but the modified SBMPC own-ship started to turn earlier than the SBMPC own-ship. This happened because the modified SBMPC knew that ship 1 would turn from the intention data about ship 1's planned waypoints. The modified SBMPC gave a higher CPA distance relative to obstacle ship 1 and also achieved higher scores for $\mathcal{S}^8$, $\mathcal{S}^{14}$ and $\mathcal{S}^{16}$ compared to the SBMPC. Relative to obstacle ship 3, the two algorithms achieved approximately the same metric scores. A higher CPA distance relative to obstacle 3 would be achieved if the own-ship waited longer before returning to her nominal path. The metric scores relative to obstacle ships 2 were equal with both algorithms.

Another interesting observation is the behavior of SBMPC obstacle ship 3. This obstacle ship had conflicting roles: give-way relative to obstacle ship 2 and stand-on relative to the own-ship. With the SBMPC, obstacle ship 3 was able to turn starboard and satisfy the COLREGs requirement for the crossing situation with passive obstacle ship 2. However, with the modified SBMPC, the stand-on role caused a penalty for maneuvering. Therefore, the obstacle ship 3 did not make any substantial heading changes with the modified SBMPC.

As long as a safe distance is kept, no turning is preferred since turning makes the situation harder to interpret. Overall, the modified SBMPC performed better in this scenario because it made obstacle ship 3 maneuver less and made own-ship achieve higher safety score relative to obstacle ship 1.

With SBMPC				With modified SBMPC			
	Obs. 1	Obs. 2	Obs. 3		Obs. 1	Obs. 2	Obs. 3
Rules	8,14,16	8,15,16	8,13,16	Rules	8,14,16	8,15,16	8,13,16
r_{cpa}	433 m	2080 m	447 m	r_{cpa}	749 m	2474 m	416 m
$\mathcal{S}_{\text{safety}}$	0.58	1.00	0.66	$\mathcal{S}_{\text{safety}}$	0.84	1.00	0.65
$\mathcal{S}^8$	0.76	0.99	0.88	$\mathcal{S}^8$	0.90	0.99	0.87
$\mathcal{S}^{13}$	-	-	0.64	$\mathcal{S}^{13}$	-	-	0.64
$\mathcal{S}^{14}$	0.89	-	-	$\mathcal{S}^{14}$	0.92	-	-
$\mathcal{S}^{15}$	-	0.97	-	$\mathcal{S}^{15}$	-	0.97	-
$\mathcal{S}^{16}$	0.54	0.97	0.64	$\mathcal{S}^{16}$	0.78	0.97	0.64

Table 7.12: Metric scores for the scenario where the own-ship is overtaking a SBMPC obstacle ship while being in a head-on situation and a crossing situation with passive obstacle ships.

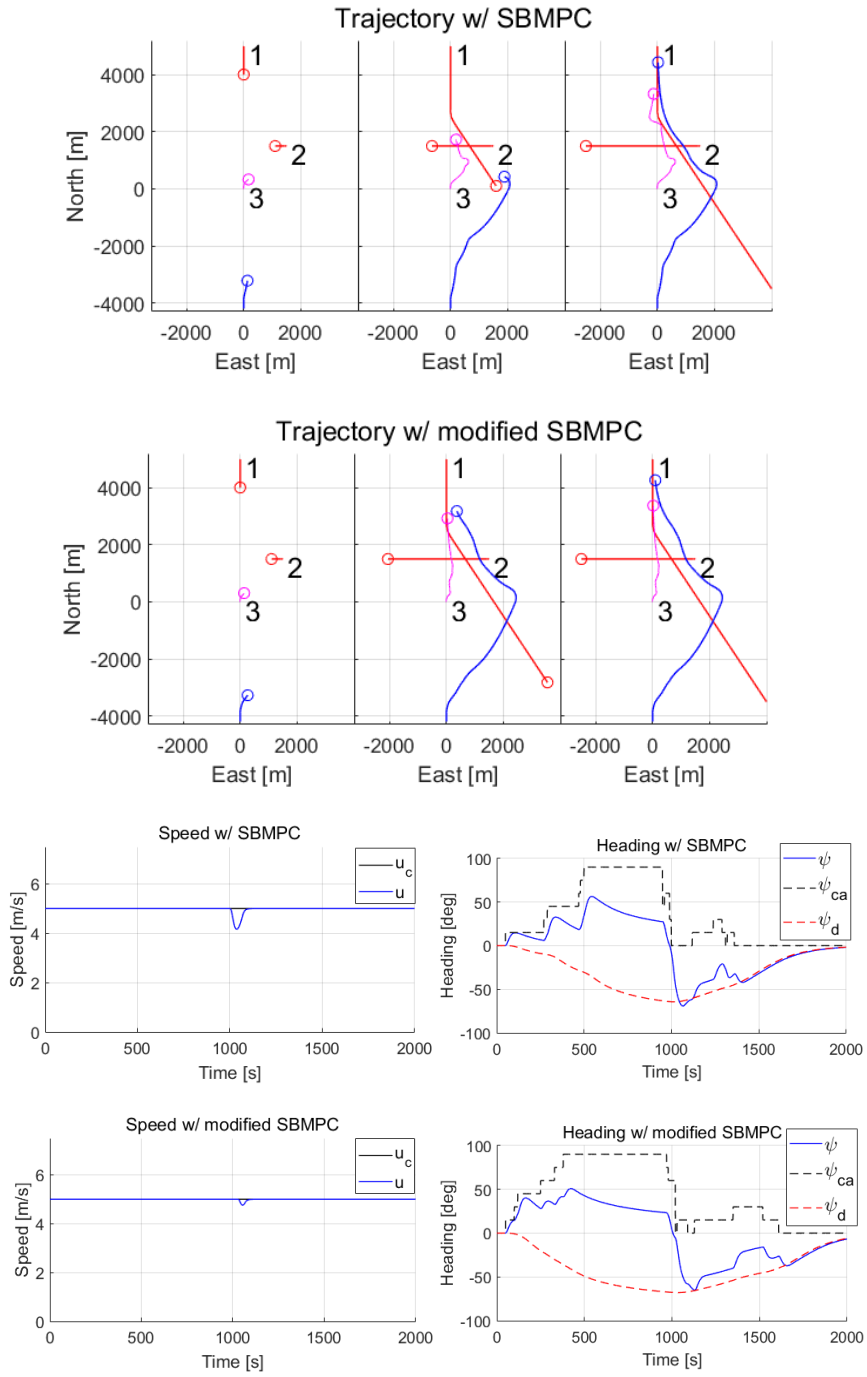

Figure 7.12: Simulation results from the scenario where the own-ship is overtaking a SBMPC obstacle ship while being in a head-on situation and a crossing situation with passive obstacle ships.

7.2.5 Scenarios with four obstacle ships

Own-ship is in head-on and crossing situations with four passive obstacle ships

The simulation results and metric scores from a scenario with four passive obstacle ships can be seen in Figure 7.13 and Table 7.13. The own-ship was initially in a head on-situation with obstacle ships 1, 2 and 4 and in a crossing situation with obstacle ship 3. In this case, the own-ship had give-way responsibility relative to all ships. The own-ship, obstacle ships 1, 3 and 4 had a speed of 3 m/s while obstacle ship 2 had a speed of 5 m/s.

Both algorithms avoided collision, but there were some differences in the performance of the two algorithms. The SBMPC decided to turn starboard earlier than the modified SBMPC. This caused the SBMPC to have a lower safety score relative to obstacles 2 and 3 compared to the modified SBMPC. However, because the maneuver started earlier, the SBMPC achieved a higher score for $\mathcal{S}^8$, $\mathcal{S}^{14}$ and $\mathcal{S}^{16}$ relative to obstacles 1 and 4. An earlier starboard maneuver resulted in a lower safety score because it made the own-ship go closer to obstacle ship 2. If obstacle ship 2 did not turn, an earlier maneuver would be better.

From Table 7.13 it can be observed that the SBMPC did have higher scores for the majority of the COLREGs metrics compared to the modified SBMPC. However, when the difference in COLREGs metrics is small, it is assumed that safety is more important than high scores for the COLREGs metrics in complicated scenarios. Therefore, the modified SBMPC did perform slightly better in this scenario. The modified SBMPC own-ship utilized intention data to predict where obstacle ship 2 would travel, which made the modified SBMPC achieve a higher safety score relative to obstacle ship 2. This maneuver also increased the safety score relative to obstacle ship 3. However, it would be preferred to have even higher safety scores relative to obstacles 3 and 4.

With SBMPC					With modified SBMPC				
	Obs. 1	Obs. 2	Obs. 3	Obs. 4		Obs. 1	Obs. 2	Obs. 3	Obs. 4
Rules	8,14,16	8,14,16	8,15,16	8,14,16	Rules	8,14,16	8,14,16	8,15,16	8,14,16
r_{cpa}	878 m	511 m	229 m	247 m	r_{cpa}	875 m	629 m	271 m	243 m
$\mathcal{S}_{\text{safety}}$	0.92	0.62	0.38	0.40	$\mathcal{S}_{\text{safety}}$	0.92	0.68	0.42	0.39
$\mathcal{S}^8$	0.96	0.81	0.68	0.69	$\mathcal{S}^8$	0.91	0.81	0.67	0.65
$\mathcal{S}^{14}$	0.89	0.00	-	0.87	$\mathcal{S}^{14}$	0.83	0.00	-	0.83
$\mathcal{S}^{15}$	-	-	0.37	-	$\mathcal{S}^{15}$	-	-	0.37	-
$\mathcal{S}^{16}$	0.91	0.60	0.37	0.39	$\mathcal{S}^{16}$	0.79	0.55	0.37	0.34

Table 7.13: Metric scores for the scenario where the own-ship is head-on relative to three passive obstacle ships while being in a crossing situation with a forth passive obstacle ship.

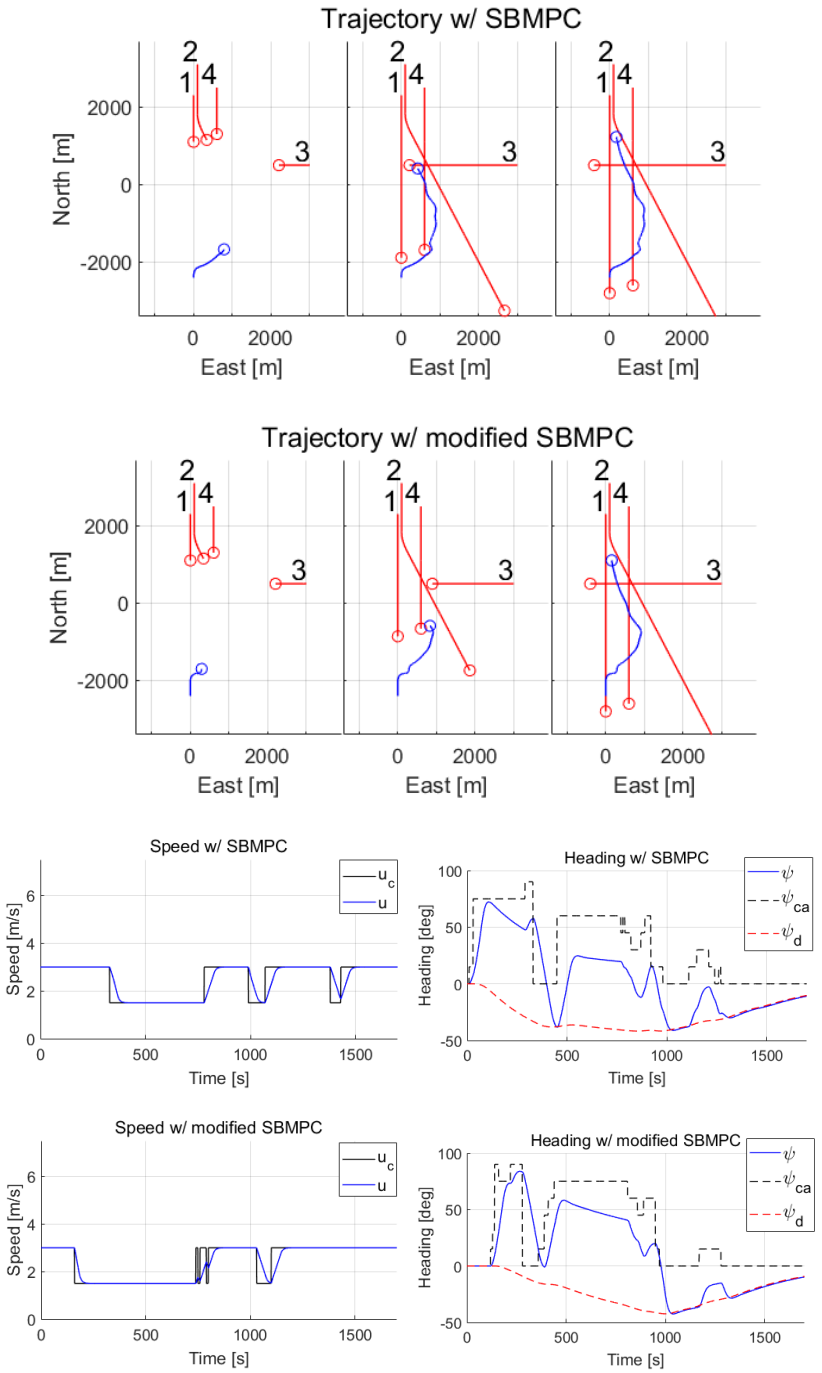

Figure 7.13: Simulation results from the scenario where the own-ship is head-on relative to three passive obstacle ships while being in a crossing situation with a forth passive obstacle ship.

Own-ship is in crossing situations with four obstacle ships

Simulation results from another scenario with four obstacle ships can be seen in Figure 7.14 and Table 7.14. The own-ship was in a crossing situation with four obstacle ships. The own-ship had stand-on responsibility relative to obstacle ships 1, 3 and 4, and give-way responsibility relative to obstacle ship 2.

The behavior of the SBMPC and the modified SBMPC was quite different in this scenario. With the SBMPC algorithm, the own-ship performed a significant starboard turn to avoid collision with the crossing obstacle ships 1, 3 and 4. In contrast, the modified SBMPC utilized the intention data about the planned roles of obstacle ships 3 and 4 to be give-way, which made the own-ship keep an almost constant heading. The modified SBMPC reduced the speed as an attempt to increase CPA distances.

The SBMPC achieved a higher safety score relative to obstacles 1 and 4, but did have a dangerous passing right in front of obstacle ship 3. On the sea, passing that close ahead of anther ship is considered to be very dangerous. Obstacle ship 3 should have performed a starboard turn. Overall, the modified SBMPC did perform better in this scenario by letting the own-ship keep her stand-on role. Acceptable safety scores were achieved with the modified SBMPC, and less maneuvering is preferred in complicated situations because it makes the situation a lot easier to interpret for human navigators.

With SBMPC					With modified SBMPC				
	Obs. 1	Obs. 2	Obs. 3	Obs. 4		Obs. 1	Obs. 2	Obs. 3	Obs. 4
Rules	15,17	8,15,16	15,17	15,17	Rules	15,17	8,15,16	15,17	15,17
r_{cpa}	2162 m	3441 m	345 m	1775 m	r_{cpa}	510 m	1598 m	1288 m	560 m
$\mathcal{S}_{\text{safety}}$	0.85	1.00	0.63	1.00	$\mathcal{S}_{\text{safety}}$	0.72	1.00	0.88	0.65

Table 7.14: Metric scores for scenario where the own-ship is in a crossing situation with four different obstacle ships.

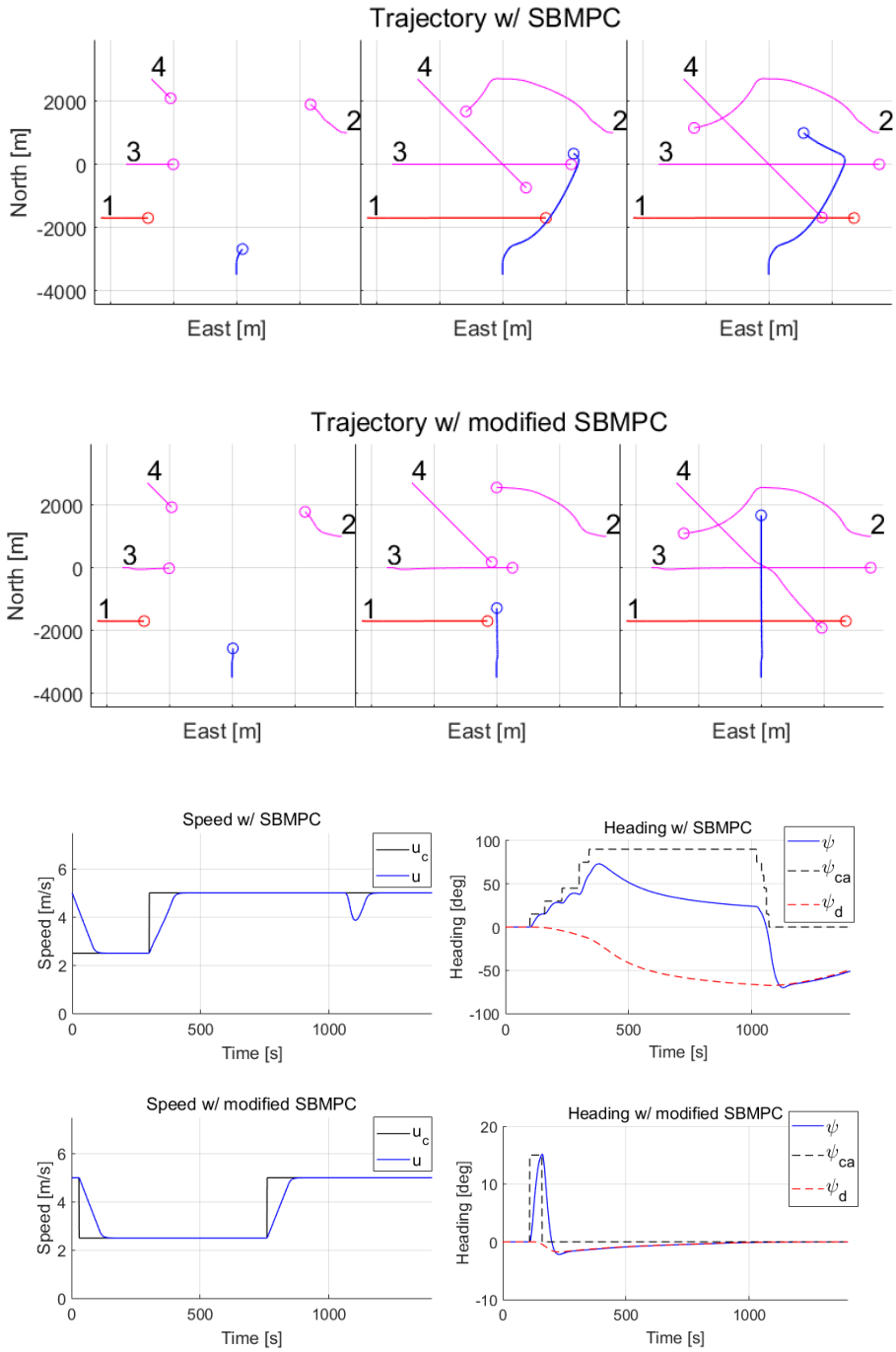

Figure 7.14: Simulation results from the scenario where the own-ship is in a crossing situation with four different obstacle ships.

Chapter 8

Discussion of the Simulation Results

The simulation study in the previous chapter compared the performance of the SBMPC and modified SBMPC algorithms in a wide range of scenarios with varying difficulty. The goal was to investigate if the inclusion of intentions could improve the collision avoidance performance. As discussed in chapter 5, the only difference between the two algorithms is that the modified SBMPC uses intention data about the obstacle's planned trajectory and the obstacle's planned role as either a stand-on or give-way vessel. For each scenario, the metric scores from chapter 6 were calculated to quantify the performance of the algorithms. The simulation results from scenarios with multiple obstacles were also discussed with a navigator from DNV GL.

Both the SBMPC and modified SBMPC algorithms used the same set of tunable parameters. However, some scenarios illustrated a weakness in the chosen parameter values. The two collision avoidance algorithms did turn back to the nominal path too early after performing a collision avoiding maneuver. This sometimes resulted in a fairly low CPA distance, especially in overtaking situations. The reason why the own-ship turned back too quickly was that the hazard function in the collision avoidance algorithms received a penalty whenever the own-ship deviated from the nominal path. Lowering the penalty for deviation from the nominal path could fix the issue.

The simulation results showed that the choice of tuning parameters gave too much penalty for port turns. Lowering the penalty for port turns could have increased the CPA distance in some of the scenarios. Also, the chosen set of parameters in the collision avoidance algorithms made the own-ship prefer a small CPA distance. Therefore, the parameters should be re-tuned to make the own-ship prefer larger CPA distances. The penalty for risk of collision could be increased to help solve the problem with small CPA distances.

Although some issues with the choice of tuning parameters were found, the SBMPC and modified SBMPC algorithms had acceptable overall performance. Both algorithms managed to avoid collision with obstacle ships and grounding with static obstacles in all scenarios. The use of intentions did not seem to improve the ability to avoid static obstacles. However, utilization of intention data did affect the ability to avoid obstacle ships. The two algorithms had some differences in terms of safety of the maneuvers made and the degree of COLREGs compliance achieved.

The scenarios with a single obstacle ship showed the clearest sign of performance improvement from utilizing intention data. The results were a bit more challenging to interpret for situations with several obstacle ships due to higher complexity. However, the modified SBMPC did have better performance than the SBMPC algorithm in the majority of the scenarios tested. There were primarily two types of situations where the modified SBMPC had the most improvement.

The first type of situation was scenarios where a passive obstacle ship changed direction and did not follow a straight path. In these cases, utilization of intention data about the obstacle's planned waypoints made the modified SBMPC have a better prediction of the obstacle ship's trajectory compared to the SBMPC algorithm. The SBMPC algorithm always assumed that the obstacle ship would continue along a straight path. Because of better trajectory prediction, the modified SBMPC initiated maneuvers earlier and kept a larger heading angle offset than the SBMPC. This gave more safe maneuvers with higher CPA distances. In situations where the passive obstacle ship traveled along a straight path for the entire scenario, utilizing intention data did not offer any improvements.

The second type of situation where the use of intentions gave the most improvement was in crossing situations where the own-ship had stand-on responsibility. In these cases, the original SBMPC algorithm could not make the own-ship obey the stand-on responsibility from rule 17. In contrast, the modified SBMPC followed rule 17 because of the utilization of intention data about the obstacle's planned role. With the current implementation of the modified SBMPC algorithm, the obstacle ships broadcast their intended roles as either a stand-on vessel or a give-way vessel to the own-ship. When an obstacle ship intends to take the role of a give-way vessel in a crossing situation, the modified SBMPC algorithm on the own-ship assumes that the own-ship should be stand-on. As a result, a penalty is given to the own-ship's hazard function for any change in heading or speed. This caused the modified SBMPC algorithm to comply with rule 17.

In several of the multi-obstacle scenarios, the use of intended role data made the ships with the modified SBMPC prefer to have a constant heading instead of maneuvering out of the way. The original SBMPC algorithm had a tendency of making the own-ship have a lot of back and forth motion. Less maneuvering makes the scenarios easier to interpret for human navigators. Therefore, the modified SBMPC did perform better in many of the multi-obstacle scenarios. However, preferring to keep the stand-on role can also be a disadvantage since it prevents evasive maneuvers. The behavior observed with the simulation results, where the ships preferred to have a constant heading, is acceptable as long as large enough CPA distances are kept at all times.

The modified SBMPC did not offer any improvement in the score for CPA/TCPA alarms. These alarms go off when either the estimated CPA distance or the estimated time to CPA goes below certain values. Intention data did not improve time to CPA. The modified SBMPC did increase CPA distance, but this was not enough to increase the score for CPA/TCPA alarms.

The own-ship predicts the trajectory of SBMPC obstacle ships differently in the SBMPC and modified SBMPC algorithms. However, the simulation results did not display any major improvement in the performance from the improved trajectory prediction in the modified SBMPC algorithm. In a few scenarios, better results were achieved with the modified SBMPC's trajectory prediction, but in the majority of the scenarios it did not make a difference. As discussed in chapter 5.3, using intention data from an autonomous vessel with the SBMPC or modified SBMPC implemented is problematic because the intentions change every 10th second. This made it challenging to plan maneuvers based on intention data.

Chapter 9

Conclusions

This thesis aimed to answer the research question about whether or not the inclusion of intention data can improve the performance of an existing short-term collision avoidance system. Two different collision avoidance algorithms have been implemented in this thesis: the SBMPC by Johansen et al. (2016) and the modified SBMPC that extends the original SBMPC algorithm to utilize intention data. The two primary modifications made were improving the trajectory prediction and utilization of data about the obstacle's intended role as either stand-on or give-way. It was also concluded that using VDES seemed to be the most promising method of communicating intentions.

A vessel simulator has been implemented, and was used to compare the performance of the two collision avoidance algorithms. The multi-obstacle simulation scenarios were manually designed to be similar to scenarios that often lead to collision for manually operated ships. These are scenarios where the navigator is distracted and when obstacle ships perform unexpected maneuvers. An evaluation tool consisting of different metrics, based on the work by Woerner (2016), quantified the performance of the algorithms. Additional metrics for grounding and CPA/TCPA alarms were implemented to supplement the work by Woerner (2016).

The SBMPC and modified SBMPC algorithms avoided collision and grounding in all scenarios tested. However, the chosen parameters for the algorithms did make the own-ship prefer a somewhat small CPA distance. Higher safety would be achieved if the algorithms were re-tuned to prefer higher CPA distances. The inclusion of intentions did improve the collision avoidance performance in the majority of the scenarios tested. There were mainly two types of scenarios where utilization of intentions gave the most improvement: situations where passive obstacle ships did not follow a straight path and situations where the own-ship had stand-on responsibility. The modified SBMPC showed an increase in both safety and degree of COLREGs compliance.

Promising results were obtained in this thesis, but there are some challenges concerned with using intention data for short-term collision avoidance. The performance is dependant on being able to track other ships accurately, and it must be assumed that that the intention data is always correct and up to date. Also, utilizing intention data from autonomous ships with the SBMPC or modified SBMPC is challenging, since the intentions change every 10th second. However, with the assumptions made in this thesis, the simulation results showed that utilizing intention data in the modified SBMPC did improve the short-term collision avoidance performance of the existing SBMPC algorithm.

Chapter 10

Further work

The results from this thesis indicate that utilizing intentions can improve short-term collision avoidance performance. However, several simplifying assumptions have been made. There is still some work to be done on the simulator and algorithm implementation to gain more realistic results.

The simulator implementation assumed that there were no environmental disturbances. Inclusion of disturbances such as wind and ocean currents would provide a more accurate picture of how the SBMPC and modified SBMPC algorithms perform in real-life. Also, the effect of sensor measurement errors and communication errors should be investigated.

The algorithms should be tested in more realistic scenarios. The static obstacles used in this thesis could be replaced with real map data. Also, different types of ship models should be included. The size and maneuverability of the obstacle ships do play an essential role in deciding which maneuvers to take.

There is a potential for improving the implementation of the collision avoidance algorithms. The chosen tuning parameters could be improved to make the algorithms achieve higher CPA distances. Also, other ways of utilizing intention data in the modified SBMPC algorithm should be investigated. This thesis was only concerned with short-term collision avoidance performance. Some effort should also be put into investigating how intention data can be used in long-term collision avoidance algorithms.

There is also a potential for improving the metrics used to quantify the collision avoidance performance. The metrics used for measuring COLREGs compliance are designed for scenarios with only one obstacle ship. Adding a metric for the amount of unnecessary maneuvering could be beneficial. Less maneuvering makes the situation easier to interpret for human navigators.

Bibliography

Allen, C.H., 2005. *Farwell's Rules of the Nautical Road* (8th Edition). Naval Institute Press.

Allianz Global Corporate & Specialty, 2017. *Global Claims Review.* Technical report.

Almeida, J., Silvestre, C., Pascoal, A., 2007. Path-Following Control of Fully-Actuated Surface Vessels In the Presence of Ocean Currents. *IFAC Proceedings Volumes* 40, 26 – 31.

Bai, Y., Bai, Q., 2019. *Chapter 4 - Subsea Surveying, Positioning, and Foundation*, in: Bai, Y., Bai, Q. (Eds.), Subsea Engineering Handbook (Second Edition). Gulf Professional Publishing, Boston, pp. 81 – 121.

Balduzzi, M., Pasta, A., Wilhoit, K., 2014. A Security Evaluation of AIS Automated Identification System. *The 30th Annual Computer Security Applications Conference* , 436–445.

Beard, R.W., McLain, T.W., 2012. *Small Unmanned Aircraft. Theory and Practice*. Princeton University Press.

Bitar, G., Breivik, M., Lekkas, A.M., 2018. Energy-Optimized Path Planning for Autonomous Ferries. *11th IFAC Conference on Control Applications in Marine Systems, Robotics, and Vehicles CAMS 2018* 51, 389 – 394.

Bitar, G., Eriksen, B.H., Lekkas, A.M., Breivik, M., 2019. Energy-Optimized Hybrid Collision Avoidance for ASVs. *2019 18th European Control Conference (ECC)* , 2522–2529.

Borenstein, J., Koren, Y., 1989. Real-Time Obstacle Avoidance for Fast Mobile Robots. *IEEE Transactions on Systems, Man, and Cybernetics* 19, 1179–1187.

Bourke, P., 1988. *Minimum Distance Between a Point and a Line*. Available at: `http://paulbourke.net/geometry/pointlineplane/`. Accessed: 15/04/2020.

Bousson, K., 2008. Model Predictive Control Approach to Global Air Collision Avoidance. *Aircraft Engineering and Aerospace Technology* 80, 605–612.

Brekke, E.F., Wilthil, E.F., Eriksen, B.O.H., Kufoalor, D.K.M., Helgesen, Ø.K., Hagen, I.B., Breivik, M., Johansen, T.A., 2019. The Autosea Project: Developing Closed-Loop Target Tracking and Collision Avoidance Systems. *Journal of Physics: Conference Series* 1357, 012020.

Børhaug, E., Pavlov, A., Pettersen, K.Y., 2008. Integral LOS Control for Path Following of Underactuated Marine Surface Vessels in the Presence of Constant Ocean Currents, in: *2008 47th IEEE Conference on Decision and Control*, pp. 4984–4991.

Campbell, S., Naeem, W., Irwin, G., 2012. A Review on Improving the Autonomy of Unmanned Surface Vehicles Through Intelligent Collision Avoidance Manoeuvres. *Annual Reviews in Control* 36, 267 – 283.

Chiang, H.L., Tapia, L., 2018. COLREG-RRT: An RRT-Based COLREGS-Compliant Motion Planner for Surface Vehicle Navigation. *IEEE Robotics and Automation Letters* 3, 2024–2031.

Cockcroft, A., Lameijer, J., 2012. Part B - Steering and sailing rules, in: Cockcroft, A., Lameijer, J. (Eds.), *A Guide to the Collision Avoidance Rules* (7th Edition). Butterworth-Heinemann, Oxford, pp. 11 – 104.

Danish Maritime Authority, 2003. Casualty Report: Collision Between Chinese Bulk Carrier FU SHAN HAI and Cypriot Container Vessel GDYNIA. Copenhagen: Division for investigation of maritime accidents, Danish Maritime Authority .

Demirel, E., Bayer, D., 2015. The Further Studies On The COLREGs (Collision Regulations). *TransNav, the International Journal on Marine Navigation and Safety of Sea Transportation* 9, 17–22.

Denker, C., Baldauf, M., Fischer, S., Hahn, A., Ziebold, R., Gehrmann, E., Semann, M., 2016. e-Navigation Based Cooperative Collision Avoidance at Sea: The MTCAS Approach, in: *2016 European Navigation Conference (ENC)*, pp. 1–8.

Elkins, L., Sellers, D., Monach, W.R., 2010. The Autonomous Maritime Navigation (AMN) Project: Field Tests, Autonomous and Cooperative Behaviors, Data Fusion, Sensors, and Vehicles. *Journal of Field Robotics* 27, 790–818.

Eriksen, B.H., Breivik, M., Wilthil, E.F., Flåten, A.L., Brekke, E.F., 2019. The Branching-Course Model Predictive Control Algorithm for Maritime Collision Avoidance. *Journal of Field Robotics* 36, 1222–1249.

Eriksen, C., Gillberg, M., Vestergren, P., 2006. Sleepiness and Sleep in a Simulated "Six Hours On/Six Hours Off" Sea Watch System. *Chronobiology international* 23, 1193–202.

European Maritime Safety Agency, 2019. *Annual Overview of Marine Casualties and Incidents 2019.* Technical report.

Foss, B., Heirung, T.A.N., 2016. *Merging Optimization and Control*. A compendium used as learning material in the course TTK4135 at the Norwegian University of Science and Technology.

Fossen, T.I., 2011. *Handbook of Marine Craft Hydrodynamics and Motion Control*. Wiley & sons, Ltd.

Fukuto, J., Imazu, H., 2013. New Collision Alarm Algorithm Using Obstacle Zone by Target (OZT). *IFAC proceedings volumes* 46, 91–96.

Hagen, I.B., 2017. *Collision Avoidance for ASVs Using Model Predictive Control*. Master's thesis from the Norwegian University of Science and Technology .

Harati-Mokhtari, A., Wall, A., Brooks, P., Wang, J., 2007. Automatic Identification System (AIS): Data Reliability and Human Error Implications. *Journal of Navigation* 60, 373–389.

Hexeberg, S., Flåten, A.L., Brekke, E.F., et al., 2017. AIS-Based Vessel Trajectory Prediction, in: *2017 20th International Conference on Information Fusion (Fusion)*, IEEE. pp. 1–8.

Hobbs, A., 2018. *Rolls-Royce Finferries Test World's First Fully Autonomous Ferry*. Available at: `https://internetofbusiness.com/rolls-royce-finferries-test-worlds-first-fully-autonomous-ferry/`. Accessed 07/01/2020.

Hornauer, S., Hahn, A., 2013. Towards Marine Collision Avoidance Based on Automatic Route Exchange. IFAC Proceedings Volumes 46, 103 – 107. *9th IFAC Conference on Control Applications in Marine Systems*.

Hu, Q., Shi, C., Chen, H., Hu, Q., 2006. Enabling Vessel Collision-Avoidance Expert Systems to Negotiate. *The proceeding of IAIN/GNSS, Jeju, Korea* , 77–82.

Hu, Q., Yang, C., Chen, H., Xiao, B., 2008. Planned Route Based Negotiation for Collision Avoidance Between Vessels. *TransNav, the International Journal on Marine Navigation and Safety of Sea Transportation* 2, 363–368.

Huang, Y., Chen, L., Chen, P., Negenborn, R.R., van Gelder, P., 2020. Ship collision avoidance methods: State-of-the-art. *Safety science* 121, 451–473.

Huntsberger, T., Aghazarian, H., Howard, A., Trotz, D.C., 2011. Stereo Vision–Based Navigation for Autonomous Surface Vessels. *Journal of Field Robotics* 28, 3–18.

IEC 61174, 2015. *Maritime Navigation and Radiocommunication Equipment and Systems - Electronic Chart Display and Information System (ECDIS) - Operational and Performance Requirements, Methods of Testing and Required Test Results*. Standard. International Electrotechnical Commission.

IEC 62388, 2013. *Maritime Navigation and Radiocommunication Equipment and Systems - Shipborne Radar - Performance Requirements, Methods of Testing and Required Test Results*. Standard. International Electrotechnical Commission.

IMO, 2002. *Guidelines for the Onboard Operational Use of Shipborne Automatic Identification Systems (AIS)*. Resolution A.917(22).

IMO, 2015. *Draft e-navigation Implementation Plan*. NCSR 1/28, Annex 7.

International Association of Marine Aids to Navigation and Lighthouse Authorities, 2017. *G1117 VHF Data Exchange System (VDES) Overview*. Technical report.

International Maritime Organization, 1972. *1972 Convention on the International Regulations for Preventing Collisions at Sea*. IMO, London.

International Maritime Organization, 2013. *Guidelines for the Approval of Alternatives and Equivalents as Provided for in Various IMO Instruments*. MSC.1/Circ.1455, London .

International Maritime Organization, 2017. *Lessons Learned*. Available at: `http://www.imo.org/en/OurWork/MSAS/Casualties/Pages/Lessons-learned.aspx`. Accessed 27/01/2020.

International Maritime Organization (IMO), 1974. *International Convention for the Safety of Life at Sea (SOLAS), 1974*. Available at: `http://www.imo.org/About/Conventions/ListOfConventions/Pages/International-Convention-for-the-Safety-of-Life-at-Sea-(SOLAS),-1974.aspx`. Accessed: 01/02/2020.

Johansen, T.A., Perez, T., Cristofaro, A., 2016. Ship Collision Avoidance and COLREGS Compliance Using Simulation-Based Control Behavior Selection With Predictive Hazard Assessment. *IEEE Transactions on Intelligent Transportation Systems* 17, 3407–3422.

Kim, D., Hirayama, K., Okimoto, T., 2017. Distributed Stochastic Search Algorithm for Multi-ship Encounter Situations. *Journal of Navigation* 70, 1–20.

Kim, D.G., Hirayama, K., Park, G.K., 2014. Collision Avoidance in Multiple-Ship Situations by Distributed Local Search. *Journal of Advanced Computational Intelligence and Intelligent Informatics* 18, 839–848.

Kjerstad, K., 2019. *Collision Avoidance System for Ships Utilizing Other Vessels' Intentions*. Unpublished 5th year specialization project, written in the fall of 2019 at the Norwegian University of Science and Technology.

Kurose, J.F., Ross, K.W., 2012. *Computer Networking: A Top-Down Approach* (6th Edition). Pearson.

Kuwata, Y., Wolf, M.T., Zarzhitsky, D., Huntsberger, T.L., 2014. Safe Maritime Autonomous Navigation With COLREGS, Using Velocity Obstacles. *IEEE Journal of Oceanic Engineering* 39, 110–119.

LaValle, S.M., 1998. *Rapidly-Exploring Random Trees: a New Tool for Path Planning*. Technical report from Iowa State University, Department of Computer Science.

Lázaro, F., Raulefs, R., Wang, W., Clazzer, F., Plass, S., 2019. VHF Data Exchange System (VDES): An Enabling Technology for Maritime Communications. *CEAS space Journal* 11, 55–63.

Lee, G., Parker, J., 2007. *Managing Collision Avoidance at Sea*. The Nautical Institute.

Lee, S.M., Kwon, K.Y., Joh, J., 2004. A Fuzzy Logic for Autonomous Navigation of Marine Vehicle Satisfying COLREG Guidelines. *International Journal of Control, Automation, and Systems* 2.

Lindborg, J., Ferm, D., Andrianov, M., 2019. *Route Message System Requirements, G1*. Document published as part of the STM BALT SAFE project.

Liu, J., Jayakumar, P., Overholt, J., Stein, J., Ersal, T., 2013. The Role of Model Fidelity in Model Predictive Control Based Hazard Avoidance in Unmanned Ground Vehicles Using LIDAR Sensors. *ASME 2013 Dynamic Systems and Control Conference, DSCC 2013* 3.

Liu, Z., Squillante, M.S., Wolf, J.L., 2001. On Maximizing Service-Level-Agreement Profits, in: *Proceedings of the 3rd ACM Conference on Electronic Commerce*, Association for Computing Machinery, New York, NY, USA. p. 213–223.

Liu, Z., Wu, Z., 2003. The Human Element in Ship Collisions at Sea, in: *Asia Navigation Conference in Kobe, Japan*.

Lloyd, M., 2006. *Why Ships Really Collide*. SEAWAYS October 2006 , 10–11.

Loe, A., 2008. *Collision Avoidance for Unmanned Surface Vehicles*. Master's thesis from the Norwegian University of Science and Technology .

Låg, S., Vartdal, B.J., Knutsen, K.E., 2015. *Ship Connectivity*. DNV GL strategic research innovation position paper.

Mambra, S., 2019. *The Complete Story of the Exxon Valdez Oil Spill*. Available at: https://www.marineinsight.com/maritime-history/the-complete-story-of-the-exxon-valdez-oil-spill/. Accessed: 24/01/2020.

Mariano, K., 2017. *Remembering Doña Paz, The Deadliest Shipwreck In History Worse Than The Titanic*. Available at: https://www.elitereaders.com/remembering-dona-paz-deadliest-shipwreck-history-worse-titanic/. Accessed: 24/01/2020.

Marine Accident Investigation Branch, 2004. *Bridge Watchkeeping Safety Study*. Technical report.

Marine Insight, 2018. *Real Life Accident: Officer Of The Watch Falls Asleep, Ship Hits Seawall At 15 Knots*. Available at: https://www.marineinsight.com/case-studies/officer-of-the-watch-falls-asleep-ship-hits-seawall-at-15-knots/. Accessed: 28/01/2020.

Martinsen, A.B., Lekkas, A., 2018. Straight-Path Following for Underactuated Marine Vessels Using Deep Reinforcement Learning. *IFAC-PapersOnLine* 51, 329–334.

Minne, P.K.E., 2017. *Automatic Testing of Maritime Collision Avoidance Algorithms*. Master's thesis from the Norwegian University of Science and Technology.

Mohović, Đ., Mohović, R., Barić, M., 2015. Identifying Skill Gaps in the Knowledge and Teaching Of COLREGs, in: *17th International conference on transport science*.

MUNIN, 2016. *MUNIN Results*. Available at: `http://www.unmanned-ship.org/munin/about/munin-results-2/`. Accessed: 07/01/2020.

Naeem, W., Sutton, R., Ahmad, S.M., Burns, R.S., 2003. A Review of Guidance Laws Applicable to Unmanned Underwater Vehicles. *Journal of Navigation* 56, 15–29.

Nocedal, J., Wright, S.J., 2006. *Numerical Optimization*. Springer-Verlag New York.

Otterholm, O.S., 2019. *Extracting Mapped Hazards from Electronic Navigational Charts for ASV Collision Avoidance*. Master's thesis from the Norwegian University of Science and Technology.

Pedersen, T.A., 2018. *Exploring System Verification for Autonomous Applications*. Unpublished report from DNV GL.

Polvara, R., Sharma, S., Wan, J., Manning, A., Sutton, R., 2018. Obstacle Avoidance Approaches for Autonomous Navigation of Unmanned Surface Vehicles. *Journal of Navigation* 71, 241–256.

Porathe, T., Borup, O., Jeong, J.S., Park, J.H., Andersen Camre, D., Brödje, A., 2014. Ship Traffic Management Route Exchange: Acceptance in Korea and Sweden, a Cross Cultural Study, in: *Proceedings of the International Symposium Information on Ships, ISIS 2014*, pp. 64–79.

Porathe, T., Lützhöft, M., Praetorius, G., 2013. Communicating Intended Routes In ECDIS: Evaluating Technological Change. *Accident Analysis & Prevention* 60, 366 – 370.

Rao, L., Liu, X., Xie, L., Liu, W., 2010. Minimizing Electricity Cost: Optimization of Distributed Internet Data Centers in a Multi-Electricity-Market Environment, in: *2010 Proceedings IEEE INFOCOM*, pp. 1–9.

Recommendation ITU-R M.1371-5, 2014. *Technical Characteristics for an Automatic Identification System Using Time Division Multiple Access in the VHF Maritime Mobile Frequency Band*. Technical report. International Telecommunication Union.

Skredderberget, A., 2017. *The First Ever Zero Emission, Autonomous Ship*. Availabe at: `https://www.yara.com/knowledge-grows/game-changer-for-the-environment/`. Accessed: 07/01/2020.

Sormunen, O.V., Hänninen, M., Kujala, P., 2016. Marine Traffic, Accidents, and Underreporting in the Baltic Sea. *Scientific Journals of the Maritime University of Szczecin* 46, 163–177.

Statheros, T., Howells, G., Maier, K., 2008. Autonomous Ship Collision Avoidance Navigation Concepts, Technologies and Techniques. *Journal of Navigation* 61, 129–142.

Strauch, B., 2015. Investigating Fatigue in Marine Accident Investigations. *Procedia Manufacturing* 3, 3115 – 3122.

Sundar, S., Shiller, Z., 1997. Optimal Obstacle Avoidance Based on the Hamilton-Jacobi-Bellman Equation. *IEEE Transactions on Robotics and Automation* 13, 305–310.

Tam, C. K., B.R., Greig, A., 2009. Review of Collision Avoidance and Path Planning Methods for Ships in Close Range Encounters. *Journal of Navigation* 62, 455–476.

The Japan Times, 2019. *U.S. Destroyer Lookouts' Failure to Follow Protocol Led to Fatal 2017 Collision, Japanese Report Says*. Available at: https://www.japantimes.co.jp/news/2019/08/29/national/japan-report-us-destroyer-collision/#.Xi2GDmhKhaQ. Accessed: 26/01/2020.

The Maritime Executive, 2014. *Chesapeake Bay Weather Causes Ship Collision, Groundings*. Available at: https://www.maritime-executive.com/article/Chesapeake-Bay-Weather-Causes-Ship-Collision-Groundings-2014-04-16. Accessed 27/01/2020.

The Maritime Executive, 2019. *AIS Gets an Upgrade*. Available at: https://www.maritime-executive.com/article/ais-gets-an-upgrade. Accessed: 21/02/2020.

Weinert, B., Park, J., Christensen, T., Hahn, A., 2018. A Common Maritime Infrastructure for Communication and Information Exchange. *19th IALA Conference, At Incheon, Republic of Korea* .

Wilthil, E., Flåten, A., Brekke, E., 2017. A Target Tracking System for ASV Collision Avoidance Based on the PDAF. *Sensing and Control for Autonomous Vehicles* , 269–288.

Wingrove, M., 2018. Accident Report: Communications breakdown causes ship collision. Available at: https://www.rivieramm.com/news-content-hub/accident-report-communications-breakdown-causes-ship-collision-24959. Accessed: 27/01/2020.

Wireless, B., 2019. *Wifi On Board! How 4G/LTE Is Transforming Maritime Communications - Top 5 Questions*. Available at: https://www.bluewireless.com/post/wifi-on-board-how-4glte-is-transforming-maritime-communications-top-5-questions. Accessed: 21/02/2020.

Woerner, K., 2016. Multi-contact protocol-constrained collision avoidance for autonomous marine vehicles. PhD thesis from Massachusetts Institute of Technology.

Wöhrn, R., 2007. *Collisions at sea - Unavoidable?* Available at: http://www.gard.no/web/updates/content/51705/collisions-at-sea-unavoidable. Accessed: 27/01/2019.

Appendix A

Interviews

This appendix contains summaries of interviews conducted with navigators from DNV GL. Co-supervisor, Steinar Låg, also participated in the interviews. All interviews were held in Norwegian, and the summaries have been translated to English.

A.1 Interview with Benjamin Bjørge 10.10.2019

- **What crew is needed onboard a ship?**
  The type of crew depends on several factors: type of ship, type of waters, traffic and weather. As a minimum, there has to be an officer of the watch on the ship's bridge. There is another person on the bridge, called the lookout, responsible for keeping a lookout at night and in bad weather. The lookout detects possible dangers and obstacles. In addition, there is a captain on the ship. If CPA becomes small, the officer of the watch can ask the captain for guidance.

- **What are the different phases of a ship's voyage?**
  There are three main phases: startup, voyage on open sea and end phase. At startup, the crew make sure that the ship is seaworthy. The crew on the deck handle the ropes and a pilot enters the ship to help with navigation. The second phase, voyage on the open sea, starts when the pilot leaves the ship. At this point, there are only one or two persons on the bridge. The final phase is similar to the first phase. Again, a pilot enters the ship to help navigate and the crew handle the ropes.

- **What are some common reasons for collisions at sea?**
  Bad weather. Collisions can also happen in calm weather conditions, because in these situations, the officer of the watch does not always pay as much attention. He

is often busy with other tasks than keeping a lookout, for instance, paperwork. Fatigue is another reason. The crew often have long work hours and little rest because the shipowners want to make as much money as possible. Collisions can also happen in situations with much traffic, and when the ship is in narrow waterways with little maneuverability options. Some people lack competence and experience. It is important to know how the onboard equipment works.

- **How to maneuver to avoid collisions?**
  Maneuvers should start as early as possible and follow the COLREGs. It is possible to perform a $360°$ turn to buy some time.

- **What information about intentions is useful?**
  It is useful to know where the obstacle ship is going (destination port). The planned route is useful as long as it is up to date and the obstacle ship does not deviate from it. Also, future speed and course are important.

- **How does the officer of the watch communicate with other ships?**
  VHF radio is commonly used to agree on where the ships should travel. VHF is also used to ask what intentions the other ship have. However, the use of VHF is not recommended. It is always better to follow the COLREGs because the use of VHF can cause misunderstandings. Another option for communication is light and sound signals.

- **What equipment is used to help avoid collisions?**
  Radar and AIS data are used to detect obstacles. Manual lookout is also required. In addition, the ship has different colored lights on different sides of the ship. The lights can be used to verify if the obstacle ship is traveling towards you or not. Also, the ship horn can alert other ships when visibility is poor.

- **What are some challenges with autonomous ships?**
  The autopilot will only steer towards the ship's waypoints. Autopilots today only follow a course and does not consider other vessels. Therefore, autopilot is difficult to use in dense traffic. Automatic collision avoidance systems are not used on today's ships.

A.2 Interview with Olaf Gundersrud 10.10.2019

- **What are some common reasons for collisions?**
  One of the reasons is a lack of competence and experience. This can cause the crew to make the wrong decisions and also misinterpret collision situations. Fatigue is another problem. The crew can often work 12-15 hour shifts, which increases the chances of making mistakes. Technical errors, such as engine failure, can cause collisions since it will reduce the maneuverability. Many people take too large risks and keep a too small distance relative to other ships. Sometimes, the ship starts to maneuver too late.

- **How does the crew on the bridge cooperate?**
  Often, there is only one person on the bridge: the officer of the watch. When there are two persons, there can be problems with cooperation if they speak different languages. When there are two persons on the bridge, the officer of the watch is responsible for steering and the lookout is only responsible for keeping a lookout for potential dangers.

- **How can ships communicate?**
  Ships can communicate by taking apparent maneuvers, for instance, by changing the course with at least $30°$. The ship horn can be used in case of poor visibility. The COLREGs specify codes for sound signals for different kinds of intentions. VHF radio is not defined in the COLREGs, but can be used to communicate. However, VHF communication is not recommended. Accidents have happened in the past because VHF was misused. Collisions have happened due to communication with the wrong ship. Language barriers are a reason for why VHF radio can cause misunderstandings.

- **What intentions would be useful to know?**
  It would be beneficial to know all intentions of the obstacle ship. The problem is that they only exist in the mind of the navigator. It would be useful to know the planned route of the obstacle ship. One problem is that intentions change over time, depending on how the situation develops.

- **What technical equipment is used on a ship?**
  Radar is useful for getting an overview of the traffic situation. Radar is the main instrument used for detecting obstacles. AIS can be used to supplement the radar. The information is typically displayed on an ECDIS monitor.

- **What are some challenges with autonomous ships?**
  In narrow waterways, it would be more difficult to navigate compared to out on the open sea. Making an autonomous ship follow the COLREGs is a challenge because the COLREGs have many vague formulations. It would also be challenging to let autonomous ships and manually operated ships operate in the same areas of the sea.

A.3 Interview with Erlend Norstein 25.02.2020

- **What steps are taken in a collision situation?**
  The first step is to get an overview of the situation and detect potential dangers. In the next step, the navigator must analyze the situation and consider what maneuvers the obstacle ships are likely to perform. The third step will consist of planning a maneuver. The maneuver chosen must avoid collision with other vessels and must also avoid making the ship end up in a dangerous situation. The last step is to perform the maneuver. It is important to take maneuvers as early as possible.

- **How can a navigator detect a collision situation?**
  Both visual monitoring and navigational equipment are used to detect collision situations. The navigator can select which obstacle ships to be tracked on the radar and plot the tracked ships on an ECDIS monitor. AIS is also used to supplement the radar. Destination data from AIS can be used to interpret where a ship is going to travel. The navigation system calculates CPA and TCPA, and alarms will be given if these values go below the chosen limits. The CPA/TCPA alarms are one of the primary means of detecting collision situations.
- **How is VHF radio used?**
  VHF radio can be used to inform other ships about planned maneuvers. It is also commonly used for asking about what intentions the other navigators have. However, VHF should not be used to plan maneuvers because it can easily cause misunderstandings. Even if you plan on following the COLREGs, VHF can be used to inform other navigators more in-depth about your maneuvers.
- **How does a navigator decide on maneuvers to perform?**
  The COLREGs define what maneuvers should be taken in different situations. If other ships do not follow COLREGs, you have to do anything you can to avoid a collision. There are some problems with the COLREGs. They can be interpreted in several ways and are made for humans. They can be difficult to follow for an automatic collision avoidance algorithm. In situations with multiple obstacles, it can be impossible to comply 100% with all COLREGs. The COLREGs rules can give conflicting requirements.
- **What situations will often cause collisions?**
  Weather, traffic and speed play an important role. Situations where the navigator is distracted with other tasks can also be dangerous. Situations where multiple ships are involved can be challenging because the navigator must pay attention to several ships at the same time.
- **How can collision avoidance performance be measured?**
  The CPA distance can be used. Often, a CPA of 1.8 km is used. In situations with dense traffic, the CPA can be smaller. Also, a smaller CPA is accepted when traveling in front of a ship compared to traveling behind a ship. The type of ship also play a role. Higher CPA is required when facing large vessels with poor maneuverability.
- **What are some challenges with autonomous ships?**
  It would be challenging to make autonomous ships comply with COLREGs. Making an algorithm to follow the COLREGs is difficult because the rules contain vague formulations.

A.4 Interview with Tommi Juhani Rifaat 08.05.2020

During this interview, five different simulation scenarios with multiple obstacle ships were discussed. The discussion was based on the trajectory plots shown in Figures A.1 -

A.5. These are the same plots as in chapter 7. It should be noted that different navigators can have different views on what is considered to be best behavior. Some believe that strictly following the COLREGs is the most important. Others believe that as long as the situation is solved safely, following the COLREGs is less important.

The first scenario in shown in Figure A.1. It is always dangerous to pass ahead of an obstacle ship. The maneuver by ship 2 with modified SBMPC is acceptable here, because it keeps a safe distance to all other ships. It would not be a better solution for the own-ship to move to the right of the circle obstacles, since this would cause a conflict with obstacle ship 2. In a real situation the size and speed of the vessels would play an important role. Larger distance should be kept relative to large ships with little room for maneuverability.

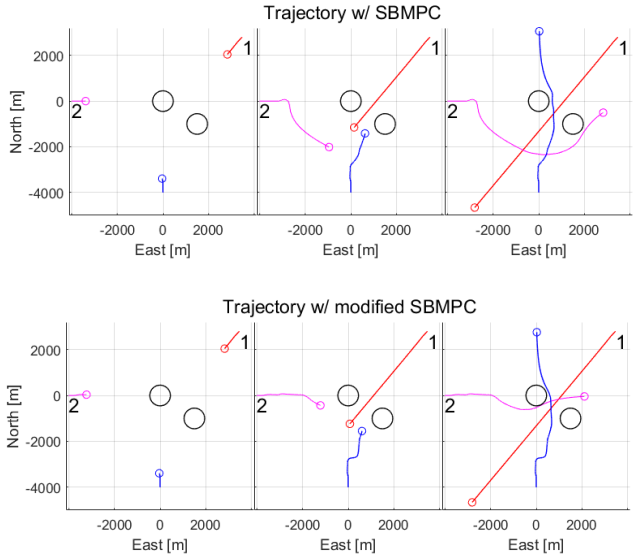

Figure A.1: Scenario where the own-ship is in a crossing situation with an SBMPC obstacle ship on the port side and a passive obstacle ship on the starboard side.

The second scenario is shown in Figure A.2. Here, the modified SBMPC results in a situation that is easier to interpret for the own-ship. Less maneuvering is positive as long as safe CPA distances are kept. It should be noted that with the modified SBMPC, ships 1 and 2 pass each other on the wrong side according to the COLREGs. The SBMPC algorithm causes too much back and forth movement, which makes the situation hard to interpret by the own-ship. Both algorithms make the own-ship turn back to her nominal path too early. In a real situation, the ships would probably use VHF radio to communicate intentions. Overall, the modified SBMPC performs better.

Figure A.3 illustrates the third scenario. Both algorithms behave similarly relative to obstacle ship 1. With the modified SBMPC, ship 2 returns back to the nominal path too early. It would be better to keep a heading offset for a longer period of time. This would make the encounter with ship 3 more safe. The encounter between ship 3 and the own-ship

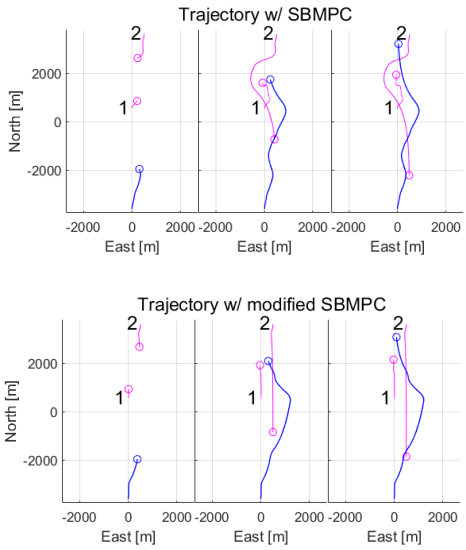

Figure A.2: Scenario where the own-ship is overtaking an SBMPC obstacle ship while being in a head-on situation with another SBMPC obstacle ship.

is clearly better with the modified SBMPC. In this case, ship 3 makes a starboard turn to comply with COLREGs. With the SBMPC, obstacle ship 3 does not make a turn, which is in violation with the COLREGs. Without the static obstacles it would be preferred if obstacle ship 3 made a hard turn to her starboard side.

The forth scenario is shown in Figure A.4. The main difference between the SBMPC and modified SBMPC is that ship 3 decides to keep a more straight course with the modified SBMPC compared to the SBMPC. Also, the own-ship make a more substantial starboard turn with the modified SBMPC. The situation becomes a bit more clear with the modified SBMPC due to ship 3 keeping a more constant course. This would make it easier for the own-ship to decide on a maneuver. It would be beneficial to have a metric based on how much the ships turn during a scenario. Less turning is often preferred because it makes the situation easier to interpret. To conclude, the modified SBMPC algorithm has the best performance.

The final scenario is shown in Figure A.5. The modified SBMPC performs best in this scenario. The own-ship's give-way responsibility relative to ship 2 is not very important, therefore it is preferred that own-ship keeps her stand-on responsibility. In complicated situations like this one, less maneuvering is preferred. The encounter between ship 3 and the own-ship in the SBMPC case is very dangerous. Passing directly ahead of other ships should always be avoided. Ship 3 should have turned to her starboard side.

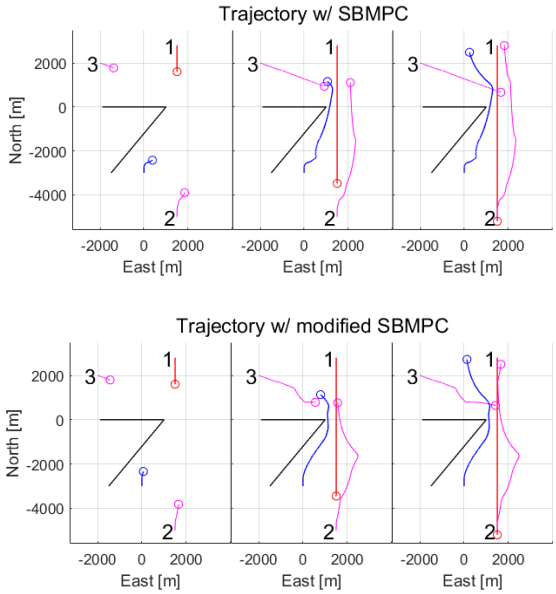

Figure A.3: Scenario where the own-ship is traveling towards a boundary obstacle and facing three obstacle ships.

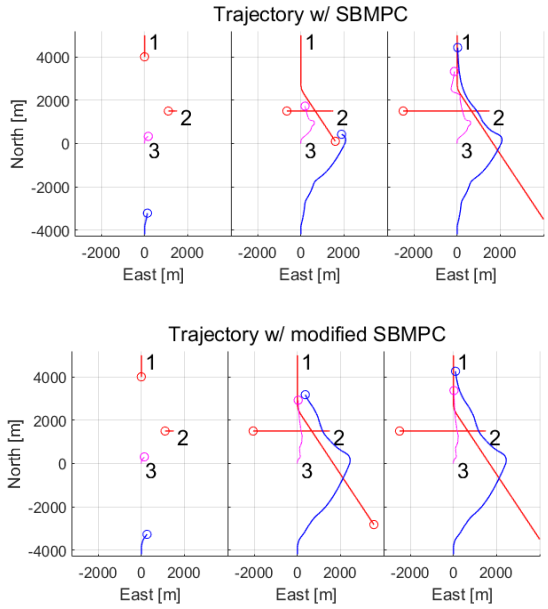

Figure A.4: Scenario where the own-ship is overtaking an SBMPC obstacle ship while being in a head-on situation and a crossing situation with passive obstacle ships.

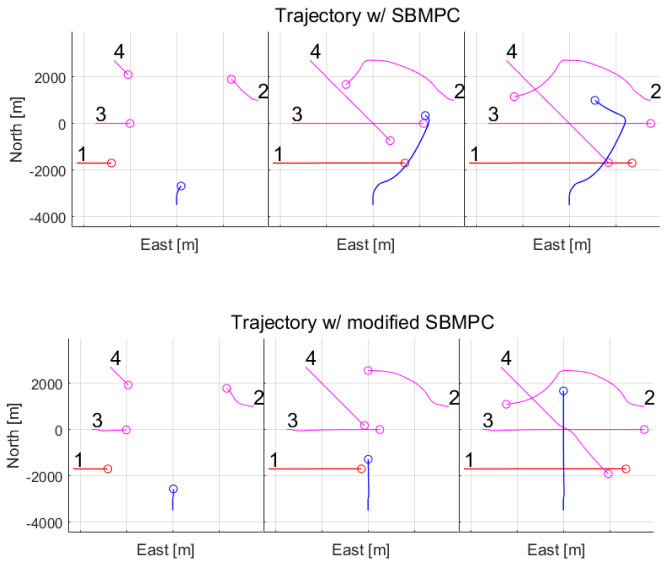

Figure A.5: Scenario where the own-ship is in a crossing situation with four different obstacle ships.

Kristian Kjerstad

Collision Avoidance System for Ships Utilizing Other Vessels' Intentions

NTNU
Norwegian University of
Science and Technology

DNV·GL